The comparison of the methods based on Wavelet Transform and Hilbert-Huang Transform in fault diagnosis of rotating machinery

JIE CHAO CHENG

A THESIS

IN

THE CONCORDIA INSTITUTE

FOR

INFORMATION SYSTEMS ENGINEERING

PRESENTED IN PARTIAL FULFILLMENT OF THE REQUIREMENTS

FOR THE DEGREE OF MASTER OF APPLIED SCIENCE (QUALITY SYSTEMS

ENGINEERING) AT CONCORDIA UNIVERSITY

MONTRÉAL, QUÉBEC, CANADA

June 2014

CONCORDIA UNIVERSITY
School of Graduate Studies

This is to certify that the thesis prepared

By: **JIE CHAO CHENG**

Entitled: **The comparison of the methods based on Wavelet Transform and Hilbert-Huang Transform in fault diagnosis of rotating machinery**

and submitted in partial fulfillment of the requirements for the degree of

Master of Applied Science in Quality Systems Engineering

complies with the regulations of this University and meets the accepted standards with respect to originality and quality.

Signed by the final examining committee:

Dr. A.Youssef Chair

Dr.C.Wang Examiner

Dr.M.Chen Examiner

Dr.Z.Tian Supervisor

Approved by _____
Chair of Department or Graduate Program Director

_____

Dean of Faculty

Date _____

ABSTRACT

As the most common mechanisms for transmitting power and motion, gears and bearings have been widely used in various mechanical equipment. Many accidents have happened because of failing to detect and replace the faulty gears or bearings in time. Hence it is very important to perform accurate fault diagnosis of gears and bearings. When a gear or bearing has a fault, the vibration signal collected from the mechanical equipment will become non-stationary and contain a series of periodic impulses that are caused by the fault. Many theories and techniques have been developed to extract the faulty information based on analyzing periodic impulses contained in the vibration signals.

It has been reported that neither time-domain analysis nor frequency-domain analysis can do well in analyzing non-stationary signals. Hence time-frequency analysis methods based on wavelet transform and Hilbert-Huang Transform (HHT) have been investigated. Wavelet transform includes continuous wavelet transform (CWT) and discrete wavelet transform (DWT). Research was reported to compare the performance of these methods in fault diagnosis of mechanical components. However, the previous works either only compared HHT based methods with CWT based methods, or only compared HHT based methods with DWT based methods, for certain applications. There are no reported comprehensive comparisons of the three methods for fault diagnosis of gears and bearings.

Cepstrum analysis can detect the periodicity and reduce the influence of the noise for the low energy signals. However, previous research usually only applied Cepstrum analysis directly to extract fault features from the entire original signal. Some other existing methods first applied DWT to decompose the original signal to obtain the detail signals, and then used Hilbert spectral analysis to analyze the periodic impulses contained in the detail signals through

identifying faulty characteristic frequency with frequency domain analysis and plotting the instantaneous amplitude with time domain analysis. Hilbert spectral analysis has the advantage in frequency domain analysis. However, sometimes it is not very sensitive in time domain analysis when the energy of the periodic impulses is not strong enough.

In this thesis, we investigate fault diagnosis of gears and bearings using two sets of vibration monitoring data collected in the lab environment: one set for gear condition monitoring and the other for bearing condition monitoring. We propose an improved DWT method that integrates Cepstrum analysis to analyze the periodic impulses contained in the data. With the proposed method, the vibration signals are first decomposed using DWT, and Cepstrum analysis is used to analyze the resulting detail signals. The results show that the proposed method performs better than the existing methods of applying Cepstrum analysis directly. Furthermore, with the help of Cepstrum analysis, the proposed method has better performance in time domain analysis than Hilbert spectral analysis in analyzing the periodic impulses contained in the detail signals.

A comprehensive study is conducted in this thesis to compare the following three methods in fault diagnosis of the gears and bearings: (1) The CWT method using time-wavelet energy spectrum, (2) the improved DWT method using Cepstrum analysis, and (3) the HHT method. The results show that in fault diagnosis of gears, the HHT method has better noise immunity and is more sensitive in frequency domain analysis than the other two methods. The proposed method shows its advantage in analyzing the periodic impulses in time domain than the other two methods. In fault diagnosis of the bearings, the fault can be more clearly detected using the CWT and DWT methods in analyzing the periodic impulse that caused by the outer race fault of the bearing. The results obtained in this thesis can assist researchers and practitioners to select suitable methods for fault diagnosis of gears and bearings.

Acknowledgments

First of all, I would like to express my greatest gratitude to my supervisor, Dr. Zhigang (Will) Tian. His warm encourage, patient guidance and talented advice have helped me a lot in building confidence, developing my knowledge and improving research shillings.

Many thanks to all the members of our lab, for their friendly, open-minded and helpful suggestions during.

I would like to thank my parents for encouraging and supporting my study and research at all time, your endless love and care always encourage me all the time.

Table of Contents

List of Figures

List of Tables

Acronyms

TSA	Time Synchronous Average
FFT	Fast Fourier Transform
STFT	Short-time Fourier Transform
WT	Wavelet transform
CWT	Continuous Wavelet Transform
DWT	Discrete Wavelet Transform
HHT	Hilbert-Huang Transform
EMD	Empirical Mode Decomposition
IMF	Intrinsic Mode Function
HSA	Hilbert Spectral Analysis
RMS	Root Mean Square
DSP	Digital Signal Process
PSD	Power Spectral Density
WVD	Wigner-Ville Distribution

Chapter 1

1. Introduction

1.1 Background

Gears and bearings, which are the common mechanisms that transmit power and motion, have applications in many mechanical driving devices. A lot of equipment's accidents have happened and caused huge economic losses due to failing to detect and replace the faulty gear or bearing in time. Hence, it has great practical and academic significance to perform accurate fault diagnosis of gears and bearings.

In practice, the running state of a healthy mechanical equipment will have a myriad of changes when it starts up. After it running in a steady state, the vibration signals collected from the equipment can be thought in a stationary state. However, when a fault of a gear or bearing has happened, its parameters such as damp and elasticity will change. Also considering the influence of the unsteady shaft rotating speed, lubrication situation, tooth stiffness variations or other reasons, the vibration signals of the equipment will then become not only non-stationary but also non-linear [1]. Hence, we can collect and analyze the vibration signals to characterize the existence of the fault. A gear's fault is usually caused by a local damage of its tooth. The typical faults include pits, cracks on the surface of gear tooth, and even more seriously, tooth wear and breakage. The typical faults of a bearing usually include cage fault, inner race fault, outer race fault, ball fault, etc. There are mainly three steps to perform fault diagnosis of gear and bearing:

1. Collect the diagnosis information (the vibration signals) from the mechanical equipment.

2. Extract fault features from the vibration signal.

3. Identify the features' states and diagnose the fault.

In practical applications, the vibration signals are usually collected by one or more accelerometer sensors installed on the equipment. When a faulty gear is running, the vibration signal usually contains its rotating frequency with the periodic amplitude and phase modulations [1]. When a bearing has a local fault, the vibration signal will also contain the periodic impulses caused by the fault. Hence, the key point for gear/bearing fault diagnosis is how to extract the impulse information from the vibration signals. Signal processing is typically used for feature extraction. There are three main categories of signal processing methods: time-domain analysis, frequency-domain analysis and time-frequency analysis.

(1) Time-domain analysis

The time-domain analysis is to analyze the amplitude and phase information of the vibration signal in time series. Traditional analysis applies descriptive statistics methods to calculate the features from the signals. The descriptive statistics include mean, peak, crest factor, root mean square, skewness, kurtosis value, etc., which are called time-domain features [2]. Time synchronous average (TSA) is also popular in time-domain analysis. These methods can detect the fault in mechanical equipment. However, when a mechanical equipment has a faulty gear or bearing, the frequency components of the signals will also change, which sometimes is hard for time-domain analysis to distinguish them.

(2) Frequency-domain analysis

Frequency-domain analysis is based on the analysis of the signals that are transformed from time domain to frequency domain. When a mechanical equipment has a fault, there will be corresponding frequency components presented in the vibration signals. Then the frequency-domain analysis has the advantage over time-domain analysis because it can easily identify and isolate certain frequency components [2]. The spectrum analysis based on fast Fourier transform (FFT) is one of the most widely used methods. The principle of spectrum analysis is to obtain the signal's frequency components and look at certain interesting frequency components to find its relationship with the amplitude, the phase or the power. And then the fault features can be extracted from the signals. The spectrum analysis mainly includes amplitude spectrum, power spectrum, Cepstrum, Hilbert spectrum, etc. However, when a gear or bearing has a fault, the vibration signal will become non-stationary and non-linearity, the spectral composition of the vibration signal will often change with time, which means that only using Fourier analysis cannot reflect such characteristics [3].

(3) Time-frequency analysis

Due to the characteristics of non-stationary vibration signal, time-frequency analysis has been investigated to analyze it in both time and frequency domain simultaneously. Traditional time–frequency analysis applied some time-frequency distributions to present a signal and show its energy distribution over the time-frequency space [4]. A time-frequency distribution is a time-frequency description of the signal [2]. The popular frequency distributions include short-time Fourier transform (STFT), Wigner-Ville distribution, Choi-Williams distribution, etc. Because

STFT only uses one window function each time, it can't take into account the need for frequency resolution and time resolution at the same time. Wigner-Ville distribution and Choi-Williams distribution belong to the Cohen class of distribution and have overcome the limitation of STFT's time-frequency resolution. But when applying them to multi-component signals, there will be interference terms caused by the transforms of Cohen class. These interference terms clutter the time-frequency plane, and make the results difficult to interpret [3, 5]. Choi-Williams distribution is insensitive to the scaling of the signal components and can provide the maximum resolution larger than the smoothed Wigner distribution, but it has poor resolution of continuously time-varying frequency components [6].

Wavelet transform is an adaptive method used for time-frequency analysis. Compared with the time-frequency distribution, it is a time-scale description of the signal. It has inherited and developed the idea of localization from STFT but overcome the disadvantage of STFT where the shape of sliding window can't change with the change of the frequency. Hence, it has the characteristic called multi-resolution or multi-scale, which means it can achieve high frequency resolutions with low time resolutions at low frequencies and high time resolutions with low frequency resolutions at high frequencies. It also works well in reducing noise in raw signals. Wavelet transform includes continuous wavelet transform (CWT) and discrete wavelet transform (DWT). Despite wavelet transform has achieved good results in fault diagnostics of rotating machinery, such as gears and bearings, it still has some issues need to be studied and improved. When applying wavelet transform method, energy leakage will occur due to the limited length of the basic wavelet function, which sometimes makes it difficult to do the accurate quantitative analysis of the frequency-time distribution. Another problem is that there

is not a general rule for selecting an optimal mother wavelet for wavelet transform, and so people usually have to propose specific rules for each specific case based on the past experience and the test results. It should also be pointed out that once the mother wavelet is selected, it will be used in the entire process.

The Hilbert-Huang Transform (HHT) was proposed by Norden E. Huang in 1998. Even though it is an empirical method without a rigorous mathematical proof, it has achieved great success in engineering areas. Through a time adaptive operation named empirical mode decomposition (EMD), a complicated signal can be decomposed into a finite and small number of intrinsic mode function (IMF). Then an energy-time-frequency distribution of the signal called as Hilbert-Huang spectrum can be obtained by applying Hilbert transform to these IMF components [7]. It can deal with the signal with larger size than wavelet transform because of the EMD step, which isn't involved with the convolution or other time resolution [8]. The frequency components contained in each IMFs will change with the signal itself. There will be no energy leakage during the Hilbert-transform. With these natures of adaptability, HHT can deal with not only linear and stationary signals but also nonlinear and non-stationary signals. However, some problems have been found at the step of EMD in some practical applications. The EMD operation sometimes is insensitive to the low-energy components of the signal, and therefore these components may be masked in the time-frequency plane. At the low-frequency region, sometimes it will generate some undesired low amplitude and frequency components. At the high-frequency region, the first IMF may cover a wide frequency range so that it cannot satisfy the definition of mono-component very well [8].

1.2 Research Motivation

There are many theories and techniques have been proposed for fault diagnosis of gears and bearings. The traditional methods, such as time-domain analysis and frequency-domain analysis, are applied in fault diagnosis based on the assumption that the vibration signal is linear and stationary. However, when a faulty gear or bearing running, the fault will generate a series of periodic impulses, which is a very important evidence to identify the existence of the fault. The vibration signal collected from the mechanical equipment will become non-stationary and its components will change with time. Hence, the time-frequency analysis, such as the methods based on wavelet transform and HHT, have been investigated in fault diagnosis of gears and bearings. Wavelet transform includes CWT and DWT.

Because of the promises of time-frequency analysis methods, research was reported to compare the performance of these methods in fault diagnosis of mechanical components. However, the previous studies either only compare HHT based methods with CWT based methods, or only compare HHT based methods with DWT based methods, for certain applications [8-12]. There are no reported studies on comprehensive comparisons of the three methods for fault diagnosis of gears and bearings.

Some existing methods first applied DWT to decompose the original signal to obtain the detail signals, and then used Hilbert spectral analysis to analyze the periodic impulses contained in the detail signals through identifying faulty characteristic frequency with frequency domain analysis and drawing the instantaneous amplitude with time domain analysis. Hilbert spectral

analysis has shown its advantage in the frequency domain analysis. However, sometimes it is not very sensitive in time domain analysis when the energy of the periodic impulses is weak.

Sometimes the faulty characteristic frequency contained in the vibration signals is masked by the noise or other components if the energy is too weak. Cepstrum analysis can detect the periodicity and reduce the influence of the noise for the low energy signal. However, the previous research usually directly applied cepstrum analysis to analyze the entire original signal.

1.3 Research Contribution

In this thesis, we use two sets of vibration monitoring data collected in the lab environment to investigate fault diagnosis of gears and bearings. One set is for gear condition monitoring and the other is for the bearing condition monitoring. We propose an improved DWT method that integrates Cepstrum analysis to analyze the periodic impulses contained in the data. The results show that the proposed method performs better than the existing methods of applying Cepstrum analysis directly. Moreover, with the help of Cepstrum analysis, the proposed method has better performance in time domain analysis than Hilbert spectral analysis in analyzing the periodic impulses contained in the detail signals.

We conduct a comprehensive study to compare the following three methods in fault diagnosis of the gears and bearings: (1) The CWT method using time-wavelet energy spectrum, (2) the improved DWT method using Cepstrum analysis, and (3) the HHT method. The results show that in fault diagnosis of gears, the HHT method has better noise immunity and is more sensitive in frequency domain analysis than the other two methods. The proposed method shows the advantage in analyzing the periodic impulses in time domain than the other two

methods. In fault diagnosis of the bearings, the fault can be more clearly detected using the CWT and DWT methods in analyzing the periodic impulses that caused by the outer race fault of the bearing.

1.4 Thesis Organization

The rest of this thesis is organized as follows:

In Chapter 2, we conduct a detailed literature review of fault diagnosis.

In Chapter 3, we introduce the basic principles of fault diagnosis of the gearbox and the bearing. Then we present the proposed methods for fault diagnosis of the gearbox and bearing.

In Chapter 4 and 5, we apply the proposed methods to fault diagnosis of the gearbox and bearing and compare their advantages and disadvantages.

Finally, we draw conclusions from our research and present several directions of future work in Chapter 6.

Chapter 2

2. Literature review on fault diagnosis of rotating components

Diagnostics and prognostics are two important parts of Condition-based maintenance, which is an advanced maintenance strategy for performing maintenance activities based on the information collected from the age data and condition monitoring. The tasks of diagnostics is to detect and identify the fault when it occurs. Fault detection is to indicate whether there is something wrong with the system. Fault identification is to find out which component has fault [2]. The method of vibration signal analysis has been applied in fault diagnostics of the mechanical equipment for a long time. Numerous techniques and algorithms of signal processing have been presented in order to detect and diagnose the impending or existing faults in rotating machinery. These methods are mainly in three categories: time-domain analysis, frequency-domain and time-frequency analysis, which will be reviewed respectively in the following parts.

2.1 Time domain analysis

The basic time domain indicators include root mean square (RMS), peak, crest factor, skewness, kurtosis value, shock pulse measurement, etc. Tandon [13] has made a comparative study of detecting the bearing defects among RMS, peak, crest factor and shock pulse measurement. Vecer [14] has compared 13 indicators' capacity of in detecting the fault of gearbox and the

results indicates that RMS and peak can track the condition of the tested gearbox very well. But both of them only show whether there is a fault but can't indicate the fault's location. Time synchronous average (TSA) is also one of the most powerful algorithm in time domain analysis for vibration signal analysis. Bechhoefer [15] made a review of time synchronous average (TSA) and applied it with the indicators above to detect the gearbox's fault. However, its experimental process are too complicated and the results are not intuitive enough. Dalpiaz [16] compared the approaches based on time-frequency analysis with TSA analysis in gearbox fault diagnosis. It demonstrated that the results are better than those obtained by TSA. It should be noted that the effectiveness and the sensitivity of TSA are effected by choosing the filtering band and the transducer location. Another drawback of TSA is that it has to repeat the TSA analysis of each gear to obtain a complete gearbox diagnosis. In general, time domain analysis of the vibration signal is not enough for fault diagnosis of the rotating machinery.

2.2 Frequency domain analysis

Fourier transform has built a bridge between the time domain and the frequency domain to extract the characteristic frequency from the vibration signal. For a given integral function $f(t)$, its Fourier transform $\mathrm{F}(w)$ is given as follows [17]:

$$\mathrm{F}(w) = \int_{-\infty}^{+\infty} f(t) e^{-jwt} dt \tag{1}$$

where $w = 2\pi f$ and $j = \sqrt{-1}$

Many methods of conventional frequency analysis are based on Fourier transform, which has three basic assumptions: linear, Gaussian and stationary. The general idea of Fourier analysis is

to treat the signal as a composition of sine or cosine signals in different frequencies and then use Fourier transform to get the amplitude spectrum. So the frequency corresponding to the larger amplitude (higher energy) can be found.

2.2.1 Fast Fourier transform

When the Fourier transform is discrete in time domain and frequency domain, it is called discrete Fourier transform. Fast Fourier transform (FFT) is an algorithm of the discrete Fourier transform to reduce the computational time. For a sequence of N complex numbers $\{x_0, x_2, ..., x_{N-1}\}$, its discrete Fourier transform $X(k)$ is defined as [18]:

$$X(k) = \sum_{n=0}^{N-1} x(n) e^{-j2\pi kn/N} \tag{2}$$

where $j = \sqrt{-1}$

For N points, FFT reduces the number of computations from $O(2N^2)$ to $O(N \log N)$, where *log* is the base-2 logarithm [19]. FFT is a powerful tools in frequency analysis and the foundation of many methods in frequency domain analysis. Betta [20] integrated FFT in a DSP (Digital Signal Process)-based architecture for the on-line monitoring and diagnosis of the rotating machine. FFT analysis may also work with time-frequency analysis to deal with non-stationary signal. Rai [21] shown the effectiveness of incorporating FFT with Hilbert-Huang transform in bearing fault diagnosis.

2.2.2 Power spectral density

Power spectral density (PSD) or power spectrum reflects the power distribution of a signal's frequency components. It can reveal the useful information of a signal such as the implied periodicity. When there is a failure of a mechanical equipment, obvious peaks will appear near the certain frequencies. Hence, the peak position corresponds to the frequency can be easily found in the PSD. After comparing with the characteristic frequency of the equipment, the type of the fault can be identified. It can be singly used to detect and diagnosis the fault of some simple rotating machinery, such as electromotor, bearing of pump and Massey Ferguson gearbox [22-24]. In general, it is often used in the fault detection and diagnosis of mechanical equipment incorporating other signal processing methods, such as wavelet decomposition [25] and mode decomposition (EMD) [26].

2.2.3 Cepstrum analysis

There are several definitions of the Cepstrum. The most common one is to take the inverse Fourier transform (IFT) of the logarithm of the signal's power spectrum [27]. It converts the complex convolution to a simple linear superposition so that it will be more easily to identify the feature of the signal. For a time-domain signal $f(t)$, the Cepstrum $C(\tau)$ is defined as [28]:

$$C(\tau) = | F^{-1}\{\log(| F\{f(t)\} |^2)\} |^2 \tag{3}$$

where F and F^{-1} is Fourier transform and inverse Fourier transform, respectively, and τ represents the time parameter of Cepstrum.

There are mainly two categories of Cepstrum analysis: real Cepstrum and complex Cepstrum. Complex Cepstrum analysis has preserved the total information of the signal while real Cepstrum analysis only preserves the amplitude information without the phase information. The real Cepstrum is usually applied in the engineering field.

When a rotating machinery is running with a fault, there will be a series of sidebands generated around the carrier frequency in the power spectrum. Hence, it will be more difficult to identify the fault because the spectrum becomes more complex. Furthermore, sometimes the components of the faulty frequency are covered by the noise. Cepstrum analysis can reduce the noise's influence for a low energy signal and separate the sidebands. Hence, it performs better than other spectra in identifying the frequency. It can also detect the components of the periodic components contained in vibration signal. There will be wave's crests the corresponding to the faulty information in the Cepstrum, therefore it can be easily extracted the concerning frequency components from the vibration signal and identified them for fault diagnosis. However, Cepstrum analysis has a deficiency that it is not stable around the very low frequency and sometimes generates many undesired large peaks near the zero point. Hence, the boundary of the Cepstrum are usually ignored.

Cepstrum is a popular method widely applied in fault diagnosis of rotating machinery. Van der Merwe [29] proposed a modified Cepstrum: linear& threds holded Cepstrum in bearing detection. Bajric [30] compared the effectiveness of some popular vibration analysis techniques for damage identification in gear pairs and pointed out that Cepstrum analysis could identify the fault earlier because it is clear and easier to see the changes of the frequency. Due to the advantage of Cepstrum, it has shown its own advantage in identifying the fault part from the

different types of the mechanical equipment [34-38]. When applied in fault diagnosis of the gearbox, Cepstrum analysis can locate the shaft on which there is a faulty gear. But if there are more than one gear on it, it can't identify which gear has a fault. Moreover, the research above only apply Cepstrum to analyze the entire original signal, which can't take the advantage of the Cepstrum completely.

2.2.4 Hilbert transform and spectrum analysis

When the mechanical equipment running with a fault, such as tooth fracture of the gearbox and fatigue spalling of the rolling bearing, it will generate a periodic pulse impact. Hence, the collected vibration signal will contain the amplitude and phase modulation caused by the fault. Then we can demodulate the signal to extract the fault information from the signal. There are many demodulation methods has been presented for fault diagnosis such as wideband demodulation [36] and resonance demodulation [37]. The Hilbert demodulation is one of the most popular techniques. The fundamental of Hilbert demodulation is Hilbert Transform. A real signal can be transformed by Hilbert Transform to a complex-valued form of the signal that called 'analytic signal', which can simplify results and methods in some cases [38]. For any giving time-domain signal $f(t)$, its Hilbert transform $H[f(t)]$ is [38]:

$$H[f(t)] = \widehat{f}(t) = \frac{1}{\pi}\int_{-\infty}^{+\infty}\frac{f(\tau)}{t-\tau}d\tau \tag{4}$$

where t is the time parameter and τ is translation parameter.

In order to accomplish the demodulation, the analytic signal $A[f(t)]$ of $f(t)$ is defined as:

$$A[f(t)] = f(t) + i\widehat{f}(t) = a(t)e^{j\varphi(t)} \tag{5}$$

where $j = \sqrt{-1}$,

$$a(t) = \sqrt{f^2(t) + \widehat{f}^2(t)} \tag{6}$$

$a(t)$ is the Hilbert envelope signal of $f(t)$. The instantaneous amplitude of the signal can also be obtained by plotting $a(t)$ in time area, which can reflect the periodic impulses if it is contained in the signal.

$$\varphi(t) = \arctan\left[\frac{\widehat{f}(t)}{f(t)}\right] \tag{7}$$

$\varphi(t)$ is the instantaneous phase of the analytic signal $A[f(t)]$.

Hence, the instantaneous frequency f_{ins} of the analytic signal $A[f(t)]$ can be obtained from the instantaneous phase:

$$f_{ins} = \frac{1}{2\pi}[d\varphi(t)/dt] \tag{8}$$

The vibration signal is usually collected by the accelerometers installed on the faulty machinery. Because the amplitude value of collected signal is in proportion to the square of the frequency, the modulation signal is almost invisible in the low frequency and the peak values are crowded with sidebands in the high frequency [39]. Hence, it is difficult to diagnose the fault by the amplitude spectrum. However, after applying the Hilbert modulation and envelope spectrum analysis, the fault information contained in the modulating components can be easily identified.

Different from Fourier transform, which converts a signal from the time domain to the frequency domain, Hilbert transform is a time-domain convolution that does not change the domain of the variable [40]. It is also a frequency-independent 90^{o} phase shifter, so it will not affect the non-stationary characteristics of modulating signals [1]. Due to the characteristics of the Hilbert transform, it has been wildly used in many areas, for example, estimating the correlative functions of a stationary random signal. However, the vibration signal of the gearbox is non-stationary, then Hilbert transform can't show how the signal change with time. Hence, Hilbert transform usually integrates with the other methods, for example Wavelet transform [1, 41-44], in fault diagnosis of the rotating machinery. The Hilbert transform based on EMD, which is also called Hilbert-Huang transform, is one of the most popular methods. It can analyze not only the linear-stationary signal but also the non-linear and non-stationary signal. We will present it in detail in the following chapters.

2.3 Time-frequency analysis

Fourier analysis and the other frequency analysis methods derived from it have established an ideal model of linear transformation and it is a steady state conversion. Therefore, they are suitable for dealing with linear and stable signal, and performing global analysis to the signal. However, when a mechanical equipment has a fault, the vibration signal usually becomes non-stationary. The key to process non-stationary signal is the local time-frequency analysis. In practical applications, it has been found that Fourier analysis is difficult to process the nonlinear and non-stationary signal. Hence, time-frequency analysis has been developed for the non-stationary vibration signal.

2.3.1 Short-time Fourier transform

Short-time Fourier transform is a basic time-frequency analysis that comes from the Fourier transform. It uses a window function to slide on the non-stationary vibration signal and then divide it into several equal length segments. The inside signal of the segments is supposed to be stationary. After that Fourier transform is applied in each segment to find out the frequencies contained in that segment. Hence, the signal will be represented by two elements of: time and frequency [45]. For a signal $x(t)$, its short-time Fourier transform is defined as follows [6]:

$$STFT_x(t,w) = \int_{-\infty}^{+\infty} x(\tau) w(\tau - t) e^{-jw\tau} d\tau \tag{9}$$

where $j = \sqrt{-1}$, $w(\tau - t)$ is the window function such as such as rectangular, triangular, Hamming, etc., and τ is the variable that slides the window across the signal $x(t)$.

Once the window function is chosen, the time and frequency resolution are fixed. So there is a trade-off to choose a proper window function between the time resolution and the frequency resolution: a longer window will lead to a higher frequency resolution with a lower time frequency and vice versa. This is referred to the Heisenberg uncertainty principle: The resolution in time and frequency cannot be arbitrarily small, once a window function has been selected, the signal can be analyzed with either good time resolution or good frequency resolution [46].

STFT has been widely used in the machinery diagnosis, such as wind turbine blade [47]. Cocconcelli [48] presented a new procedure based on STFT for bearing fault detection in a varying speed motor while many previous experiments are based on a stable speed motor.

Many studies have also been done to compare STFT with other signal processing techniques. Kemal [49] compared STFT and wavelet transform in electroencephalography signals to determine epileptic seizure activity. It was found that STFT took the shortest processing time that was applied for online diagnostics while wavelet transform had a high performance for visualization in recognizing the signal. Long [50] compared STFT and HHT in fault diagnosis of rolling bearings and indicated that if STFT has a good time-frequency identification rate and it can extract the fault features from signal well, while HHT is a good method for adaptive signal processing and is very suitable for nonlinear and non-stationary signal analysis.

2.3.2 Wigner-Ville distribution

The Wigner-Ville distribution (WVD) plays an important role in the time-frequency signal analysis as it has overcome the limit of STFT and provided a high-resolution in both time and frequency for non-stationary signals. The total energy of the signal is analyzed by instantaneous power in time domain and energy spectrum in frequency domain [51]. In the time domain, Wigner-Ville distribution is defined as [52]:

$$Wx(t,w) = \int_{-\infty}^{+\infty} x(t+\frac{\tau}{2})x^*(t-\frac{\tau}{2})e^{-jw\tau}d\tau \tag{10}$$

where t is the time domain variable, w is the frequency domain variable, $x(t)$ is restricted to a complex continuous time analytic signal and its Fourier transform is $X(f)$, $x^*(t)$ is the complex conjugate of $x(t)$, and $j = \sqrt{-1}$.

WVD is an effective method for non-stationary signal in time-frequency analysis and has been widely used in fault diagnosis of machinery [53, 54]. However, there are several disadvantages

in directly applying the Wigner-Ville distribution because of its inherent nature. It will cause the interference of the cross terms while analyzing a multicomponent signal. The interferences of the cross terms may have significant amplitude which can corrupt the transform space [55]. In practice, the vibration signal collected from the gearbox is the multicomponent signal. It usually contains the mesh frequencies and their harmonics, and occasionally some components called ghost components. The interferences among these strong components, between these strong components or the other low level parts of the signal such as the modulation sidebands, may produce complicated results which is difficult to be interpreted [56]. Choy [52] made a comparison between WVD and Wavelet transform in the damage identification of a gear transmission. The results has shown that the wavelet transform method can provide a more direct quantification than using WVD. In order to take its advantage, WVD has been combined with some methods such as wavelet transform [57] and EMD [58] for fault diagnosis of the rotating machinery.

2.3.3 Wavelet Transform

There are mainly two categories of the time-frequency analysis: One is the quadratic method that covers the time-frequency distributions, such as STFT and WVD that we have presented above. The other is the linear approach including the Gabor transform, the Zak transform and the wavelet transform analysis [51]. Wavelet was first introduced by Morlet and then became a powerful mathematical tool. For N points, the computations of wavelet transform is $O(N)$, which is smaller than that of FFT that is $O(N \log N)$.

Wavelet transform is an adaptive transform that has overcome the resolution problem of STFT. It has the basic properties such as linearity, translation, dilation, symmetry, etc. Due to its properties, it is suitable for making multi-scale analysis for a non-stationary signal in both time domain (through translation) and frequency domain (through dilation) [51]. Both continuous wavelet transform and discrete wavelet transform have been widely used in fault diagnosis of the machinery.

2.3.3.1 Continuous wavelet transform (CWT)

Suppose a function $\psi(t) \in L^2(R)$ where $L^2(R)$ represents a real space that the square can be integration, which means signal space's energy is limited. Its Fourier transform $\widehat{\psi}(w)$ is [51]:

$$\widehat{\psi}(w) = \int_{-\infty}^{+\infty} (\psi)(t) e^{-jwt} dt \tag{11}$$

If $\widehat{\psi}(w)$ satisfies the admissibility condition:

$$C_\psi = \int_{-\infty}^{+\infty} \frac{|\widehat{\psi}(w)|^2}{|w|} dw < \infty \tag{12}$$

Then $\psi(t)$ is called mother wavelet.

As the wavelets is a family of functions constructed from translation and dilation of the mother wavelet $\psi(t)$, then the wavelets $\psi_{a,b}(t)$ is defined by [51]:

$$\psi_{a,b}(t) = \frac{1}{\sqrt{a}} \psi(\frac{t-b}{a}) \tag{13}$$

where $a \in R, a \neq 0$ is called a scaling (dilation) parameter that measures the degree of scale,

$b \in R$ is a translation (location) parameter which determines the time location of the wavelet, and $\frac{1}{\sqrt{a}}$ is used to ensure energy preservation.

The typical continuous wavelets include Meyer wavelet, Mexican hat wavelet, Morlet wavelet, etc. For a given signal of limited energy $f(t)$, its continuous wavelet transform is defined as [51]:

$$W_f(a,b) = \int_{-\infty}^{+\infty} f(t) \frac{1}{\sqrt{a}} \psi^*(\frac{t-b}{a}) dt \tag{14}$$

where $\psi^*(t)$ is the complex conjugate function of $\psi(t)$, $a \in R, a \neq 0$ is called a scaling parameter and $b \in R$ is a translation parameter.

Compared with the kernel e^{-jwt} in the Fourier transform in Eq. (1), it can be found that kernel $\psi_{a,b}(t)$ in Eq. (14) plays the same role. Hence, continuous wavelet transform is linear like Fourier transform. However, it is the transform based on any wavelets $\psi_{a,b}(t)$ which is different from Fourier transform which is only based on e^{-jwt} [51].

Similar to the window function $w(\tau - t)$ in Eq. (9) for STFT, $\psi_{a,b}(t)$ looks like a time-frequency window function to 'observe' a signal. However, the shape of it is not fixed and will change with the parameters a and b. For a fixed parameter b, when the parameter a increases, the length of the frequency window will become wider while the length of time window will become narrower. The comparison of them are shown in figure 1. We can find the area and the shape of STFT is fixed during the whole transform while only the area of wavelet transform is fixed but the shape will change the time and frequency. Wavelet transform uses wide time window and

narrow frequency window at low frequencies to get high frequency resolutions while using narrow time window and wide frequency at high frequencies to get high time resolutions. That's why wavelet transform is called adaptive.

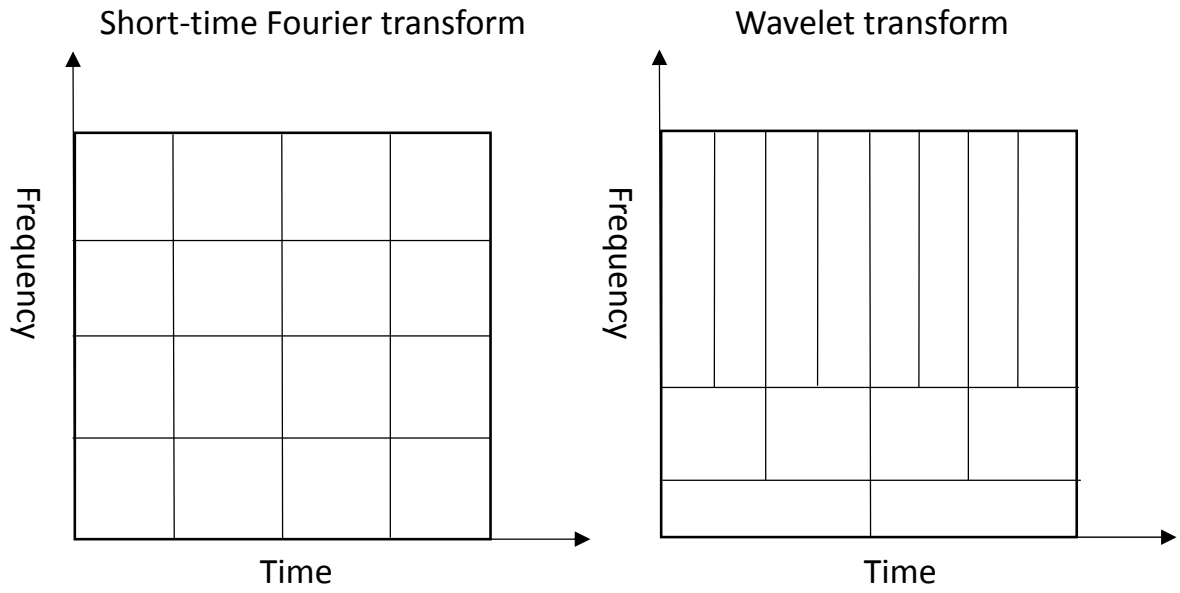

Figure 1 Comparison of the window function between STFT and wavelet transform [59]

Continuous wavelet transform has been successfully applied many areas. Vikhe [60] presented that CWT performed better than STFT in the detection of the abnormal heart sound. It also widely used in fault diagnosis of the rotating machinery. Lin [61] used Morlet wavelet transform for ball bearing diagnosis from the machine sound. Baydar [62] applied Gabor-based wavelet to detect the gear failures from both vibration signal and acoustic signal. Some improved methods that combines with other methods have also been introduced: Zheng [63] presented the time-

averaged wavelet spectrum based on Morlet continuous wavelet transform for gear fault diagnosis. Rubini [64] applied the envelope spectrum analysis in Morlet transform to diagnose the early faults in ball bearing. Elbarghathi [65] proposed a method that using time synchronous average (TSA) to remove the noise and then applying continuous wavelet transformation for fault detection and diagnosis of the gearbox.

2.3.3.2 Discrete wavelet transform (DWT)

In many applications of the signal processing, it needs to consider the discrete expression of the continuous wavelet transform because the data are in the form of a finite number of values. In order to get discrete wavelet transform, the two parameters a and b of CWT in Eq. (14) should be converted into a discrete one that a and b only take integral values as follows [66]:

- The discretization of the scaling parameter a

  Normally it takes $a = a_0^j$ where j is an integer and $a_0 > 1$.Then the corresponding wavelet is:

$$\frac{1}{\sqrt{a_0^j}}\psi(\frac{t-b}{a_0^j}) = a_0^{-j/2}\psi(a_0^{-j}(t-b)) \tag{15}$$

- The discretization of the translation parameter b

  For $j = 0$, in order to discretize b, it only takes the integer (positive and negative) multiples of one fixed b_0 (arbitrarily fix $b_0 > 0$) where b_0 is appropriately chosen so that the $\psi(x - nb_0)$ can 'cover' the whole time axis and the signal information won't lose.

  For different values of j, because the width of $a_0^{-j/2}\psi(a_0^{-j}(t-b))$ is a_0^j times the width of $\psi(\mathrm{t})$, so that the sampling interval can be expanded a_0^j times without losing the signal

information, then the choice $b = nb_0 a_0^j$ will make sure the discretized wavelets at the level m can 'cover' the whole time axis and preserve the whole signal information.

Hence, the discretized expression of the parameters a and b is:

$$a = a_0^j \ , \ b = nb_0 a_0^j \tag{16}$$

where j and n are integers and $a_0 > 1$, $b_0 > 0$.

Then the wavelet $\psi_{j,n}(t)$ after discretizing without losing information can be presented as follows:

$$\psi_{j,n}(t) = a_0^{-j/2} \psi \left(\frac{(t - nb_0 a_0^j)}{a_0^j} \right) = a_0^{-j/2} \psi (a_0^{-j} t - nb_0) \tag{16}$$

We can transfer value nb_0 to the integer k by adjusting time axis, then the modified discrete wavelet function $\psi_{j,k}(t)$ can be expressed as:

$$\psi_{j,k}(t) = a_0^{-j/2} \psi (a_0^{-j} t - k) \tag{17}$$

For a given signal $f(t) \in L^2(R)$, its discrete wavelet transform can be defined as [66]:

$$(W_\psi f)(j,k) = \left\langle \psi_{j,k}(t), f(t) \right\rangle \int_{-\infty}^{+\infty} f(t) \psi_{j,k}^*(t) dt \tag{18}$$

where $\psi_{j,k}^*(t)$ is the complex conjugate function of $\psi_{j,k}(t)$.

It should note that discrete wavelet transform only discretizes the parameters a and b of the analysis wavelet $\psi_{a,b}(t)$ but doesn't convert the parameter t of the analysis wavelet $\psi_{a,b}(t)$ or the signal $f(t)$ into discretization. The typical discrete wavelets include Daubechies (DB) wavelets, Haar wavelets, Symmlet wavelets, etc.

Discrete wavelet transform has greatly reduced the redundancy of continuous wavelet transform and has been widely in the field of the signal and image processing. Like continuous wavelet transform, there are many applications in the field of fault diagnosis of rotating machinery. Lu [67] presented a method of based on the Daubechies-40 wavelets for fault diagnosis of induction motor rotor. Prabhakar [68] applied DWT to detect single and multiple faults in ball bearings. Su [69] and Liu [70] respective proved the effective of DWT in fault diagnosis of gearbox. There are also many improved methods based on DWT for fault diagnosis. For example, the method combining DWT and Hilbert Transform achieved success in the fault detection and diagnosis of the gears, bearings and rotor bar [43, 44, and 71]. In recent years, an idea that applying DWT for feature extraction and intelligent techniques for classification has been developed and many new methods has been proposed and applied in gearbox [72], bearing [73], and induction motors [74].

2.3.4 Hilbert-Huang Transform (HHT)

The above time-frequency analysis methods have been widely applied in many cases of fault diagnosis of the rotating machinery, however each method also have their own limitations. Hence, Hilbert-Huang transform is proposed as a new type of time-frequency analysis for

analyzing nonlinear and non-stationary signal. The HHT methods are mainly consisted by two parts: empirical mode decomposition (EMD) and Hilbert spectral analysis (HSA).

2.3.4.1 Empirical mode decomposition

The 'empirical mode decomposition' is the key process of HHT to deal with the non-stationary and nonlinear data. It has the largest computation complexity of the whole process. After EMD decomposition, the complicated signal can be presented as the sum of a finite and small number of 'intrinsic mode functions' (IMF). IMF is a function that satisfies the following functions [7]:

1. In the whole dataset, the number of extrema and the number of zero-crossings must either equal or differ at most by one.
2. At any point, the mean value of the envelope defined by the local maxima and the envelope defined by the local minima is zero.

An IMF represents a simple oscillatory mode as a counterpart to the simple harmonic function, but it is much more general: the IMF can have a variable amplitude and frequency as functions of time while a simple harmonic component only has constant amplitude and frequency [75]. The EMD is a sifting process that decomposes the signal into IMF components. The decomposition is based on the following assumptions [7]:

1. The signal has at least two extrema: one maximum and one minimum.
2. The characteristic time scale is defined by the time lapse between the extrema.

3. If the data were totally devoid of extrema but contained only inflection points, then it can be differentiated one or more times to reveal the extrema. Final results can be obtained by integrations of the components.

For a given signal $x(t)$, the procedures of its empirical mode decomposition is given in the following steps [7]:

1. Identify all the local extrema from the signal $x(t)$, then connect all the local maxima by a cubic spline line as the upper envelope.
2. Repeat the procedure for the local minima to produce the lower envelope. The upper and lower envelopes should cover all the data between them.
3. Compute the mean of the upper and lower envelopes designated as m_1, and the difference between the signal $x(t)$ and m_1 is the first component h_1:

$$h_1 = x(t) - m_1 \tag{19}$$

Ideally, h_1 should satisfy the definition of an IMF because the construction of h_1 describes above should have made it satisfy the requirements of IMF. However, there common exist overshoots and undershoots in reality, which will also generate new extrema and shift or exaggerate the existing ones. Even if the fitting is perfect, a gentle hump on a slope can be amplified to become a local extrema which will change the local zero from a rectangular to a curvilinear coordinate system. After the first round of sifting, the hump may become a local maximum.

4. In order to eliminate riding waves and making the wave's profiles more symmetric, the sifting process of Eq. (19) will repeat many times to reduce the extracted signal to an IMF.

   Repeat the steps 1-3 by treating h_1 as the signal in the subsequent sifting processes,

$$h_{11} = h_1 - m_{11} \tag{20}$$

   After repeating siftings up to k times until h_{1k} becomes an IMF, that is

$$h_{1k} = h_{1(k-1)} - m_{1k} \tag{21}$$

   Then the first IMF of the signal designated as c_1 has been obtained:

$$c_1 = h_{1k} \tag{22}$$

   There is a criterion to stop the sifting process accomplished by calculating of the normalized squared difference SD between two successive sifting operations:

$$SD = \sum_{t=0}^{T} \left[\frac{|h_{k-1}(t) - h_k(t)|^2}{h_{k-1}^2(t)} \right] \tag{23}$$

   If SD is smaller than a predetermined value which is between 0.2 and 0.3, the sifting process will stop. Overall, the first IMF c_1 should contain the finest scale or the shortest period component of the signal.

5. Remove the first IMF c_1 the signal and get the residue of the signal r_1

$$r_1 = x(t) - c_1 \tag{24}$$

   The residue r_1 still contain longer period variations than the previous component.

6. Treat r_1 as a new signal and repeat steps 1-4 to obtain the second IMF c_2.

7. Repeat steps 1-5 to obtain the series of IMFs c_i ($i = 1, 2, ..., n$) and the final residue r_n until the sifting process satisfies any of the following predetermined criteria: either when the component c_n or the residue becomes so small that is less than the predetermined value of substantial consequence, or when the residue r_n becomes a monotonic function from which no more IMFs can be extracted.
8. Sum up all the IMFs and the final residue, we can reconstruct the original signal $x(t)$:

$$x(t) = \sum_{i=1}^{n} c_i + r_n \tag{25}$$

Hence, the decomposition of the signal has been completed and the residue r_n can be either the mean trend or a constant.

2.3.4.2 Hilbert spectral analysis

After obtaining all the IMFs, Hilbert transform is applied to each IMF component and calculate the instantaneous frequency based on Eq. (4)-(8). Then the original signal $x(t)$ can be expressed as [7]:

$$x(t) = \mathrm{Re}\left\{ \sum_{i=1}^{n} a_i(t) \exp\left(j \int w_i(t) dt \right) \right\} \tag{26}$$

where $a_i(t)$ is the Hilbert envelope signal of each IMF, $\mathrm{Re}\{.\}$ represents the real part of a complex quantity and $j = \sqrt{-1}$.

The residue r_n has been left out because it is either a monotonic function or a constant. Eq. (26) can represent the instantaneous amplitude, frequency and time of the signal $x(t)$ in a three-

dimensional plot, where the amplitude can be drawn on the frequency-time plane. This frequency-time distribution of the amplitude is called as Hilbert spectrum $H(w,t)$. Then a measure of the total amplitude (or energy) contribution from each frequency value called Hilbert marginal spectrum $h(w)$ can be defined as:

$$h(w) = \int_0^T H(w,t)dt \tag{27}$$

Hilbert marginal spectrum represents the accumulated amplitude over the entire signal span in a probabilistic sense.

Hilbert-Huang transformation has been proved as an effective method that can extract the features from nonlinear and non-stationary signal. It has been applied to numerous scientific investigations, such as structural safety [75], geophysics [76], and nuclear physics [77]. HHT has also been done in fault diagnosis of the rotating machinery, such as bearings [78-80] and gearbox [81-83]. Some expanding research base on HHT also has been presented. Cheng [84] introduced a concept of local Hilbert energy spectrum and combined it with frequency family separation based on EMD in the gear fault diagnosis. Su [85] presented a new singular value decomposition method based on Hilbert-Huang transform in gears fault identification and classification, which has overcome the problem of reconstructing a feature matrix of singular value decomposition. Wang [86] proposed an integration method by applying continuous wavelet transform to detect the simulated sensor fault and diagnose it with HHT.

2.3.5 Comparative research in time-frequency analysis

As there are many techniques for time-frequency analysis, each one has its own advantage and disadvantage. Hence, it is necessary to make a comparison research among them. Douglas [6] made a resolution comparison of several time-frequency distributions of STFT, Wigner distribution, Choi-Williams distribution and other distributions. He concluded that there was not a distribution that can be considered as the best approach for all kinds of time-frequency analysis. Each distribution has its own advantage in some specify conditions. Peng [87] made a review of wavelet transform, STFT, Wigner-Ville distribution (WVD), Choi-Williams distribution and other techniques. These methods are compared in many areas of the machine fault diagnostics, such as time-frequency analysis of signals, fault feature extraction, singularity detection, etc. The results shows that wavelet transform has better performance in these areas. Lin [88] used an adaptive wavelet filter based on the Morlet wavelet and compared the result obtained by discrete wavelet transform in gearbox fault diagnosis. The results shows that the adaptive Morlet wavelet filter is more effective for capturing impulses.

Although wavelet transform and Hilbert-Huang transform are the most popular methods for analyzing nonlinear and non-stationary signals, they still have their own limitations. For example, although wavelet transform has the properties of analyzing nonlinear and non-stationary signals and is suitable for diagnosing the fault from the vibration-based machine, it still has some inevitable deficiencies including the interference terms, border distortion and energy leakage. The same situation also applied to HHT, who suffers the shortcomings caused by the EMD: First, the EMD will sometimes generate undesirable IMFs at the low-frequency region that may cause misinterpretation. Second, depending on the different analyzed signals,

the first obtained IMF may cover too wide a frequency range so that it cannot achieve the property of mono-component. Third, the EMD operation cannot separate signals that contain very low energy components [89]. Some research have been done to compare wavelet transform and Hilbert-Huang transform in fault diagnosis of rotating machinery. In the field of fault diagnosis of oil whirl, Yang [10] applied the methods of HHT and wavelet transform in rotating machinery. He summarized that the result of HHT is more sharp and clear than wavelet transform. Xiang [90] compared the analysis results of the oil whip signal by applying STFT, WVD, continuous wavelet transform and HHT. He concluded that HHT is more effective because it can detect components of low energy and displayed the distinct time-frequency distribution. Babu [91] applied HHT, FFT and CWT in the field of detection and monitoring of crack in a transient rotor. The results shown that HHT is more effective for extracting the salient features from time response of the cracked rotor because of the concept of HHT's instantaneous frequency. In the field of gearbox fault detection and diagnosis, Liu [92] investigated the results that obtained by continuous CWT and HHT. It is found that HHT is more effective than CWT because HHT can better enhance transients caused by the crack. However, after making a comparison between DWT and HHT in fault diagnosis of rotor bar in induction machines, Antonino-Daviu [9] concluded that HHT has a better representation of the left sideband harmonic up to the fundamental frequency but the patterns arising from it does not seem to be any clearer than those with the DWT approaches. Yan [11] made a comparative study of modal parameter identification based on Morlet wavelet and HHT. After comparing the results of the application in numerical simulation, impact test and ambient vibration test, the author concluded that the continuous wavelet transform and HHT have their own benefits for specific

types of vibration data, thus it is hard to say which one is superior to the other. The same conclusion also has been made by Quek [12], who applied continuous wavelet transform and HHT in the analysis of flexural wave propagation in an aluminum beam and the analysis of acoustic Lamb wave propagation in an aluminum plate.

According to the above research, we can find that many types of comparative studies have been done, such as CWT based methods versus DWT based methods, HHT based methods versus CWT based methods and HHT based methods versus DWT based methods. However, there are no reported comprehensive comparisons of the three methods for fault diagnosis of gears and bearings.

Chapter 3

3. The proposed method for fault diagnosis

In this chapter, we first analyze the signal characteristics collected from the gearbox and bearing. Then we present to the new improved DWT method which can improve the analytical capacity of periodic impulses in time domain. The CWT method using time-wavelet energy spectrum and the HHT method are also introduced in detail for the comprehensive study.

3.1 Signal analysis for gearboxes

For a healthy pair of gears, assuming that all teeth of the gears are identical and equally spaced and they are meshing under a constant load and speed, the vibration signal of the healthy gears $f(t)$ can be represented as follows [1]:

$$f(t) = \sum_{m=0}^{M} X_m \cos(2\pi m N f_s t + \phi_m) \tag{28}$$

where M is the number of tooth-meshing harmonics, X_m and ϕ_m are the amplitude and the phase of the M^{th} meshing harmonic, N is the number of the gear teeth, f_s is the shaft rotating frequency, then the meshing frequency is $N * f_s$, and t is time.

Eq. (28) indicates that the predominant frequency components of the signal collected from the healthy gears are the meshing frequency and its harmonics.

When a gear has a fault, it usually can be reflected in the vibration signals, which will contain the amplitude and phase modulations. Then the amplitude-modulating functions $a_m(t)$ and the phase-modulating functions $b_m(t)$ caused by a faulty gear tooth can be represented by [1]:

$$a_m(t) = \sum_{m=0}^{M'} A_{mn} \cos(2\pi n f_s t + \alpha_{mn}) \tag{29}$$

$$b_m(t) = \sum_{m=0}^{M'} B_{mn} \cos(2\pi n f_s t + \beta_{mn}) \tag{30}$$

where M' is the number of sidebands around tooth-meshing harmonics, A_{mn} and B_{mn} are respectively amplitudes at n^{th} sidebands of amplitude and phase-modulating signals around the m^{th} meshing harmonic, and α_{mn} and β_{mn} are respectively the phases at the n^{th} sidebands of amplitude and phase-modulating signals around the m^{th} meshing harmonic.

From Eq. (29) and Eq. (30), we can find that $a_m(t)$ and $b_m(t)$ are the periodic functions that are based on the shaft rotating frequency f_s and its frequency multiplication, which is accorded with the factual situation. Then the vibration signal $x(t)$ of a pair of meshing gears with a tooth fault can be represented by the combination of Eq. (28)-(30) as follows:

$$x(t) = \sum_{m=0}^{M} X_m \left(1 + a_m(t)\right) * \cos\left(2\pi m N f_s t + \phi_m + b_m(t)\right)$$

$$= \sum_{m=0}^{M} X_m \left(1 + \sum_{m=0}^{M'} A_{mn} \cos(2\pi n f_s t + \alpha_{mn})\right) * \cos\left(2\pi m N f_s t + \phi_m + \sum_{m=0}^{M'} B_{mn} \cos(2\pi n f_s t + \beta_{mn})\right) \tag{31}$$

Because the vibration signal from a gearbox is usually non-stationary, the frequency components of the signal will vary with time t. Thus Eq. (31) is modified to:

$$x(t)=\sum_{m=0}^{M}X_m\left(1+\sum_{m=0}^{M'}A_{mn}\cos(2\pi nf_s(t)t+\alpha_{mn})\right)*\cos\left(2\pi mNf_s(t)t+\phi_m+\sum_{m=0}^{M'}B_{mn}\cos(2\pi nf(t)_s t+\beta_{mn})\right) \quad (32)$$

According to Eq. (32), the additional frequency components $mNf_s(t)\pm nf_s(t)$ corresponding to the meshing frequency and the shaft rotating frequency, will appear in the spectrum of the signal. Hence, we can extract these important information from the vibration signal to detect and diagnose the gearbox fault.

Three diagnosis methods that are respectively based on CWT, DWT and HHT will be applied to extract fault features from the collected vibration signal. We will introduce and discuss them respectively in the following parts.

3.2 Calculation of the bearing's faulty characteristic frequency

When a bearing has a fault, it will usually occur in cage, inner race of the bearing, outer race fault of the bearing and the balls. The faulty characteristic frequency of them can be calculated as follows [93]:

$$\text{Cage Faulty Frequency}=\frac{f}{2}\left(1-\frac{d}{e}\times\cos(\beta)\right) \quad (33)$$

$$\text{Inner Race Faulty Frequency}=\frac{b\times f}{2}\left(1+\frac{d}{e}\times\cos(\beta)\right) \quad (34)$$

$$\text{Outer Race Faulty Frequency}=\frac{b\times f}{2}\left(1-\frac{d}{e}\times\cos(\beta)\right) \quad (35)$$

$$\text{Ball Faulty Frequency}=\frac{e\times f}{d}\left(1-\left(d/e\right)^2\times\cos^2(\beta)\right) \quad (36)$$

where f is the driving frequency, b is the number of rolling elements, d is the ball bearing diameter, e is the bearing pitch diameter and β is the bearing contact angle.

3.3 Methods based on Wavelet Transform

3.3.1 The CWT method using Time-wavelet energy spectrum

The time scale and its corresponding energy distribution are the two important indicators in the signal processing that can reflect the dominant components of the vibration. When there is a gear that has a local fault, the damage will generate periodic impulses. The impulses will cause the energy at that instant generate peaks. The sidebands will appear in the spectrum because of the modulation. Thus the energy spectrum will vary with the change of time and frequency that can reflect the dominant features of the vibration signal. Hence, it is possible to detect and diagnose the fault by extract these features from the vibration signal.

As mentioned before, for a given signal of limited energy $f(t)$, its continuous wavelet transform is defined as Eq. (14)

$$W_f(a,b) = \int_{-\infty}^{+\infty} f(t) \frac{1}{\sqrt{a}} \psi^*(\frac{t-b}{a}) dt \tag{14}$$

where $\psi^*(t)$ is the complex conjugate function of $\psi(t)$, $a \in R, a \neq 0$ is called the scaling parameter and $b \in R$ is the translation parameter.

Wavelet transform is isometric which means wavelet transform of $f(t)$ is energy conservation. We can obtain the following equation via Eq. (14) [94]:

$$\int_{-\infty}^{+\infty} |f(t)|^2 \, dt = \frac{1}{C_\psi} \int_{-\infty}^{+\infty} \int_{-\infty}^{+\infty} \frac{1}{a^2} |W_f(a,b)|^2 \, dadb \tag{37}$$

where $C_\psi = \int_{-\infty}^{+\infty} \frac{|\widehat{\psi}(w)|^2}{|w|} dw < \infty$ is the admissibility condition of the wavelet.

Because of the limitation of the Heisenberg Uncertainty Principle, $\frac{|W_f(a,b)|^2}{C_\psi a^2}$ can be taken as the energy density function in plane (a, b), which means it represents the energy in the space $(a \pm \Delta a, b \pm \Delta b)$. Hence, Eq. (37) can be expressed as follows:

$$\int_{-\infty}^{+\infty} |f(t)|^2 \, dt = \frac{1}{C_\psi} \int_{-\infty}^{+\infty} E(b) db \tag{38}$$

where $E(b) = \int_{-\infty}^{+\infty} \frac{1}{a^2} |W_f(a,b)|^2 \, da$ (39)

Eq. (39) is the integral of squared modulus of wavelet transform over scale [95]. It expresses the distribution of the signal's energies in time axis (the parameter b), and it is called the time-wavelet energy spectrum. It is an effective method in fault diagnosis of gears and bearings [93-95].

Morlet wavelet is one of the most popular wavelet used in signal processing, it is defined as [66]:

$$\psi(t) = \pi^{-\frac{1}{4}} (e^{-jw_0 t} - e^{-\frac{1}{2}w_0^2}) e^{-\frac{1}{2}t^2} \tag{40}$$

where $j = \sqrt{-1}$ and w_0 is the central frequency of the mother wavelet.

When $w_0 \geq 5$, the second exponential $e^{-\frac{1}{2}w_0^2}$ in Eq. (40) tends to be zero then it can be neglected in practice. Then Morlet wavelet can be modified to:

$$\psi(t) = \pi^{-\frac{1}{4}} \mathrm{e}^{-jw_0 t} \mathrm{e}^{-\frac{1}{2}t^2} \tag{41}$$

From Eq. (41), we can find it is a squared exponentially declining function that is very similar to an impulse vibration. Then it can be used to extract the impulse features from the signal of the faulty gear.

The steps of using this method are as follows:

1. Denoise the signal. We apply the approach of global threshold for wavelet denoising, which can well preserve the early characteristics of the signal.
2. Extract the fault features. We apply time-wavelet energy spectrum to analyze the denoising signal.
3. Identify the characteristics for fault diagnosis.

3.3.2 The proposed method based on DWT integrating Cepstrum analysis

We first introduce Mallet algorithm for DWT decomposition and reconstruction. Then we propose the new improved DWT method that can improve the capacity of analyzing the periodic impulse in time domain. The proposed method is based on DWT that integrates Cepstrum analysis. The results show that the proposed method performs better than the existing methods of applying Cepstrum analysis directly. Furthermore, with the help of Cepstrum analysis, the proposed method has better performance in time domain analysis than Hilbert spectral analysis in analyzing the periodic impulses contained in the detail signals.

3.3.2.1 Multi-resolution analysis and Mallet algorithm

Discrete wavelet transform is derived from continuous wavelet transform, where the scaling parameter a and translation parameter b are discretized. For a discrete wavelet $\psi_{j,k}(t) \in L^2(R)$, if the scaling and translation family $\left\{\psi_{j,k}(t) = 2^{-j/2}\psi(2^{-j}t - k)\right\}_{j,k \in Z^2}$ is an orthonormal basis of $L^2(R)$, then $\psi_{j,k}(t)$ is called as orthonormal wavelet [51]. Multi-resolution analysis (MRA) $\left(\{V_j\}_{j \in Z}, \phi(t)\right)$ is consisted by a sequence $\{V_j\}_{j \in Z}$ of closed subspaces of $L^2(R)$ and a function $\phi(t)$, which should satisfied the following properties [96]:

1. $\forall (j,k) \in Z^2, f(t) \in V_j \Leftrightarrow f(t - 2^j k) \in V_j$
2. $\forall j \in Z\ , V_{j+1} \in V_j$
3. $\forall f(t) \in V_j \Leftrightarrow f(\frac{t}{2}) \in V_{j+1}$
4. $\lim_{j \to +\infty} V_j = \bigcap_{j=-\infty}^{+\infty} V_j = \{0\}$
5. $\lim_{j \to -\infty} V_j = closure \bigcap_{j=-\infty}^{+\infty} V_j = L^2(R)$
6. $\phi(t) \in V_0$ and $\{\phi(t-k)\}_{k \in z}$ is the orthonormal basis of V_0, then $\phi(t)$ is called the scaling function of the multi-resolution.

The discrete wavelet function and the scaling function are defined as [96]:

$$\psi_{j,k}(t) = 2^{-j/2}\psi(2^{-j}t - k) \tag{42}$$

$$\phi_{j,k}(t) = 2^{-j/2}\psi(2^{-j}t - k) \tag{43}$$

DWT can analyze the signal at different frequency bands with different resolutions by decomposing it into the coarse approximation and the detail information. It applies the scaling function as low-pass filter and wavelet function as high-pass filter to decompose the signal. The high-pass filter $g(n)$ and low-pass filter $h(n)$ are defined as follows [96]:

$$g(n) = \left\langle \frac{1}{\sqrt{2}} \psi(\frac{t}{2}), \phi(t-n) \right\rangle = (-1)^{1-n} h(1-n) \tag{44}$$

$$h(n) = \frac{1}{\sqrt{2}} \left\langle \phi(\frac{t}{2}), \phi(t-n) \right\rangle \tag{45}$$

Based on Multi-resolution analysis and orthonormal wavelet, Mallat proposed a fast wavelet transform algorithm that decomposes a given signal $f(t) \in L^2(R)$ as follows [66]:

$$f(t) = \sum_{k \in z} c_k^j \phi_{j,k}(t) + \sum_{i=1}^{j} \sum_{k \in z} d_k^i \psi_{i,k}(t) \tag{46}$$

where $j \in Z^+$ is the number of decomposition level, $\phi_{j,k}(t)$ is the scaling function and $\psi_{i,k}(t)$ is the discrete wavelet, c_k^j and d_k^j is the scaling coefficient (approximation coefficient) and wavelet coefficient (detail coefficient) respectively.

The coefficients c_k^j and d_k^j can be obtained by:

$$c_k^0 = f_k(c_k^0) \tag{47}$$

$$c_k^j = \sum_n c_n^{j-1} \overline{h}_{n-2k} \tag{48}$$

$$d_k^j = \sum_n c_n^{j-1} \overline{g}_{n-2k} \tag{49}$$

where $j \in Z^+$ is the number of decomposition level, $k = 0,1,2...N-1$, N is the sample number, and f_k is the time-domain waveform of the original signal $f_k(c_k^0)$.

After the decomposition from level 1 to level j, the signal could get its approximation coefficient c_j and detail coefficients $d_1, d_2, ...d_j$. They contain the frequency band information of the signal from high frequency to low frequency with the time information of the signal. Therefore they are the time-frequency presentation of the signal. The decomposition procedure of the Mallat algorithm is shown in Figure 2:

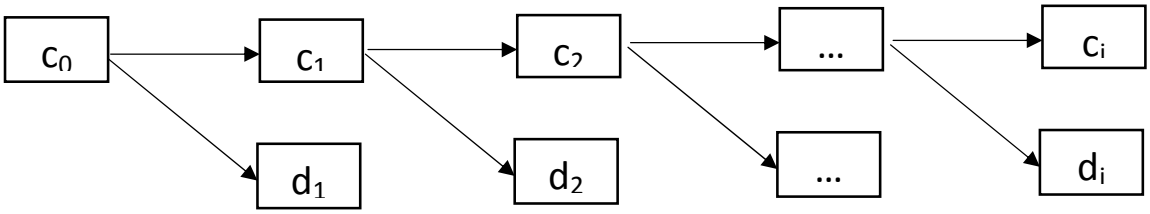

Figure 2 Decomposition procedure of the signal [96]

After the decomposition, the signal can also be reconstructed based on the following algorithm:

$$c_k^j = \sum_n c_n^{j+1} h_{k-2n} + \sum_n d_n^{j+1} g_{k-2n} \tag{50}$$

where $k = 0,1,2...N-1$, N is the sample number.

In fact, the algorithm of the reconstruction is the inverse processing of the decomposition shown in Figure 3:

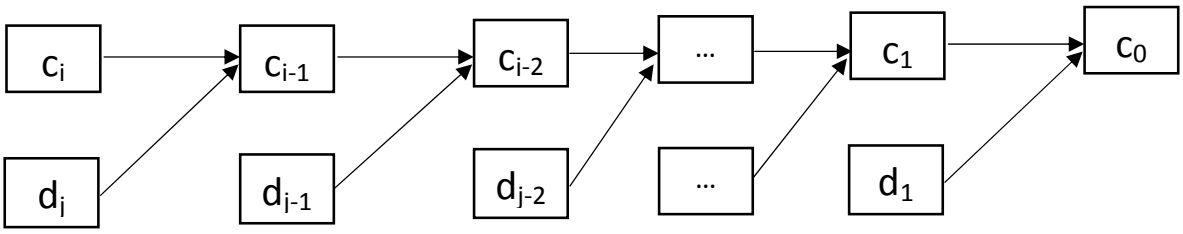

Figure 3 Reconstruction procedure of the signal [96]

In practice, the signals collected from the sampling system are usually discrete. It is the same idea to decompose the signal by passing it through a successive combinations of quadrature mirror filters: low-pass filters (scaling filter) $h(n)$ and high-pass filters (wavelet filter) $g(n)$, which is shown in Figure 4 [97]: the signal $X(n)$ is a discrete signal with 1024 sample points. Its bandwidth is $(0-\pi)$. The bandwidth of the signal at every level is marked on the figure as f, and $\downarrow 2$ means downsampling by 2. The filter groups at each level $h(n)$ and $g(n)$ are low-pass filter and high-pass filter respectively. The low-pass filter is used to smooth the signal and the high-pass filter is to obtain the difference in this detail. The signal is then decomposed into two parts by the filters at each level: high frequency part D_i ($i \in Z^+$) which is called as detail signal and low frequency A_i ($i \in Z^+$) which is called as approximation signal. And it continues to decompose the low frequency part A_i each time. Hence, the composition procedure can be presented as:

$$A_i = A_{i+1} + D_{i+1} \tag{51}$$

where $i \in Z^+$.

After the first decomposition level, the output of the $g(n)$: D_1 will have 512 sample points with the frequency band $(\pi / 2 \sim \pi)$. Then the time resolution is half of the previous one because there are only the half number of sample points to present the entire signal. However, the frequency resolution is doubled because the frequency band of the signal is the half of the previous one. Then the signal continues to pass the filters for further decomposition which will increase frequency resolution and decrease the time resolution [98].

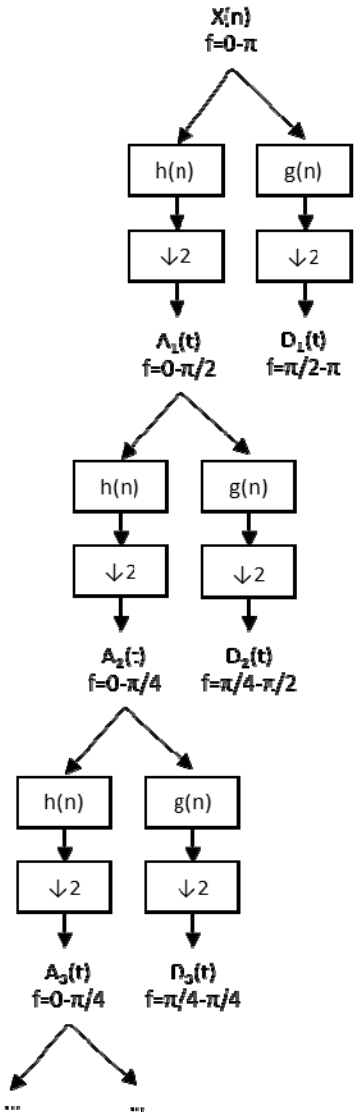

Figure 4 Decomposition of the discrete signal [97]

The reconstruction is also the inverse procedure of the decomposition and the $X(n)$ after reconstructing can be represented as:

$$X(n) = A_j + \sum_{i=1}^{j} D_{i+1} \tag{52}$$

where $j \in Z^+$ is the number of decomposition level.

The resolution of the signal, which is a measurement of the amount of detail information in the signal, is changed by the filtering operations, and the scale is changed by upsampling and downsampling operations [98].

Daubechies wavelet is a family of orthogonal wavelets that has been wildly used in fast wavelet transform. The scaling signals and wavelets have slightly longer support in the Daubechies wavelet transform. It usually used DBN to describe the Daubechies wavelet, where N is the vanishing moment. When the vanishing moment become higher, the wavelet will oscillate stronger [66]. The wavelet with a higher vanishing moment is more welcomed in practice.

3.3.2.2 The improved DWT method

After the decomposition and reconstruction steps of DWT, the information of the signal will be contained by the detail and approximation signals at different frequency bands. Many studies applied an improved Hilbert envelope spectrum to analyze the detail signal. The improved Hilbert spectral analysis is presented as follows [99]:

For a given signal $f(t)$, its analytic signal $A[f(t)]$ is given by Eq. (5), then we can define a new envelope signal

$$\mathrm{E}(t) = \left|A[f(t)]\right| - \frac{\sum\left|A[f(t)]\right|}{N} \tag{53}$$

where N is the length of $A[f(t)]$.

Then the envelope spectrum analysis $\mathrm{ES}(f)$ of $\mathrm{E}(t)$ is presented as:

$$\mathrm{ES}(f) = \left| \int_{-\infty}^{+\infty} E(t) e^{-jwt} dt \right| \tag{54}$$

$\mathrm{ES}(f)$ presents the absolute value of the Fourier transform amplitude of $\mathrm{E}(t)$. The improved Hilbert spectrum can reduce the undesirable distortion near the two ends of the region where the Hilbert transform is performed.

If there are a series of periodic impulses contained in the corresponding detail signal, Hilbert spectral analysis can detect them by plotting the instantaneous amplitude of the signal in time domain. But in practice applications, the energy of the periodic impulses contained in the vibration signal is usually not very strong, the periodic impulses are masked by the noise or other frequency components. Thus sometimes the results are not very clear and accurate.Previous studies usually only have good results in analyzing the periodic impulses in frequency.

According to the definition of Cepstrum analysis in Eq. (3), we can find it first apply Fourier transform to get the estimated spectrum of a signal. After that it apply the inverse Fourier transform of the logarithm of the estimated spectrum. Based on this process, it can make the complex convolution become a simple linear superposition. Thus Cepstrum analysis has the characteristics of detecting the periodicity and reducing the influence of the noise for the low energy signal. The 'inverted frequencies' corresponding to the wave's peaks in a Cepstrum graph present the period of the periodic impulses.

revious research usually only applied Cepstrum analysis directly to extract fault features from the entire original signal. Hence, we propose a new method that takes the advantage of Hilbert

spectral analysis and Cepstrum in fault diagnosis of gears and bearings. The steps of the improved DWT method are as follows:

1. Denoise the signal. Even though DWT can reduced some noise information by the decomposition and reconstruction, but that is not enough because the original signal usually contains a lot of noise information, which sometimes makes it is hard to interpret the results. Therefore, we apply the same signal denoising method as in section 3.3.1.
2. Decompose and reconstruct the signal. After denoising the original signal, we decompose and reconstruct the signal to obtain the detail and approximation signals for future analysis.
3. Extract the fault features. We apply Cepstrum analysis to analyze the periodic impulses in time domain and still use the improved Hilbert envelope spectrum analysis to obtain the faulty information in frequency domain from the corresponding detail signals.
4. Identify the characteristics for fault diagnosis.

The proposed method can not only extract the fault features in frequency domain as previous research did but also improve the analytical capacity of the periodic impulses in time domain.

3.4 The HHT method

Due HHT's characteristics of good noise immunity [75], we can use the original data directly for analysis. It is also an aspect of comparison with the methods based on WT. The steps of fault diagnosis using HHT are as follows:

1. Decompose the original data to a set of IMFs by EMD.

2. Extract the faulty frequency information and the impulse's period from the selected IMFs by applying Hilbert transform and Hilbert marginal spectrum.
3. Identify the characteristics for fault diagnosis.

Chapter 4

4. Case study on gearbox fault diagnosis

4.1 Case introduction

Traditional gearbox experiments usually analyze the vibration signals collected from some significant faulty gears with a chipped tooth or even a missing tooth, because these damage will generate stronger periodic impulses, which can make it easier to extract the fault features for further diagnosis.

In practice, it requires to detect and diagnose a fault as earlier as possible once it happens. Therefore we have respectively collected the vibration signals by using gears with the tooth's root been cut in different depth respectively in our experiment. The sizes of the crack at the gear tooth root are: 0% (healthy gear), 25%, 40%, 60%, and 80%. Figure 5 shows a gear with one tooth's root been cut in 80% degree. In this way we can simulate the gradual growing process of the gear damage: from a smaller damage at the beginning to a larger damage at end. Then we will apply the methods based on CWT, DWT and HHT to analyze the five sets of collected signals respectively and compare their capacity of fault diagnosis of the gearbox. We will also compare the results of Cepstrum analysis and the improved Hilbert envelope spectrum analysis at the same time because they are both based on DWT. This experiment has practical significance and can reflect the characteristics of wavelet transform and Hilbert-Huang Transform more precisely in fault diagnosis of the gearbox.

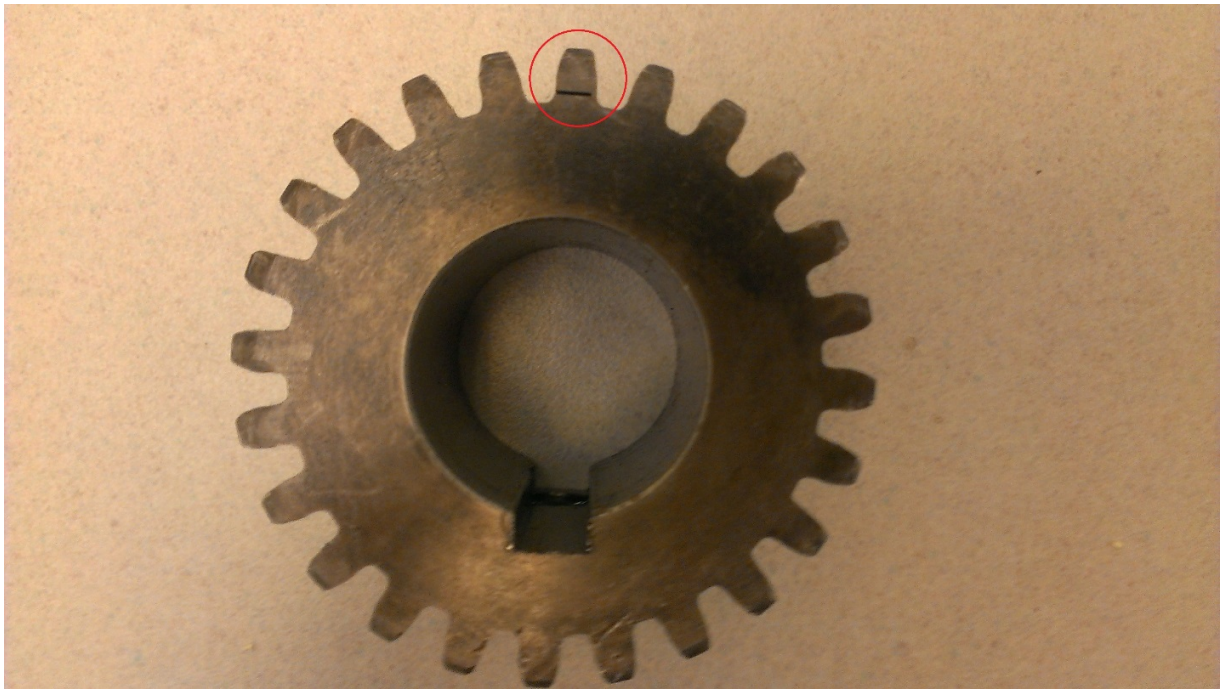

Figure 5 Gear with 80% crack

4.2 Experimental equipment

The experimental equipment is shown in Figure 6, where we can see there is an accelerometer mounted on the top of the gearbox to collect the signals. The configuration of the gearbox is shown in Figure 7: there are four gears installed on the three shafts. The gearbox's parameters are shown in Table 1. One tooth's root of the gear 3 (24 teeth) has been cut in different degrees. Then five sets of vibration data are collected by running the five different gears respectively and the sampling frequency is 256000Hz.

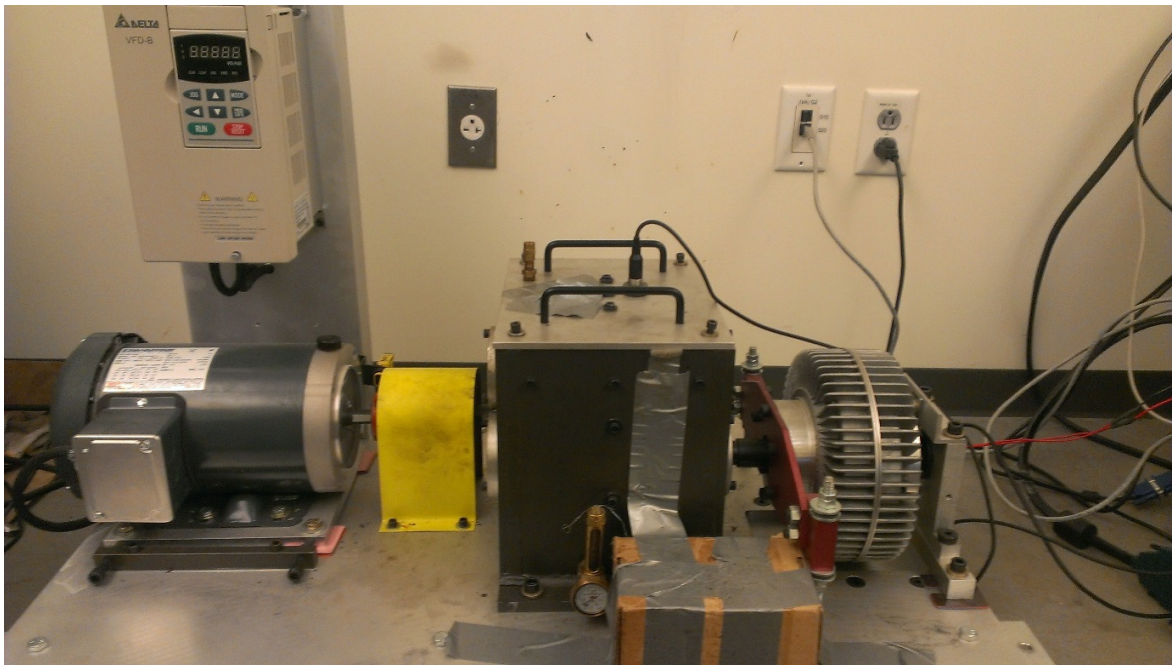

Figure 6 Experimental equipment

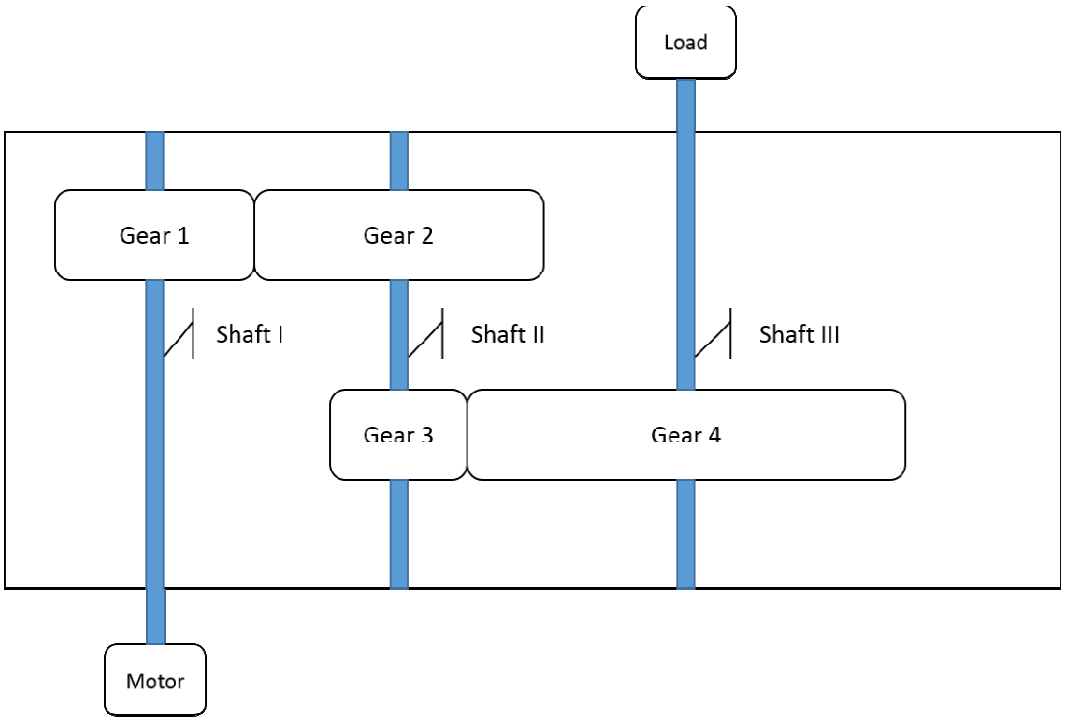

Figure 7 The configuration of the gearbox

Table 1 Gearbox parameters

Gear	1	2	3	4
Number of teeth	36	48	24	72
Rotating frequency(Hz)	30	22.5	22.5	7.5
Meshing frequency(Hz)	1080		540	
Shaft	**I**	**II**		**III**
Rotating frequency(Hz)	30	22.5		7.5

4.3 Comparison of the methods

In this part, we will apply the above methods to analyze the signals collected from the gearbox and extract the characteristic frequency of the faulty gear.

4.3.1 Time-wavelet energy spectrum

The method of time-wavelet energy spectrum will generate two spectral: time-wavelet spectrum that describes the instantaneous energy distributed along with time axis x and the frequency distribution of the time-wavelet spectrum. We have used Morlet wavelet for continuous wavelet transform. The signal has been pre-processed by the method of global threshold for wavelet denoising to reduce the influence of the noise.

4.3.1.1 Healthy gear

The time-domain waveform of the healthy gear collected from the gearbox is shown in Figure 8 and its Fast Fourier transform is shown in Figure 9. There exist a series of the peak valves: 609.4Hz, 1045Hz, 1653Hz, 2088Hz, 2698Hz in the frequency domain in Figure 9, which reflect the meshing frequency of gear 1&2 (1080Hz), the meshing frequency of gear 3&4 (540Hz) and their harmonic frequency respectively. Figure 10 is the time-wavelet spectrum and there

doesn’t exist obvious vibration period in it, which means there are no periodic impulses. Figure 11 is the frequency distribution of the time-wavelet spectrum and there are two biggest peaks values: (29, 3.211e-5) and (1044, 1.347e-05). The frequency 1044Hz is significant because it is the sum of the meshing frequency of gear 1 and gear 2(1080Hz) and second order harmonic of the meshing frequency of gear 3 and gear 4 (540Hz).

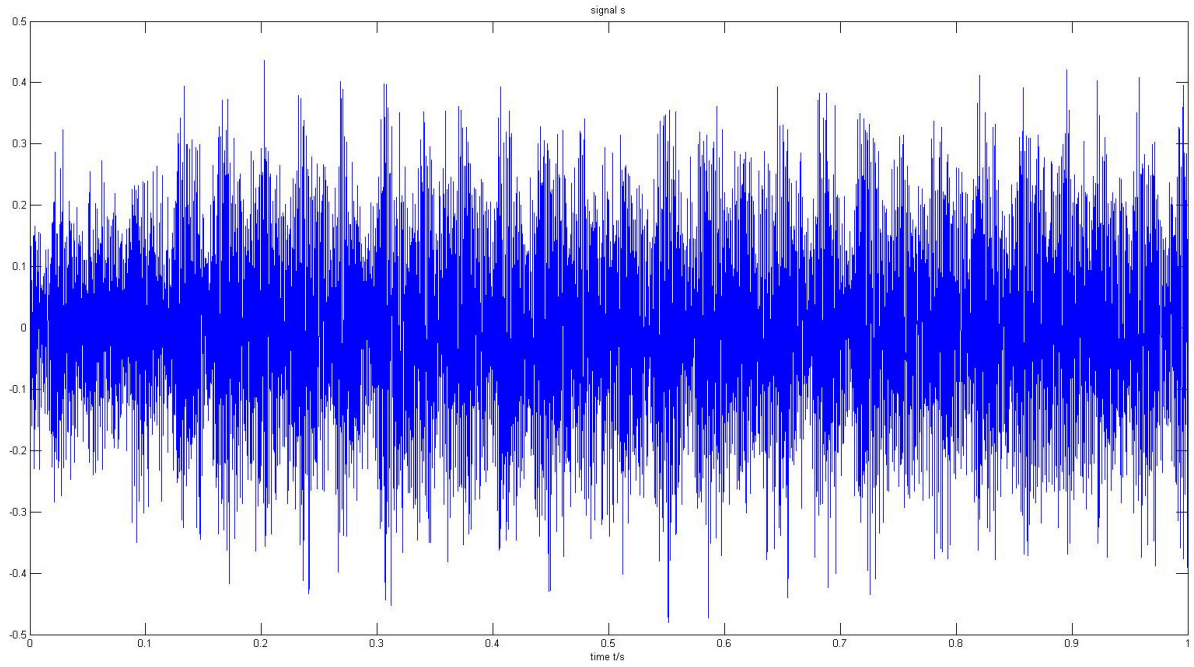

Figure 8 Time-domain waveform for the healthy gear

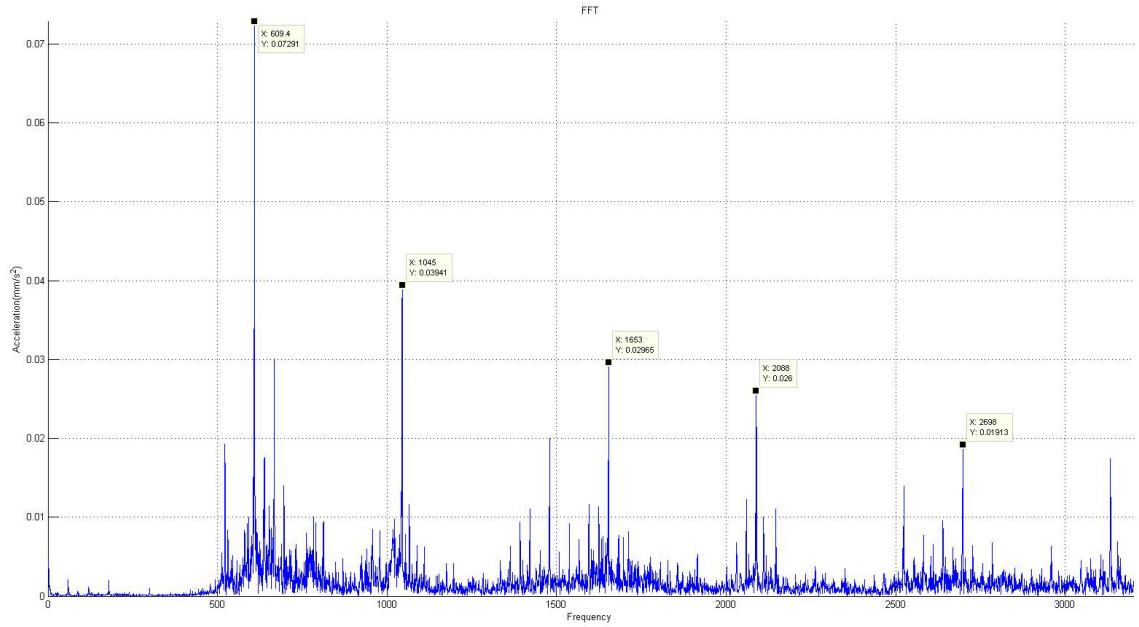

Figure 9 FFT for the healthy gear

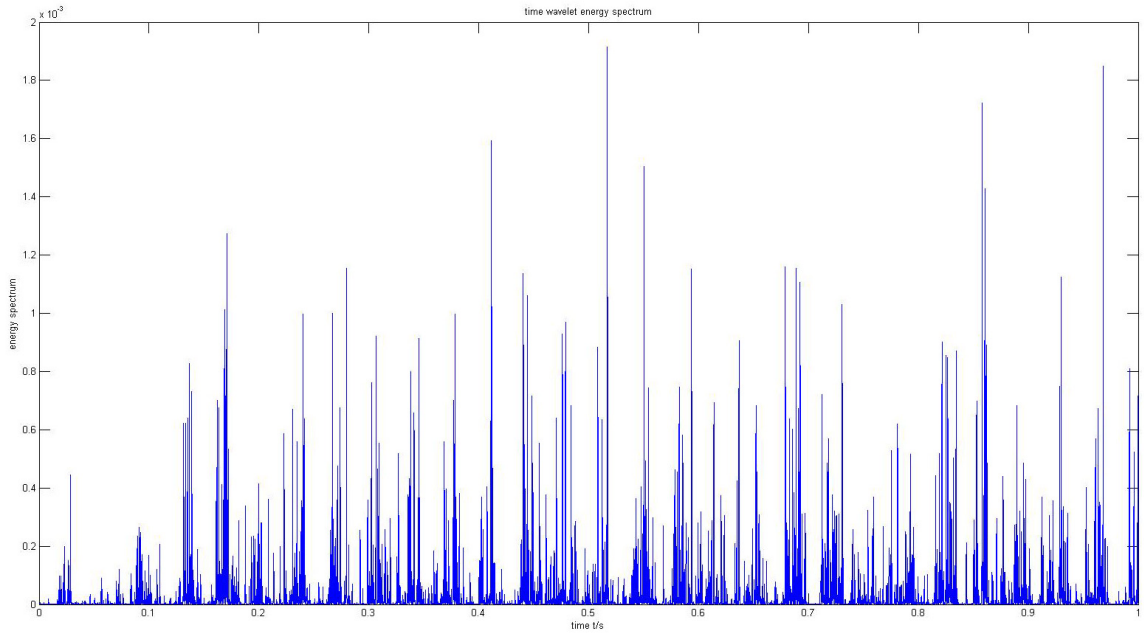

Figure 10 Time-wavelet spectrum for the healthy gear

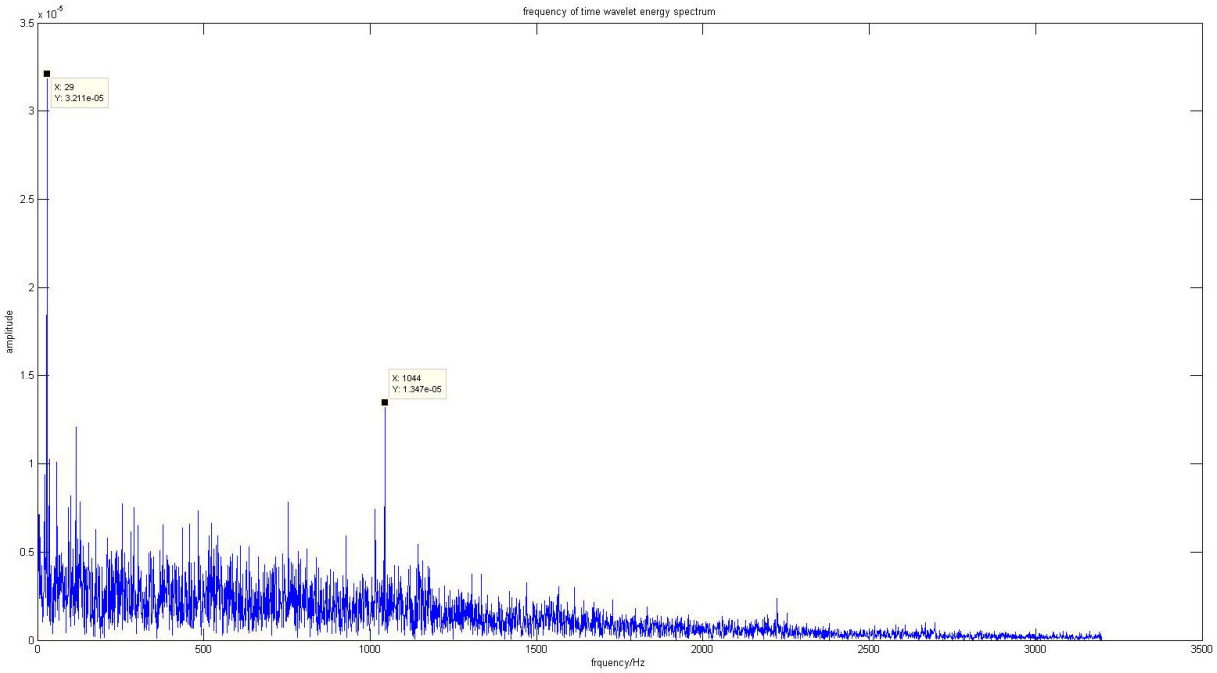

Figure 11 Frequency distribution of the time-wavelet spectrum for the healthy gear

4.3.1.2 Gear with 25% crack

Figure 12 is the time-domain waveform of the faulty gear with 25% crack. Figure 13 is the Fast Fourier transform analysis where there are a series of the peak valves: 680.5Hz, 1063Hz, 1594Hz, 2125Hz frequencies corresponding to the meshing frequency of gear 1&2 (1080Hz), the meshing frequency of gear 3&4 (540Hz) and their harmonic frequencies respectively. Figure 14 and Figure 15are the Time-wavelet spectrum and Frequency distribution respectively. There doesn't exist obviously vibration period in Figure 14. The frequencies corresponding to the peaks in Figure 15 are: 37Hz, 401Hz, 863Hz and 1092Hz. As the fault characteristics of the fault gear can't be identified, it can't detect and diagnose the gear's fault in 25% degree.

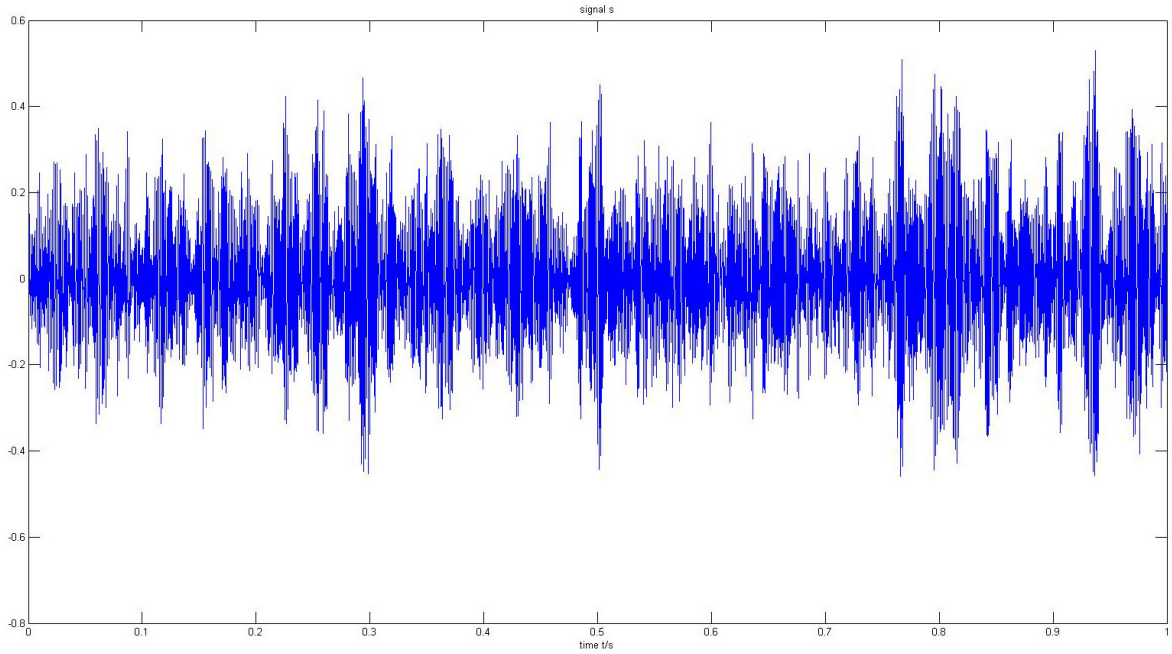

Figure 12Time-domain waveform for the gear with 25% crack

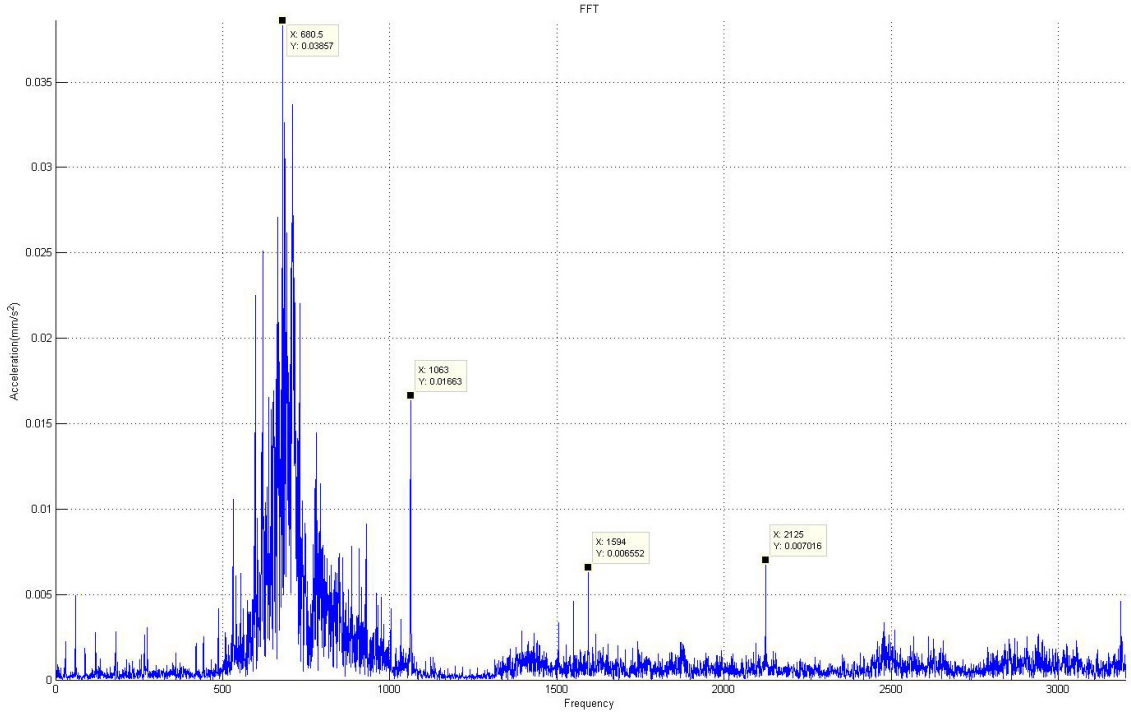

Figure 13 FFT for the gear with 25% crack

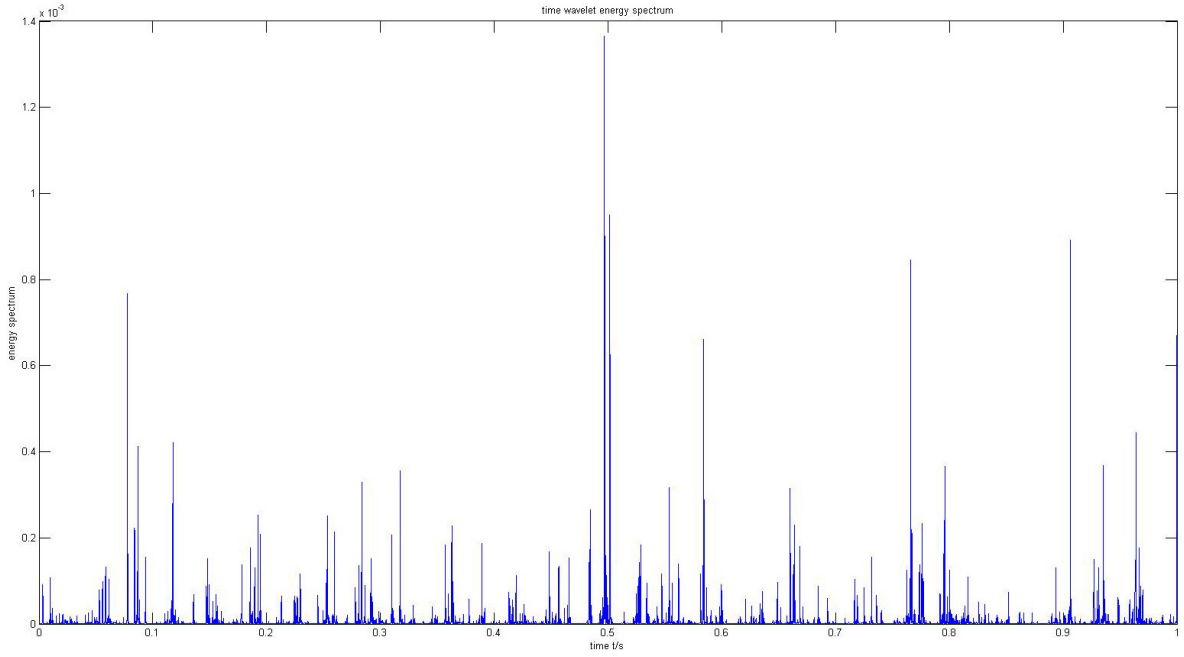

Figure 14 Time-wavelet spectrum for the gear with 25% crack

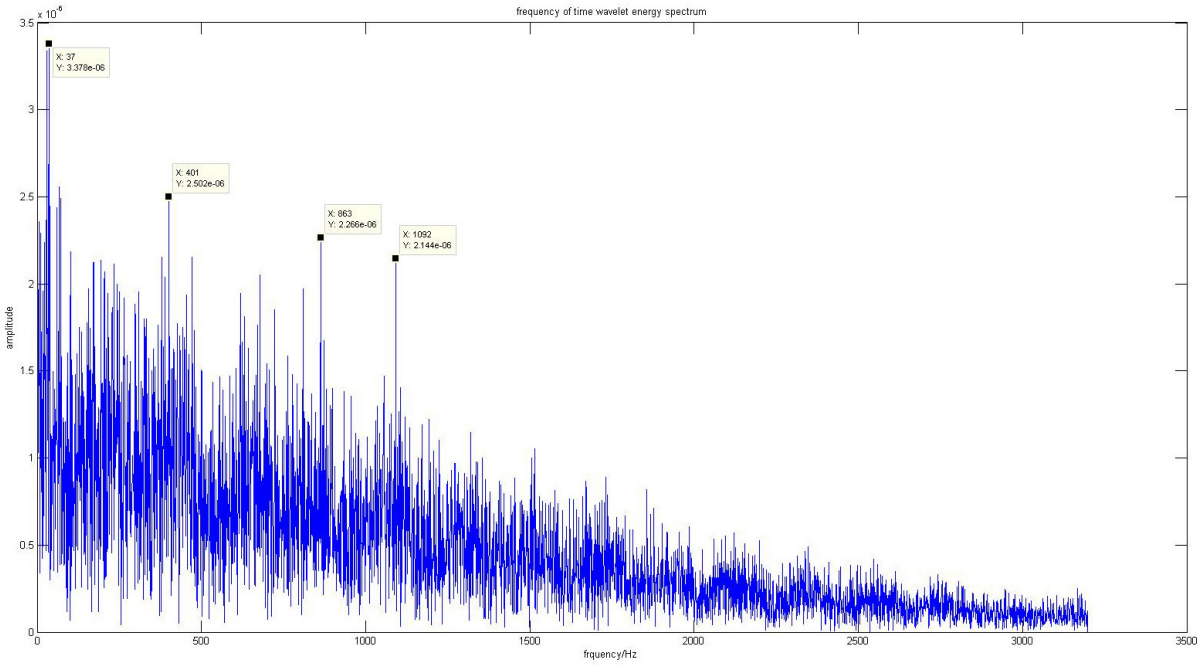

Figure 15 Frequency distribution of the time-wavelet spectrum for the gear with 25% crack

4.3.1.3 Gear with 40% crack

The time-domain waveform and its Fast Fourier transform are shown in Figure 16 and Figure 17. There are many peaks in the Time-wavelet spectrum (Figure 18), but the vibration period is not very obvious. The frequency of the highest peak in the Frequency distribution (Figure 19) is 29Hz, which is corresponding to gear 3's rotating frequency 22.5 Hz. The meshing frequency of gear 3 &4 (540Hz) and its harmonic can also be found in Figure 19: 517 Hz and 1051 Hz. However, they are not very clear and obvious. Hence, it can't detect and diagnose the gear with 40% crack.

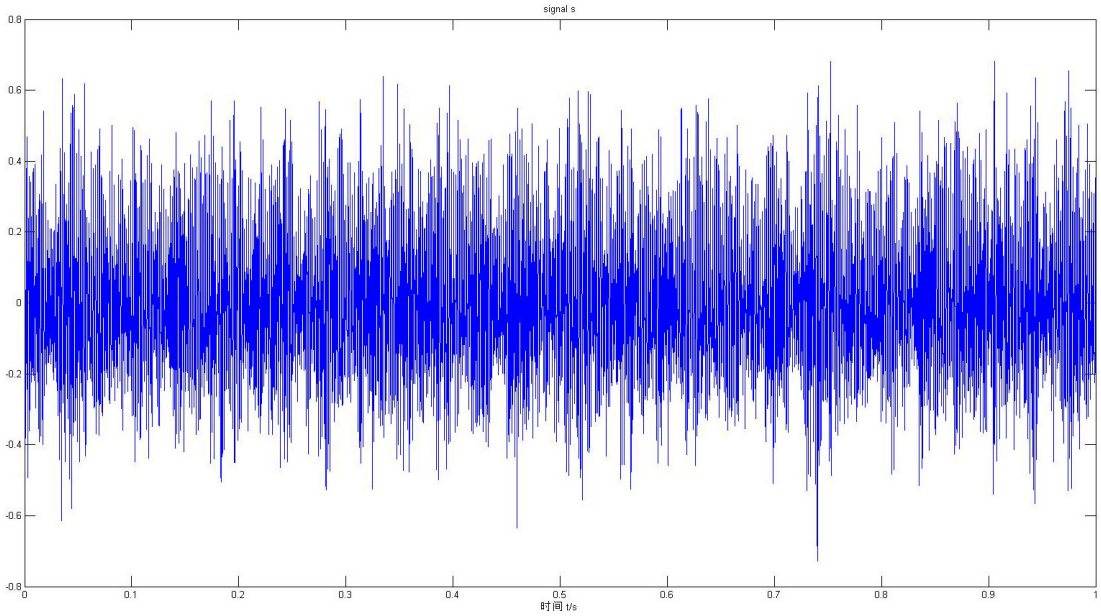

Figure 16 Time-domain waveform for the gear with 40% crack

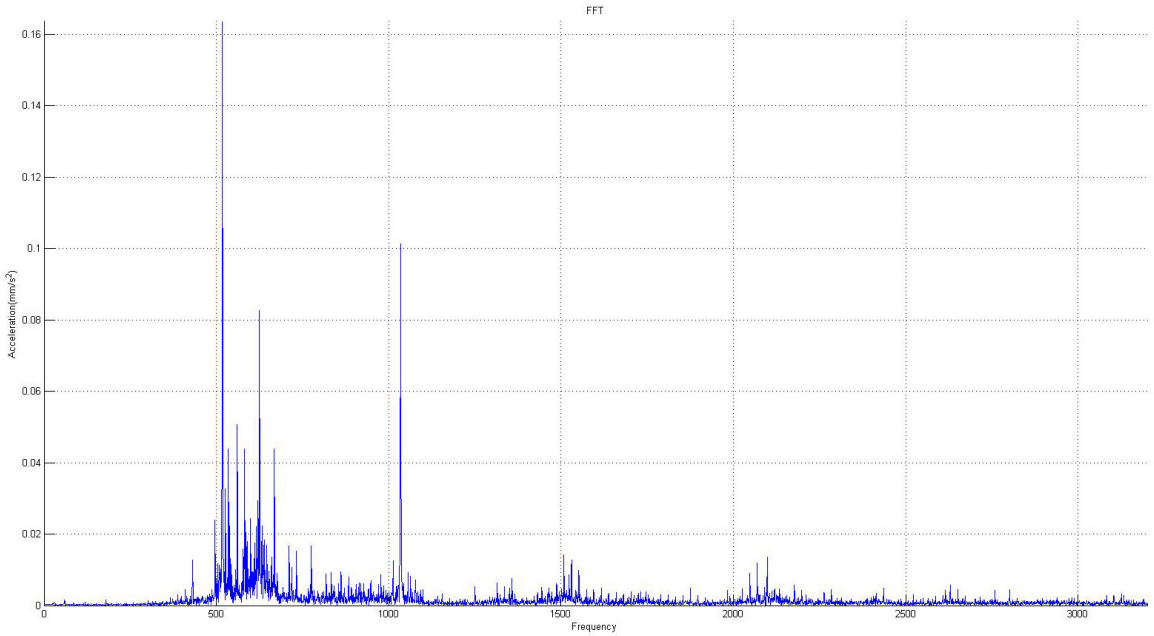

Figure 17 FFT for the gear with 40% crack

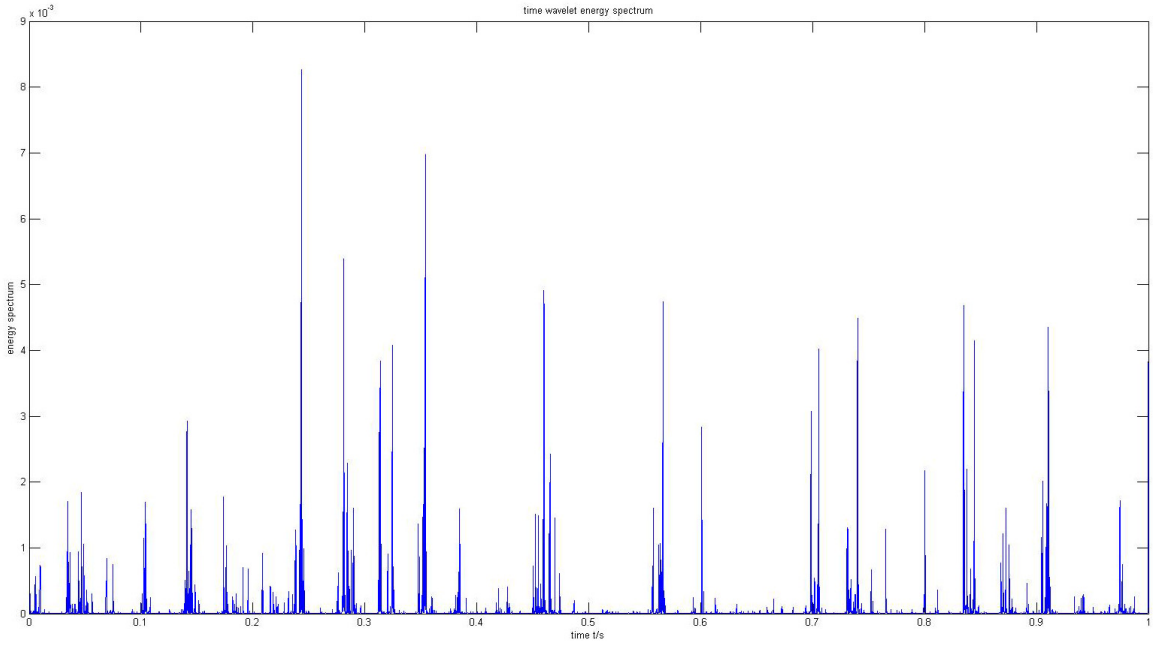

Figure 18 Time-wavelet spectrum for the gear with 40% crack

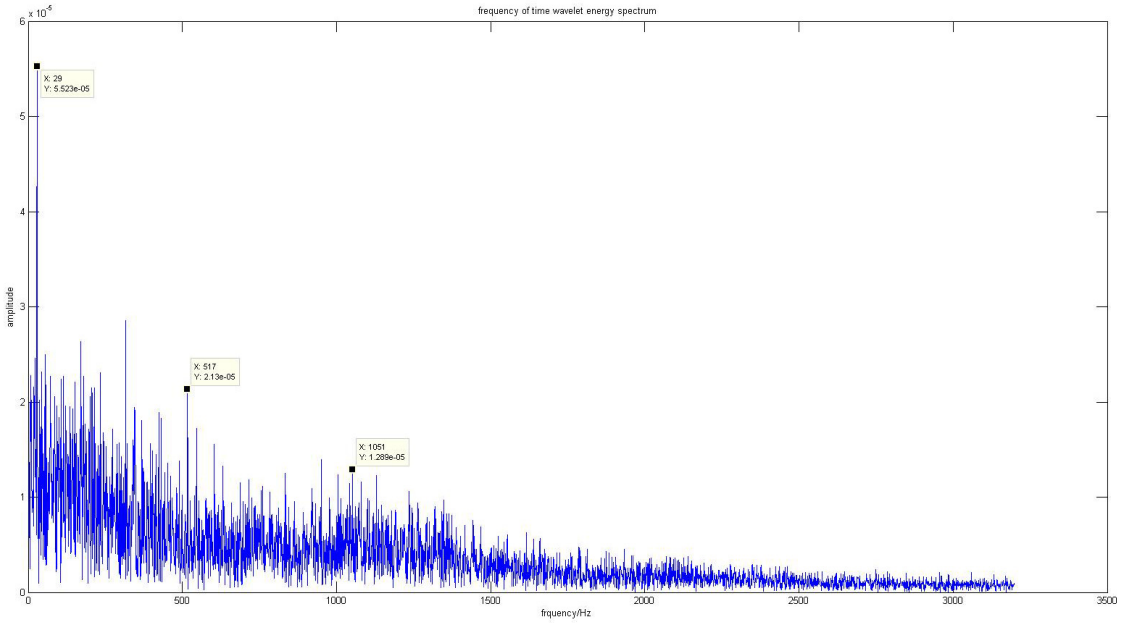

Figure 19 Frequency distribution of the time-wavelet spectrum for the gear with 40% crack

4.3.1.4 Gear with 60% crack

The time-domain waveform and its Fast Fourier transform are shown in Figure 20 and Figure 21. The meshing frequency of gear 1&2 (1080Hz), the meshing frequency of gear 3&4 (540Hz) and their harmonic frequency can also be reflected in Figure 21. There doesn't exist obvious vibration period in the time-wavelet spectrum shown in Figure 22. However, there are a series of the peak values that exist in the frequency distribution of the time-wavelet spectrum shown in Figure 23: (29, 4.283e-5) is corresponding to gear 3's rotating frequency 22.5Hz, (489, 1.475e-5) & (518, 1.443e-5) are corresponding to its meshing frequency, (1007, 1.49e-5) & (1036, 1.443e-5) are corresponding to its meshing frequency's second harmonic frequency. Compared with the frequency distribution of the healthy gear shown in Figure 11, it can be found that the amplitude of the 29Hz has greatly increased. The meshing frequency (540Hz) doesn't appear in Figure 11 but has appeared in Figure 23. Based on the two features, it can

conclude that there is a fault in gear 3. Hence, this method can detect and diagnosis the gear with 60% crack, but it is not accurate enough in frequency-domain and can't analyze the signal in time-domain.

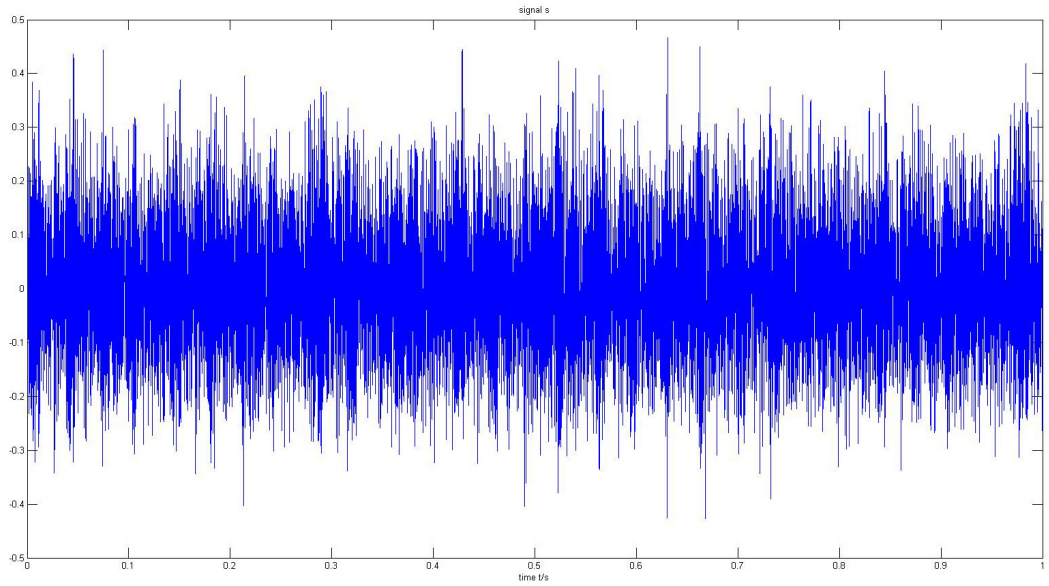

Figure 20 Time-domain waveform for the gear with 60% crack

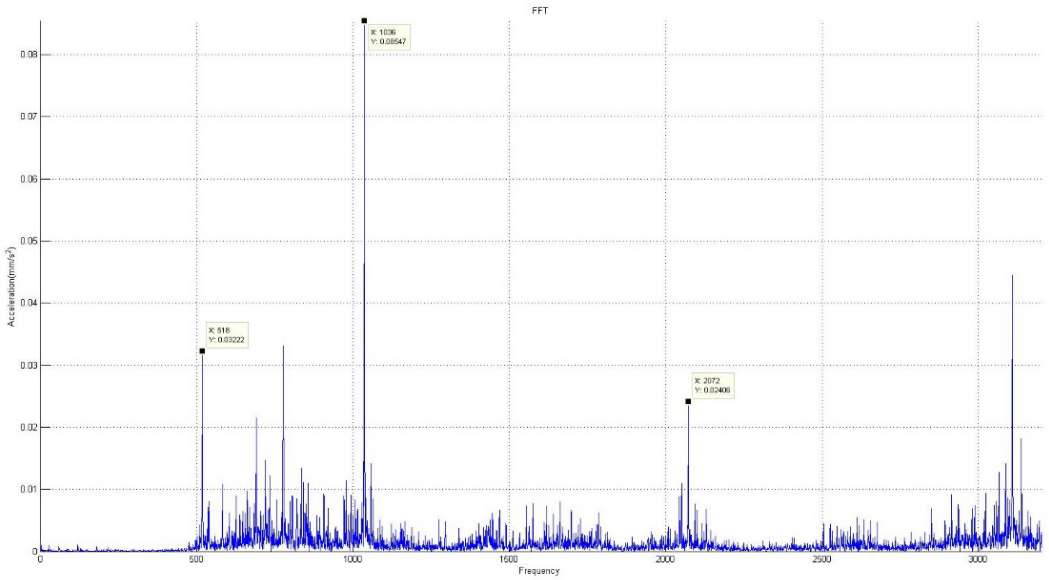

Figure 21 FFT for the gear with 60% crack

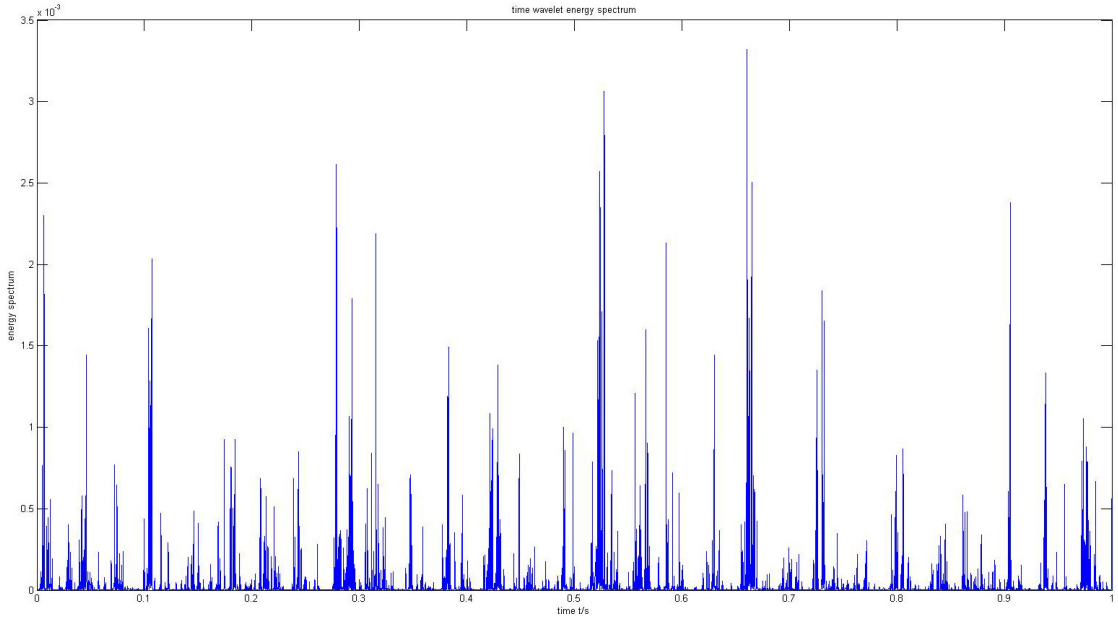

Figure 22 Time-wavelet spectrum for the gear with 60% crack

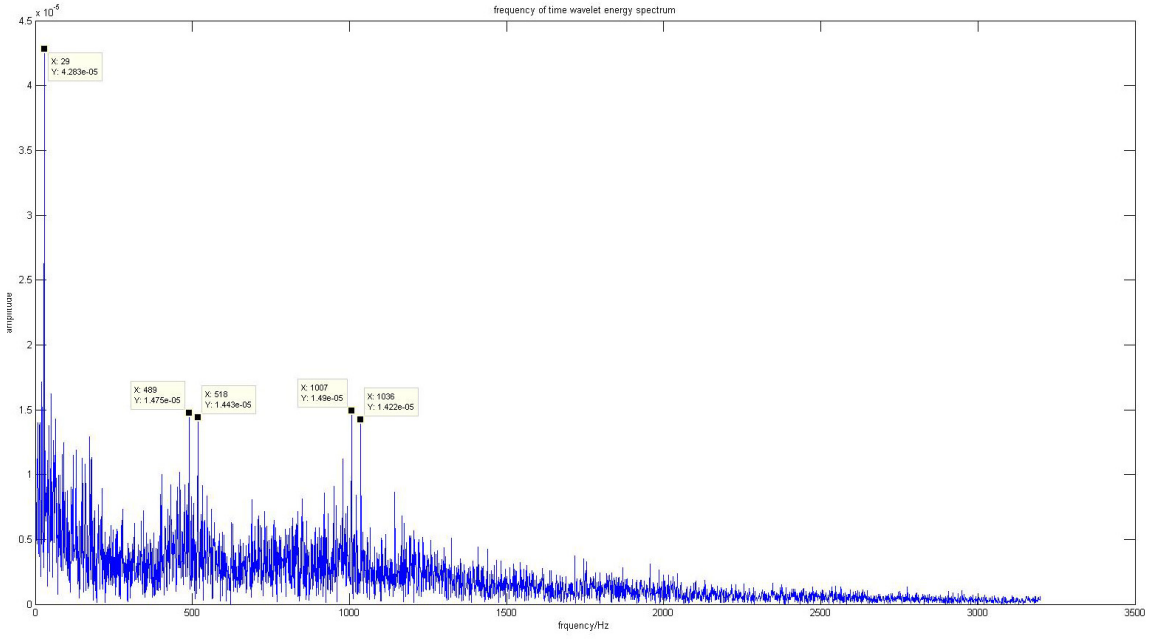

Figure 23 Frequency distribution of the time-wavelet spectrum for the gear with 60% crack

4.3.1.5 Gear with 80% crack

Figure 24 is the time-domain waveform. Figure 25 is the Fast Fourier transform, where the meshing frequency of gear 1&2 (1080Hz), the meshing frequency of gear 3&4 (540Hz) and its harmonic frequency are presented. The vibration period in the time-wavelet spectrum shown in Figure 26 is $T \approx 0.0413s$ and its frequency is $\frac{1}{T} = 24.2Hz$, which is corresponding to gear 3's rotating frequency. There are significant peaks in Figure 27 (the frequency distribution of the time-wavelet spectrum). The peak vales are as follows: (29, 5.432e-5), (583, 3.354e-5) and (1036, 2.274e-05), which are corresponding to the rotating frequency of the gear 3 (22.5Hz), the meshing frequency of gear 3 & gear 4 (540Hz) and its higher order harmonics. Then we can detect that there is a fault in gear 3. . Hence, this method can detect and diagnosis the gear's fault in 80% degree by analyzing the signal in time-frequency domain.

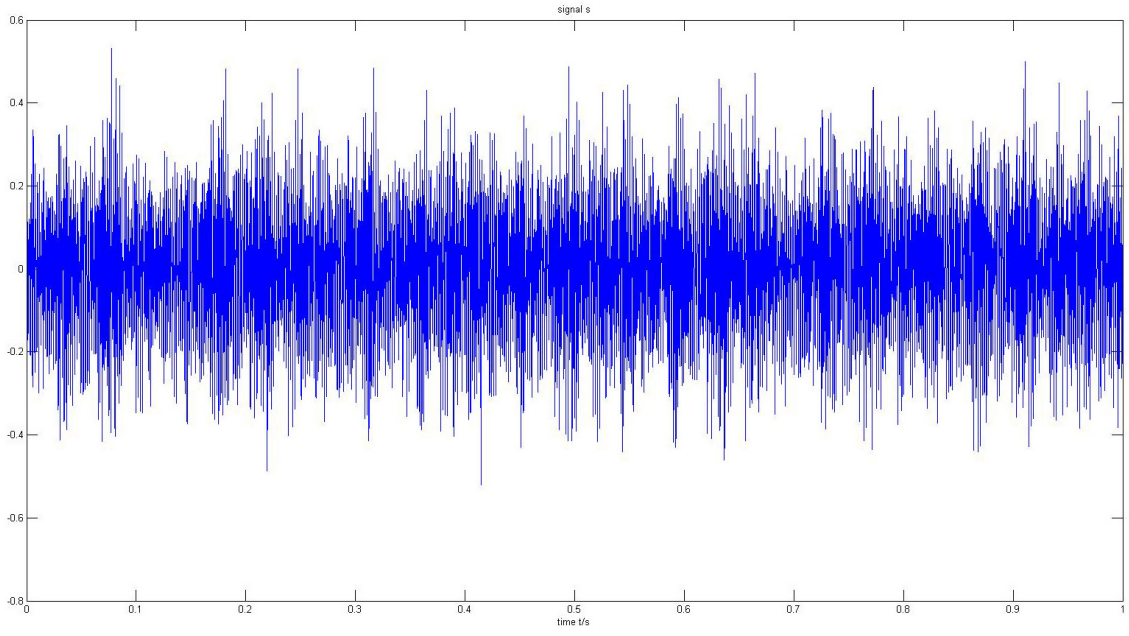

Figure 24 Time-domain waveform for the gear with 80% crack

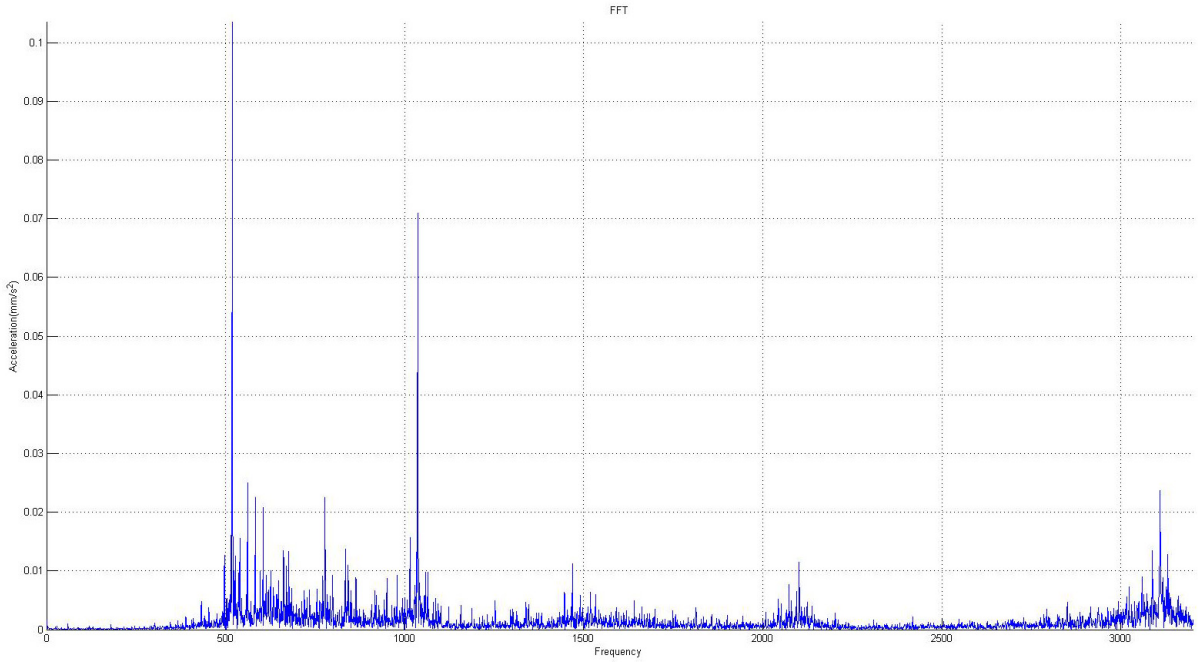

Figure 25 FFT for the gear with 80% crack

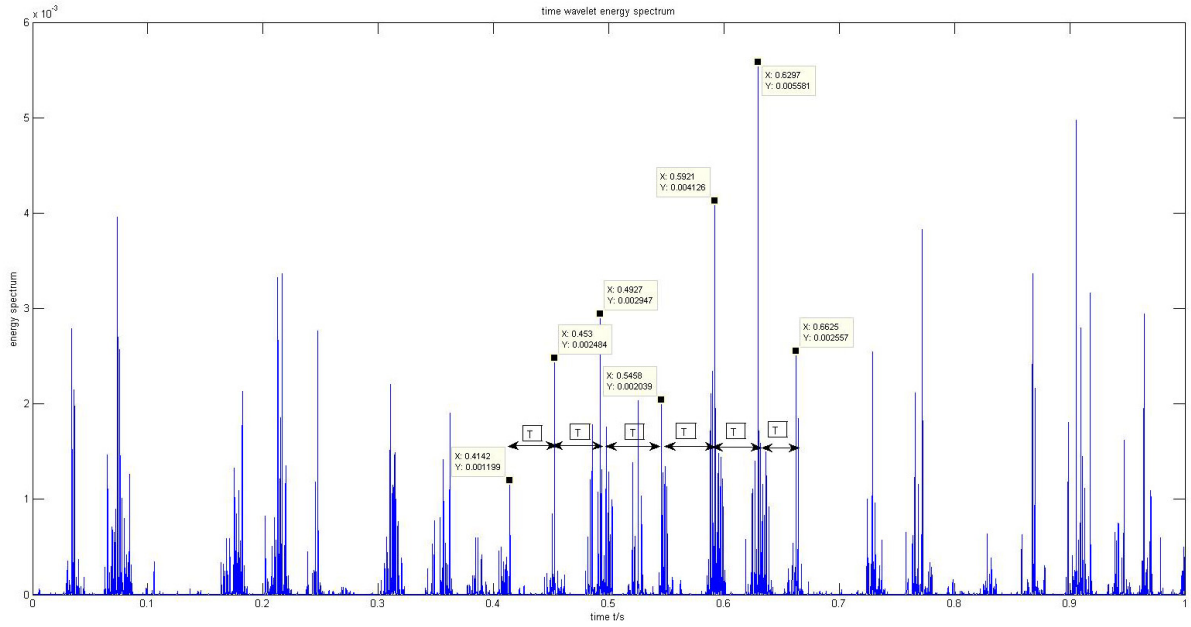

Figure 26 Time-wavelet spectrum for the gear with 80% crack

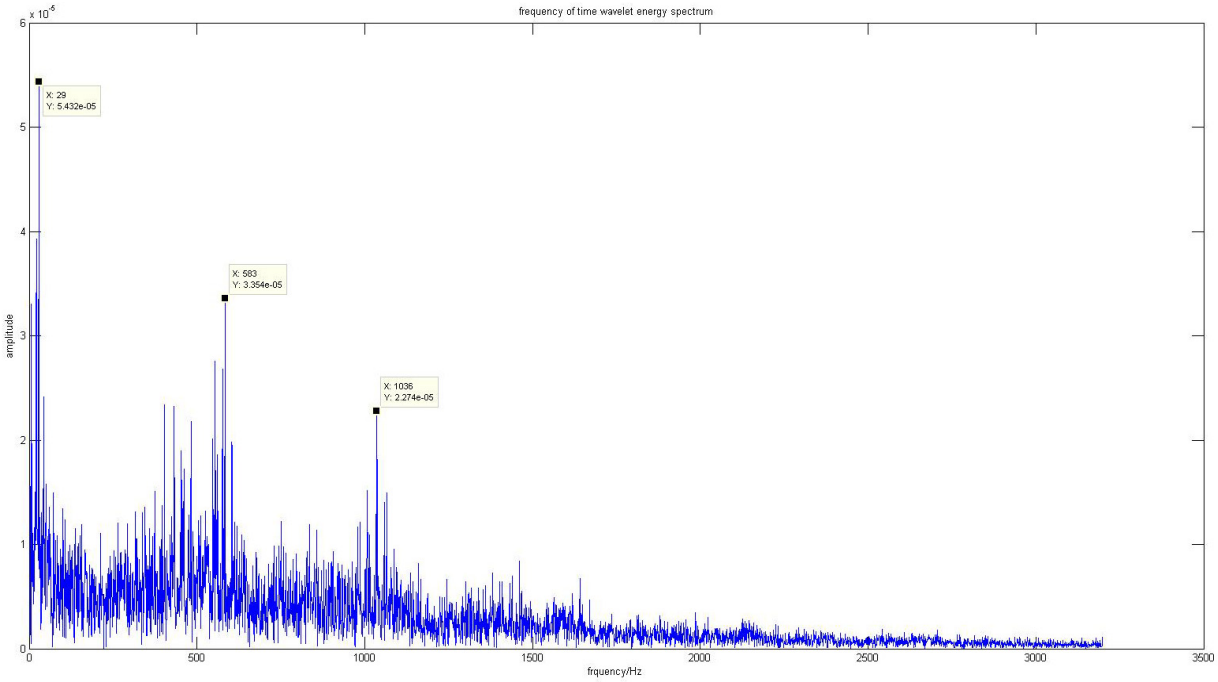

Figure 27 Frequency distribution of the time-wavelet spectrum for the gear with 80% crack

4.3.2 The improved DWT method

Same as CWT, the signal will be first denoised. Then we decompose the signal in 5 levels with DB 20 (Daubechies 20) wavelet and reconstruct it to obtain the approximation signal named ‘a5’ and five detail signals named ‘d1’ to ‘d5’. The approximation signal is an approximate to the original and detail signals contain the detail information of the signal. The ‘instantaneous amplitude’ analysis based on Hilbert transform is an analysis method in time domain, which can reflect the period of the impulses. Hence, we used it as a comparison with Cepstrum analysis to find out the impulse’s period in time domain.

4.3.2.1 Healthy gear

The approximation signal ‘a5’ and the five detail signals from ‘d1’ to ‘d5’ are shown in Figure 28. Figure 29 is the Hilbert envelope spectrum analysis from d1 to d5. There exist the peaks values:

(29, 6.716), (522, 2.756) and (1044, 2.11), which are corresponding to gear 3's rotating frequency (22.5Hz), its meshing frequency and the sum of the meshing frequency of gear 1 & 2 (1080Hz) and second order harmonic of the meshing frequency of gear 3 and gear 4 (540Hz). Figure 30 shows the instantaneous amplitude of d1 and there doesn't exist obvious vibration period. Figure 31 and Figure 32 are Cepstrum analysis of the entire original signal and the detail signal 'd5', we can see there doesn't exist obvious vibration period. There are a set of unusual peaks around the zero point due to its deficiency, which are usually ignored in practice.

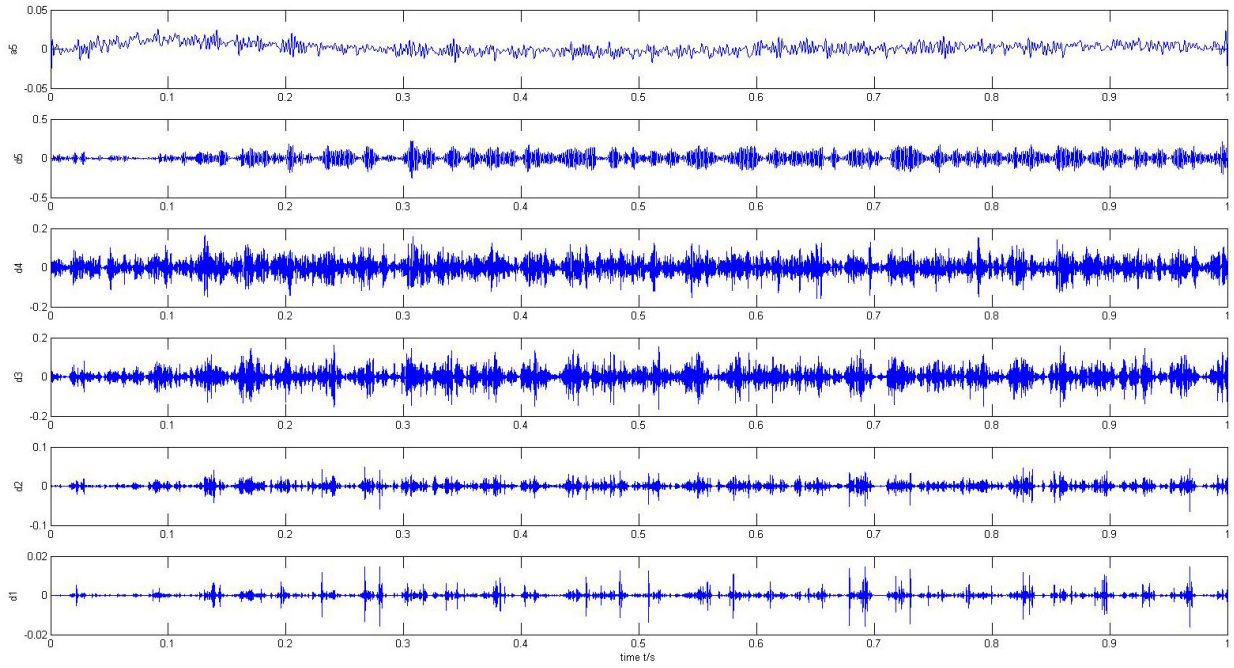

Figure 28 Approximation signal and detail signals for the healthy gear

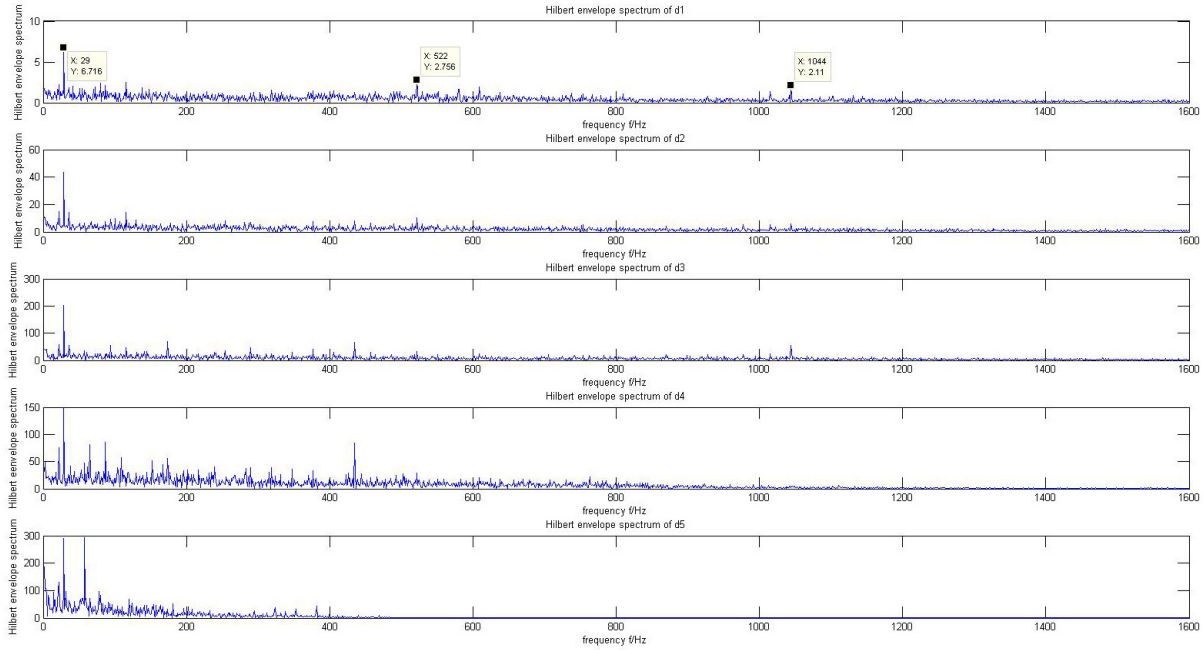

Figure 29 Hilbert envelope spectrum analysis for the healthy gear

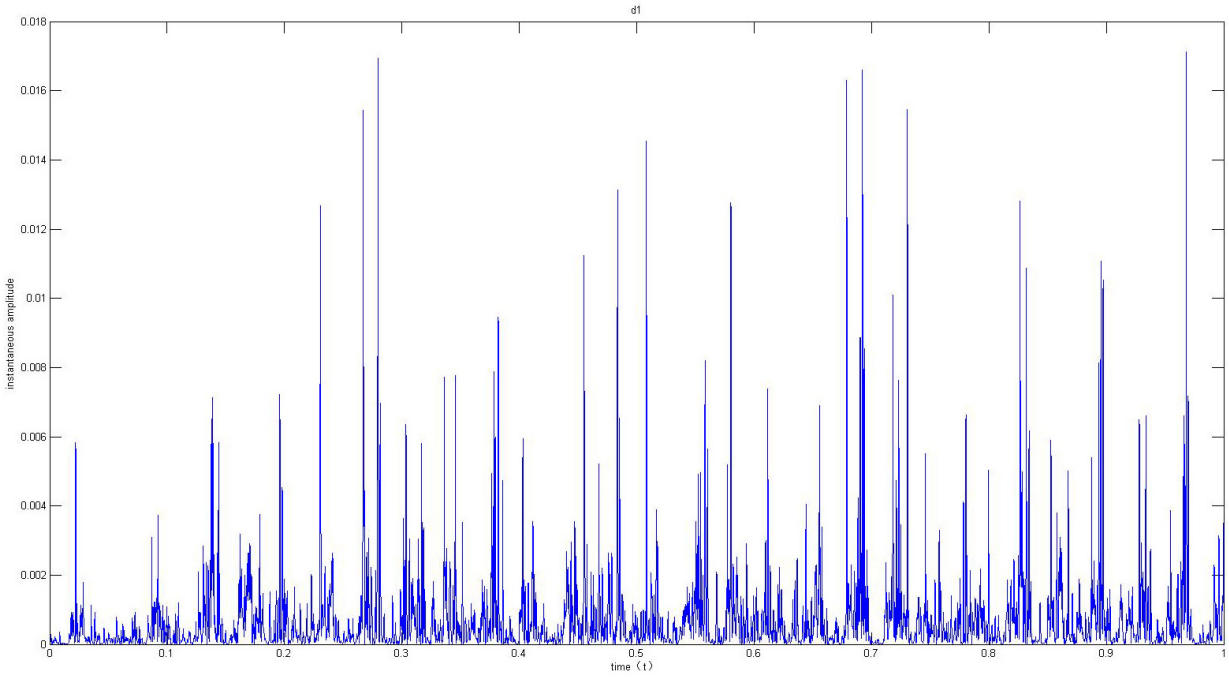

Figure 30 Instantaneous amplitude of d1 for the healthy gear

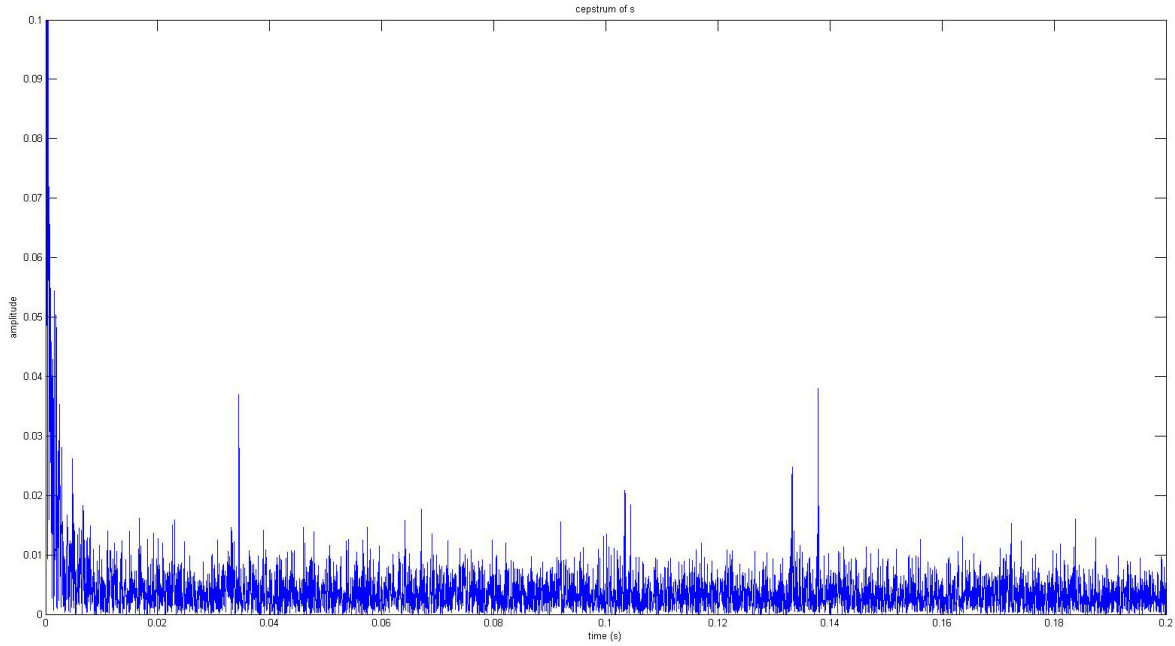

Figure 31 Cepstrum analysis of the entire original signal for the healthy gear

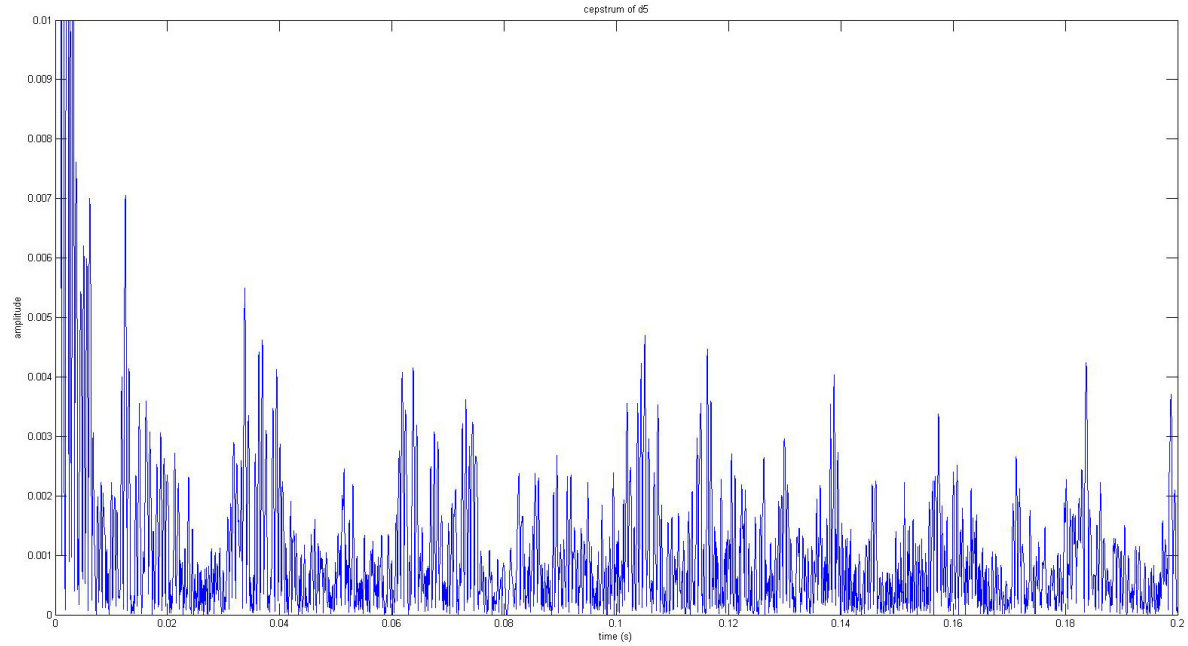

Figure 32 Cepstrum analysis of d5 for the healthy gear

4.3.2.2 Gear with 25% crack

According to the results shown from Figure 33 to Figure 37, neither Cepstrum analysis nor Hilbert envelope spectrum analysis extract the fault features from the vibration signals.

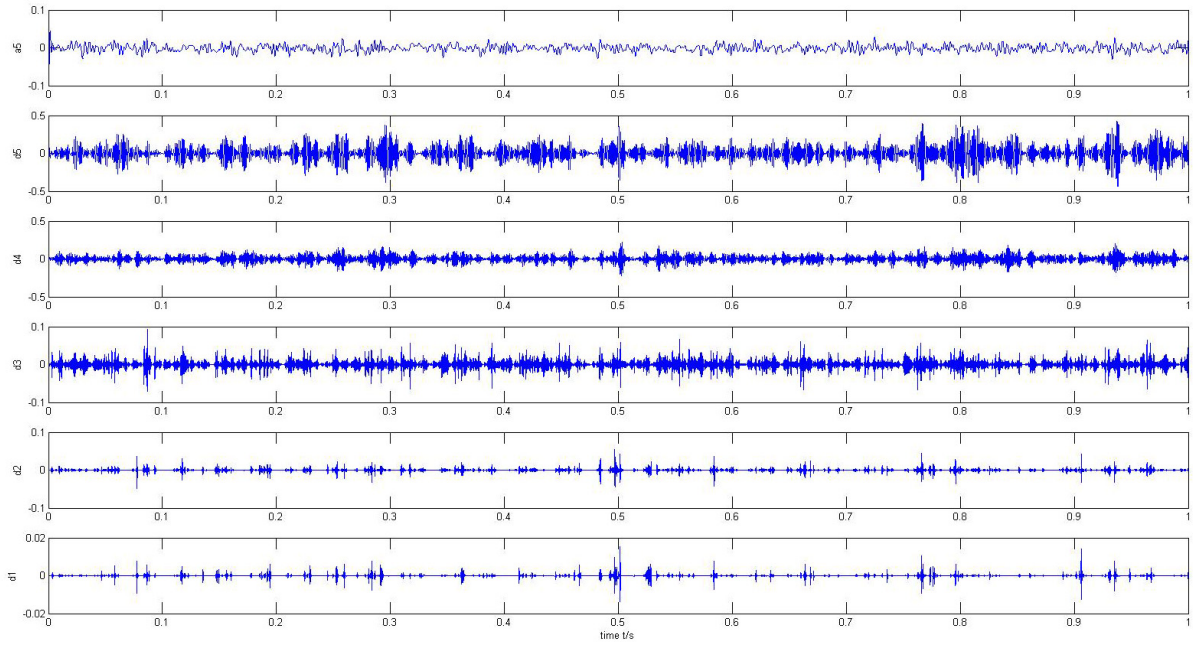

Figure 33 Approximation signal and detail signals for the gear with 25% crack

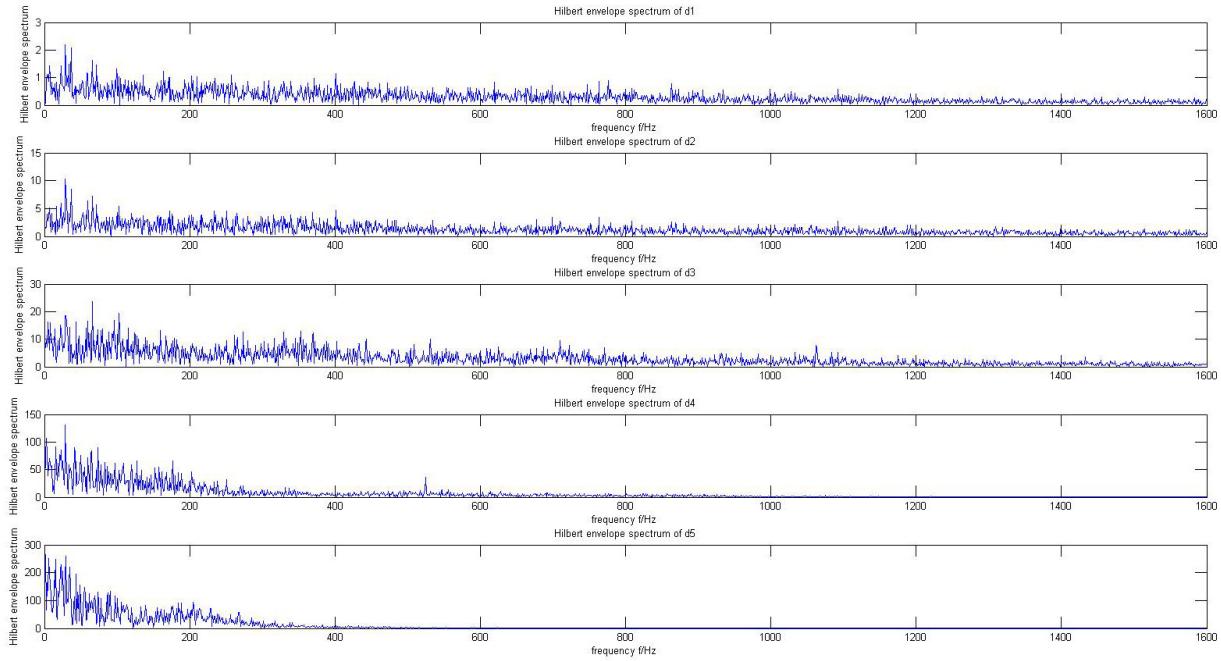

Figure 34 Hilbert envelope spectrum analysis for the gear with 25% crack

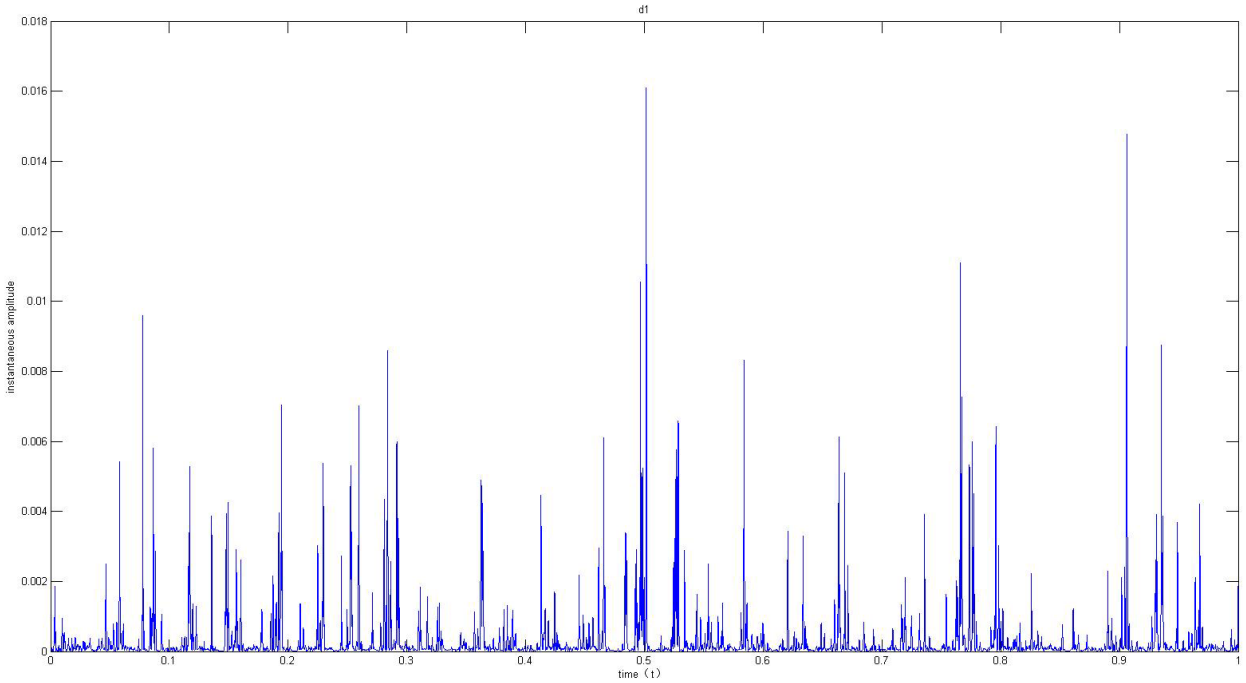

Figure 35 Instantaneous amplitude of d1 for the gear with 25% crack

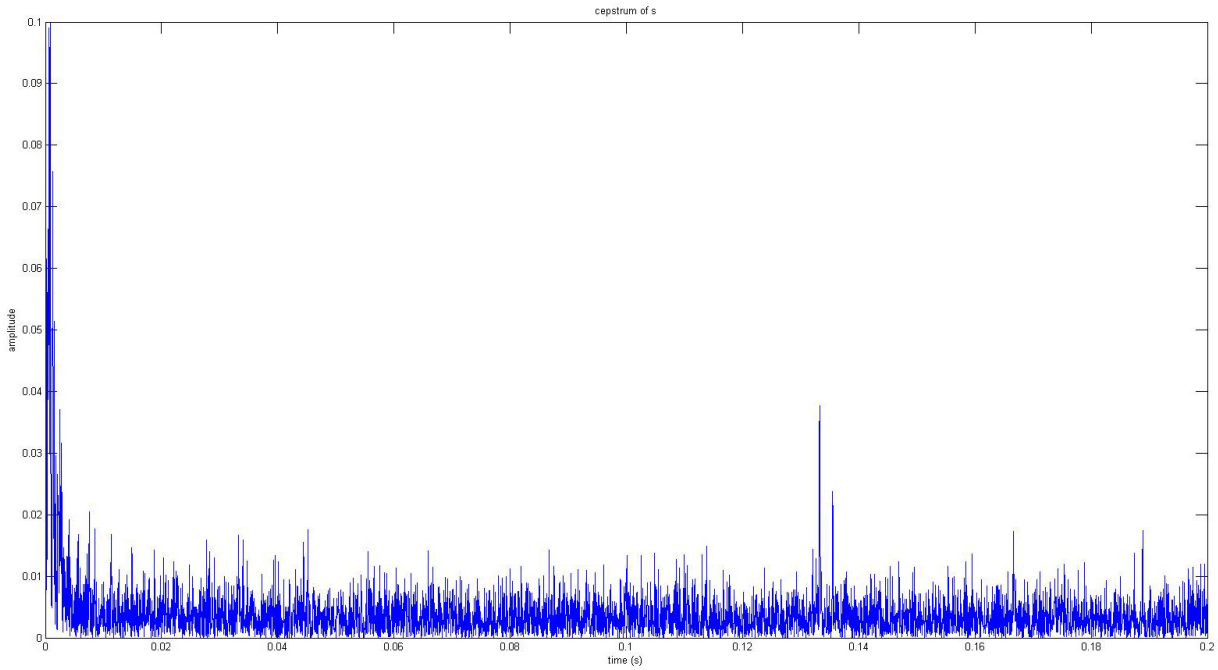

Figure 36 Cepstrum analysis of the entire original signal for the gear with 25% crack

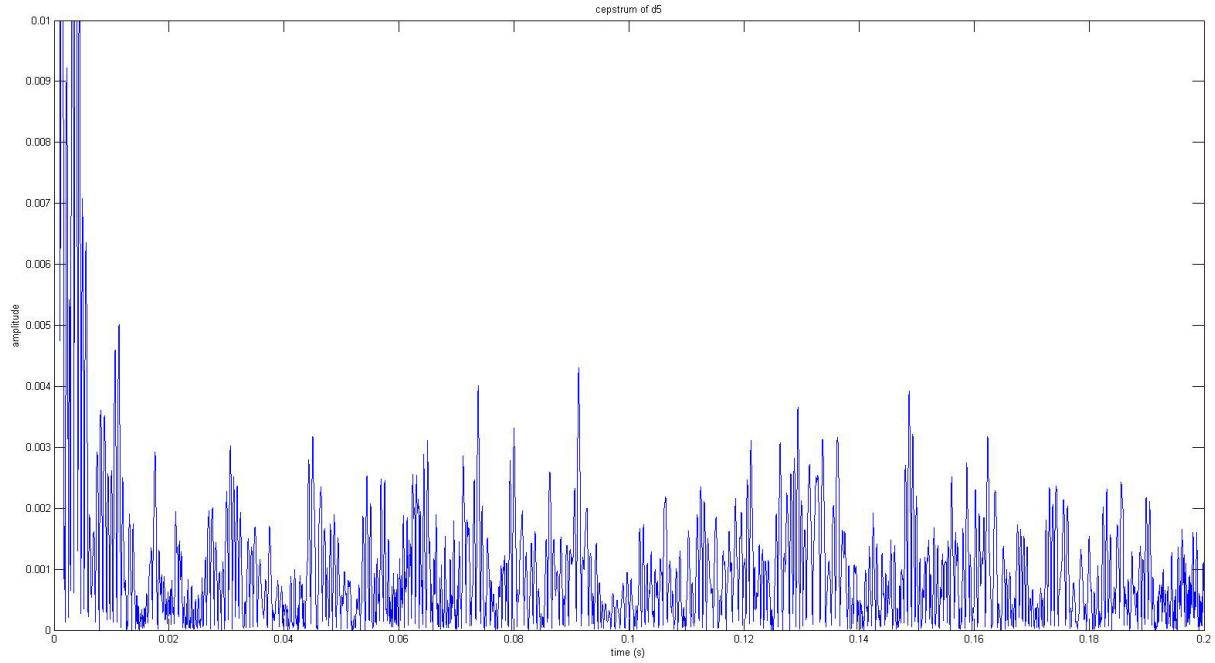

Figure 37 Cepstrum analysis of d5 for the gear with 25% crack

4.3.2.3 Gear with 40% crack

In Figure 39, we can find a series of the peaks values: the highest peak (29, 12.3) is corresponding to gear 3's rotating frequency, and compared with the healthy gear (29, 6.716), its value has highly improved. The peaks (517, 3.032) and (1051, 2.036) are the meshing frequency and its second harmonic. There doesn't exist obvious vibration periods in Figure 40. In Figure 41 the period of the impulses can be identified with $T \approx 0.0464s$ and its frequency is $\frac{1}{T} = 21.6Hz$. We can also identify the period of the impulses in Figure 42 with $T \approx 0.04583s$ and its frequency is $\frac{1}{T} = 21.8Hz$. Both of their frequencies are corresponding to the rotating frequency of the shaft II. However, there are two gears on it and the meshing frequency of gear 3 is not significant enough. Hence, we can only conclude that the faulty gear is probably gear 3 based on time domain analysis and frequency domain analysis.

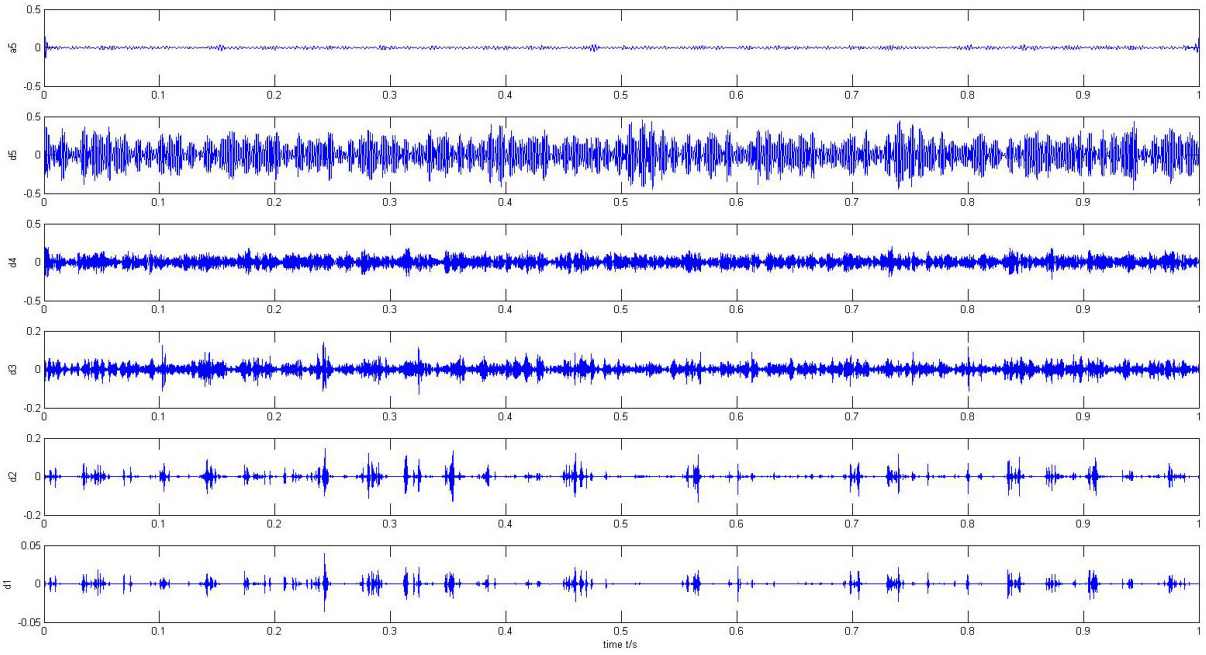

Figure 38 Approximation signal and detail signals for the gear with 40% crack

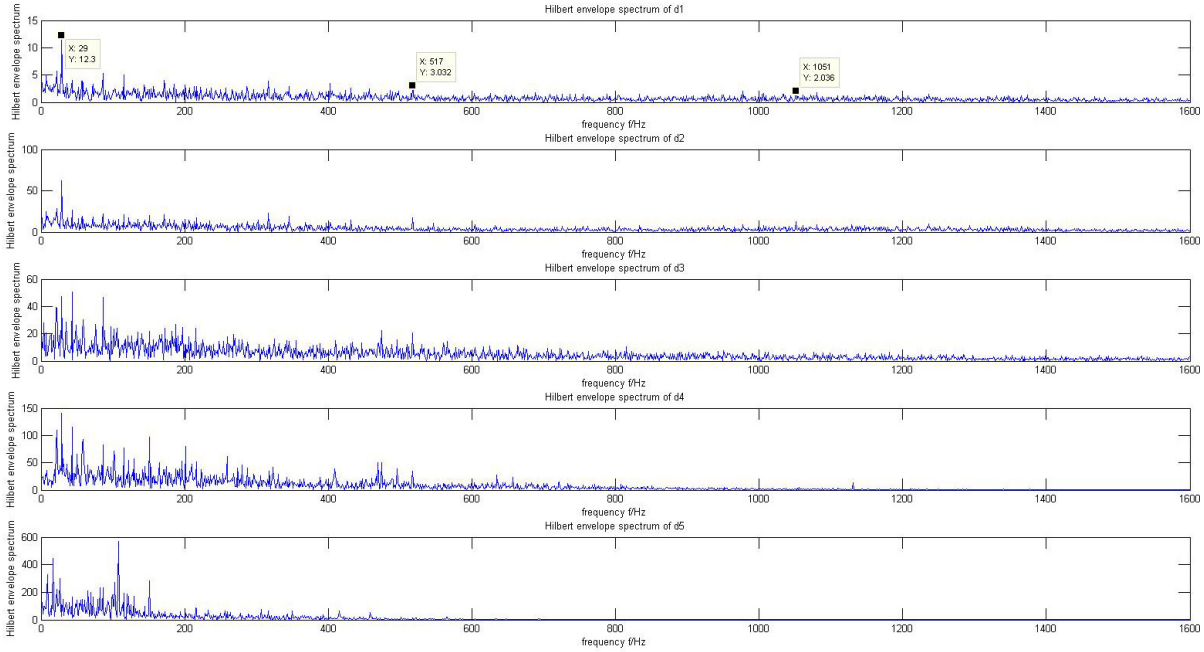

Figure 39 Hilbert envelope spectrum analysis for the gear with 40% crack

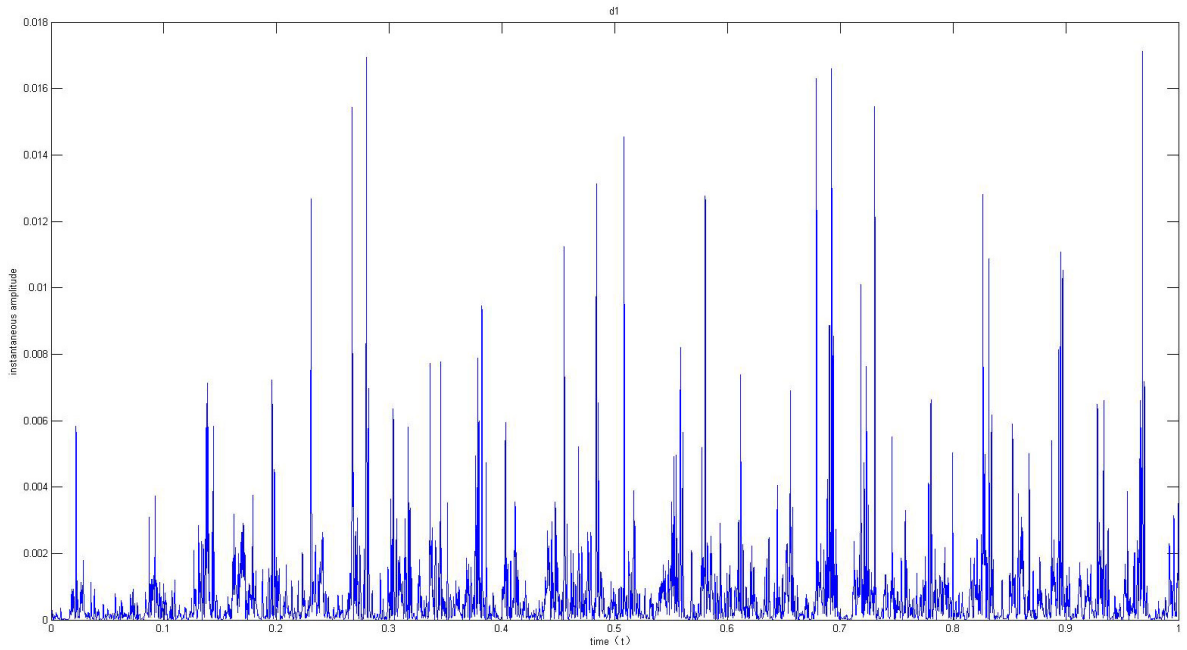

Figure 40 Instantaneous amplitude of d1 for the gear with 40% crack

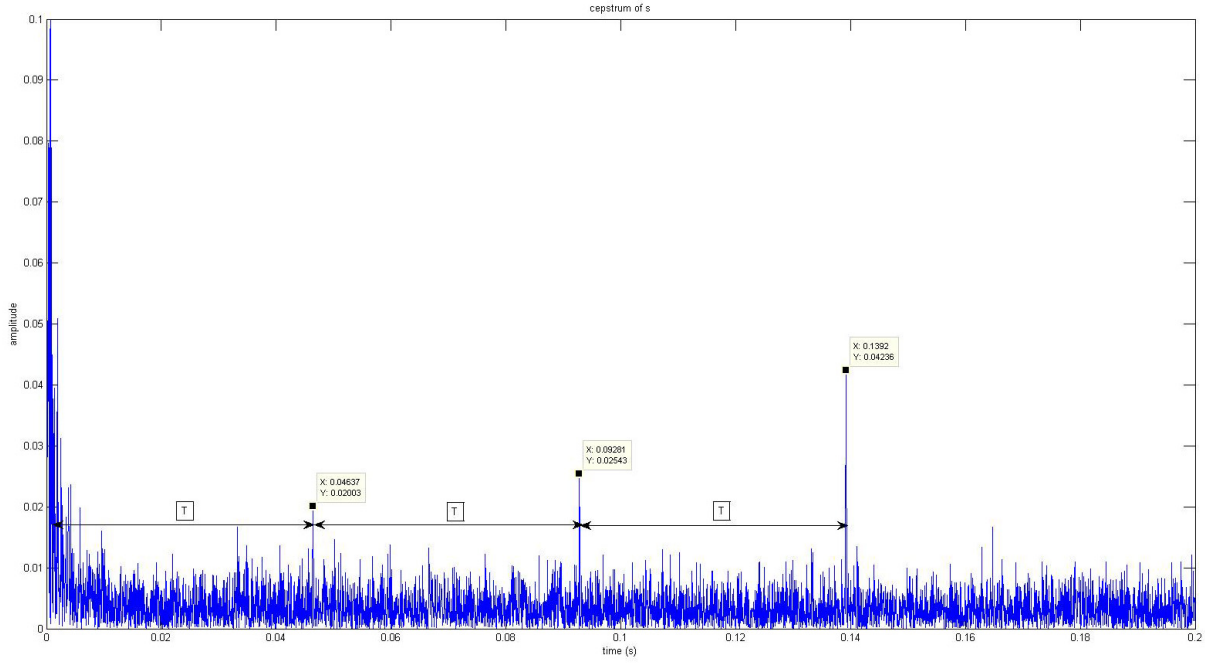

Figure 41 Cepstrum analysis of the entire original signal for the gear with 40% crack

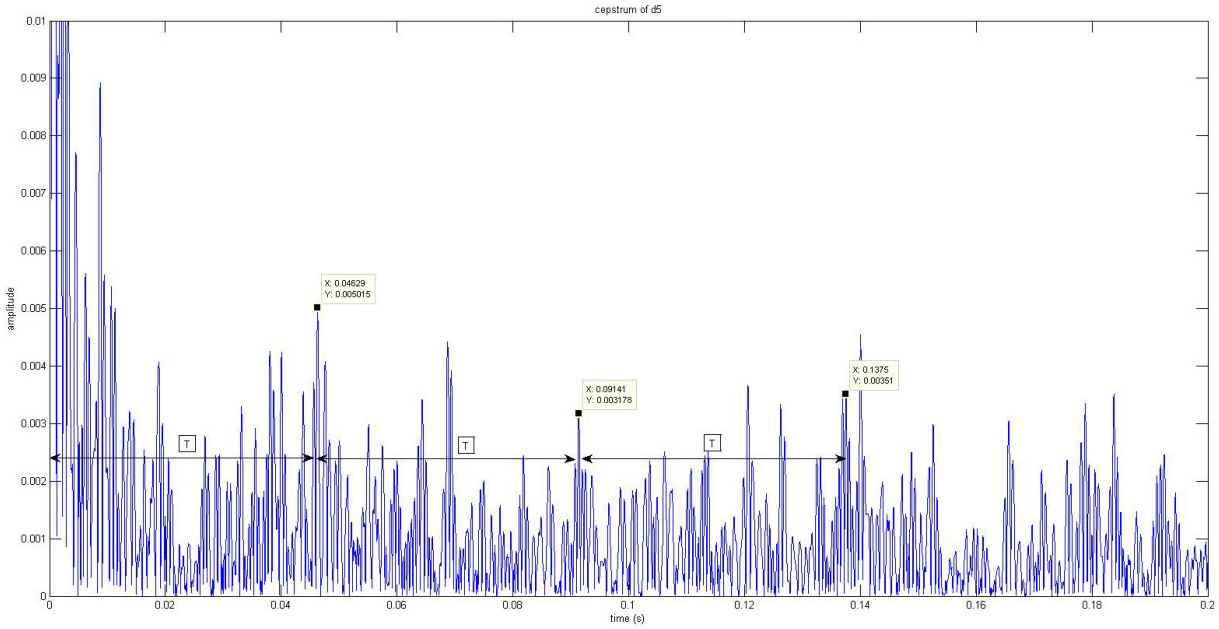

Figure 42 Cepstrum analysis of d5 for the gear with 40% crack

4.3.2.4 Gear with 60% crack

In the Hilbert envelope spectrum analysis (Figure 44), there are peaks values: (29, 9.76) corresponding to gear 3's rotating frequency and (518, 2.747) corresponding to its meshing frequency. Compared with the healthy gear, the value at the point of the rotating frequency is highly increased. There still doesn't exist obvious period in the instantaneous amplitude of d1 (Figure 45). We can find gear 3's rotating frequency in the Cepstrum analysis of the entire original signal (Figure 46) with $T \approx 0.0463s$, and its frequency is $\frac{1}{T} = 21.6Hz$. There also exists the obvious periods in the Cepstrum analysis of the detail signal 'd5' (Figure 47) with $T \approx 0.0462s$, and its frequency is $\frac{1}{T} = 21.6Hz$ corresponding to gear 3's rotating frequency. Hence, we can conclude there is a fault on gear 3. Besides, the result of the proposed method is more clear and intuitive than that of applying Cepstrum analysis directly.

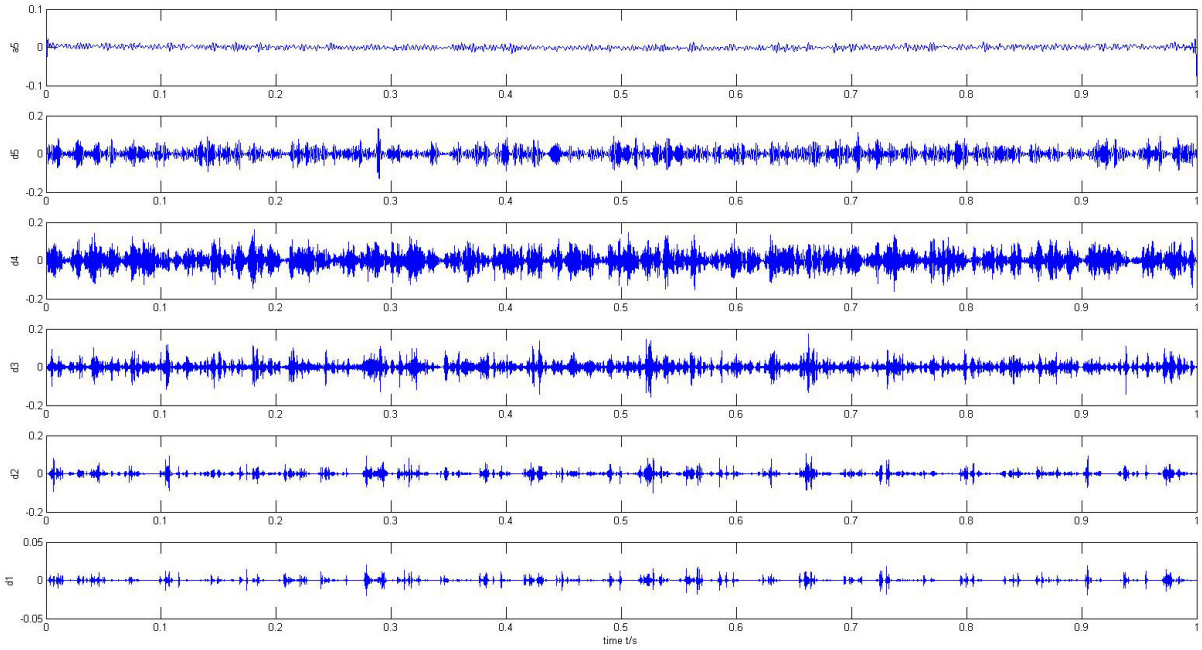

Figure 43 Approximation signal and detail signals for the gear with 60% crack

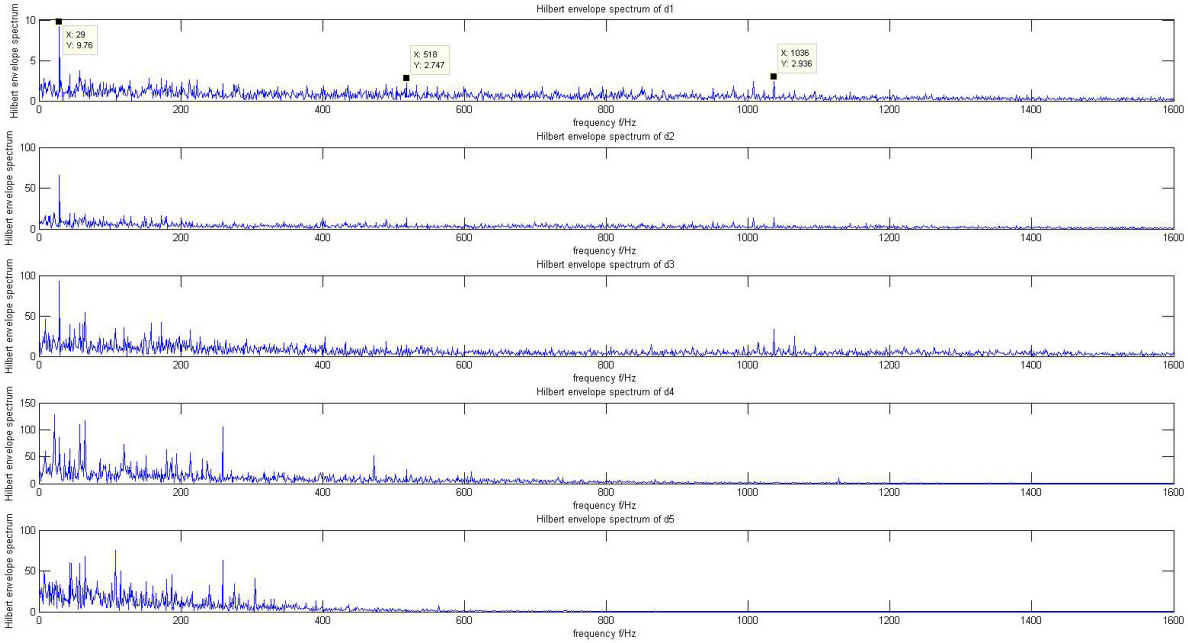

Figure 44 Envelope spectrum analysis for the gear with 60% crack

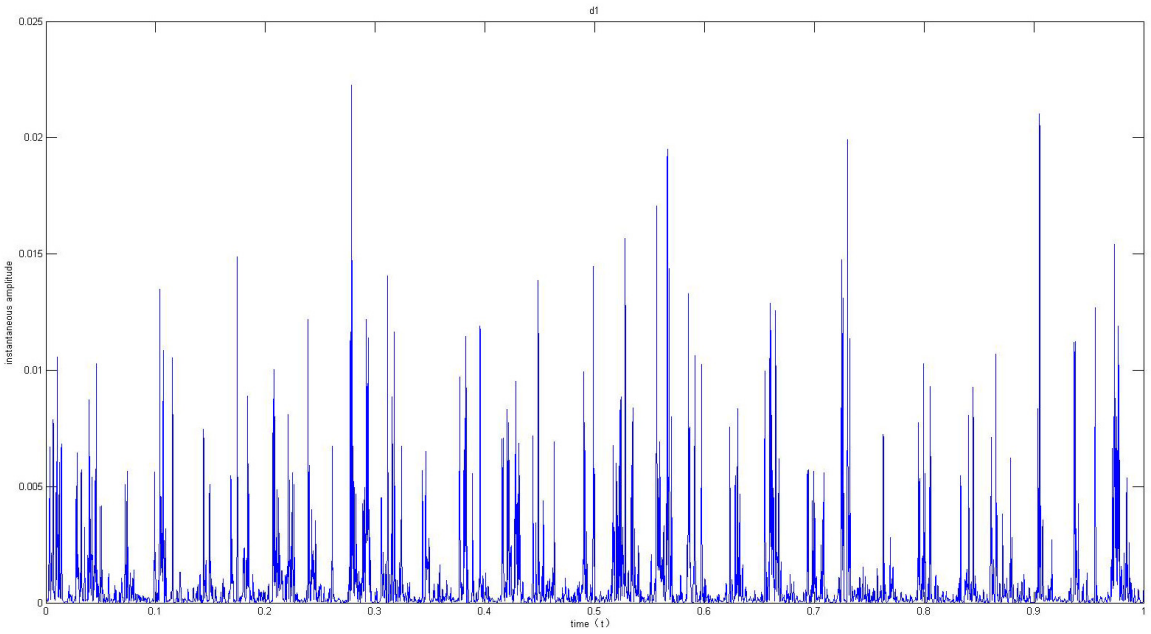

Figure 45 Instantaneous amplitude of d1 for the gear with 60% crack

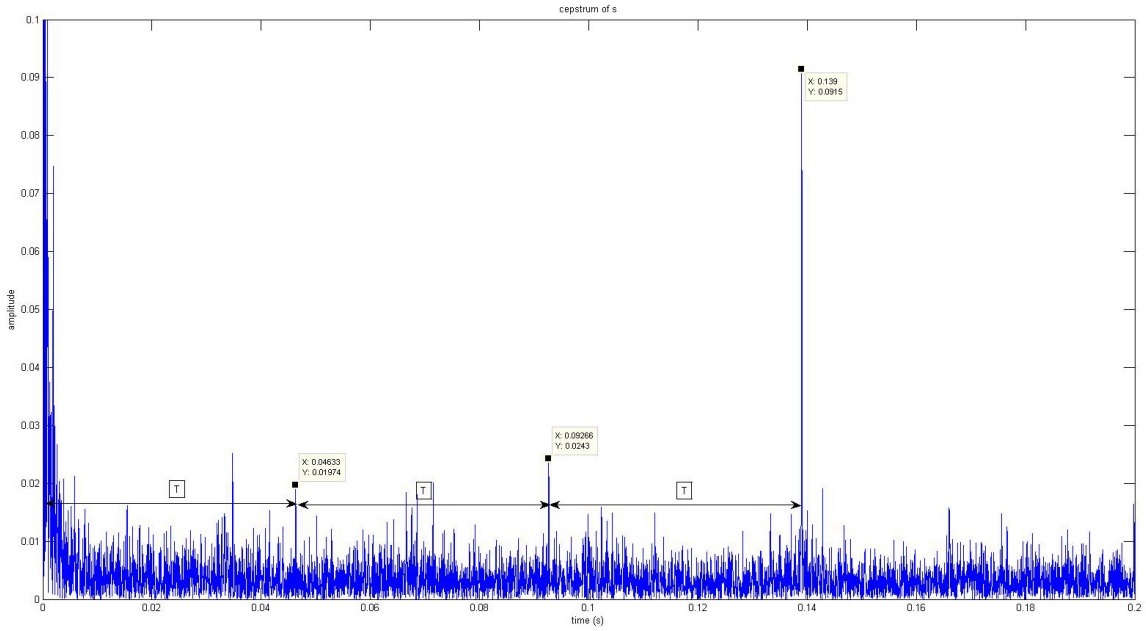

Figure 46 Cepstrum analysis of the entire original signal for the gear with 60% crack

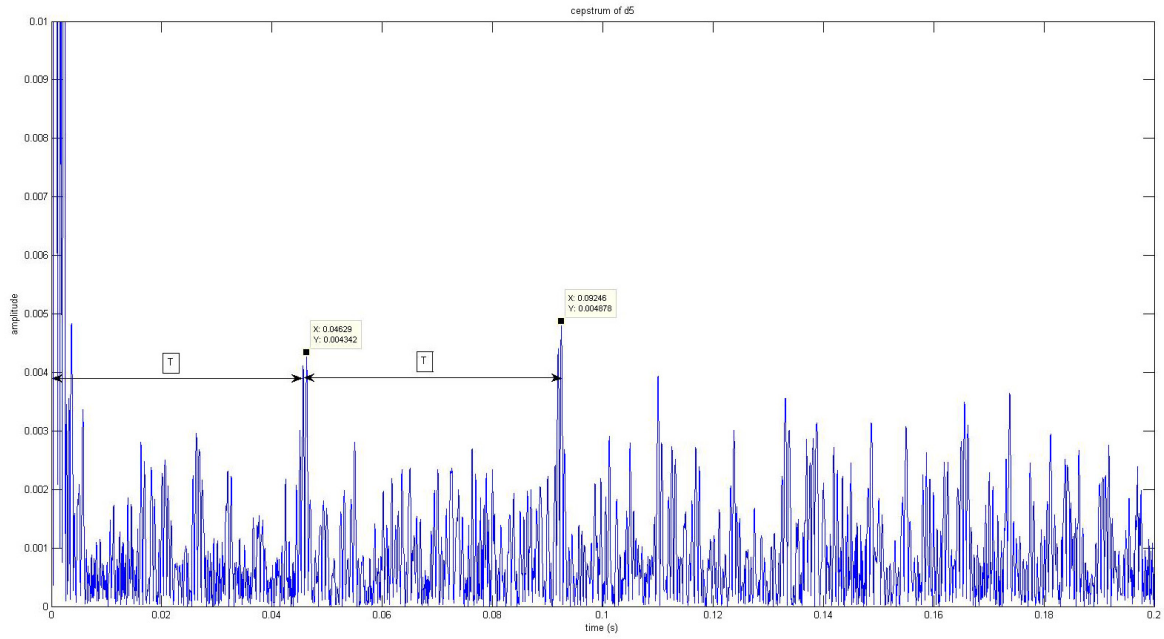

Figure 47 Cepstrum analysis of d5 for the gear with 60% crack

4.3.2.5 Gear with 80% crack

In Figure 49, there are peaks values: (29, 9.242) corresponding to gear 3's rotating frequency and (554, 3.427) corresponding to its meshing frequency. Compared with the healthy gear, the value at the point 29Hz has greatly increased. There exist a period $T \approx 0.0456s$ and $f = \frac{1}{T} = 21.9Hz$ in the instantaneous amplitude of d1 (Figure 50), which means there are periodic impact in the signal. It is near the rotating period of gear 3. We can find gear 3's rotating frequency in the Cepstrum analysis of the entire original signal (Figure 51) but it is not very obvious. In Figure 52, there also exists obvious period with $T \approx 0.0463s$, and its frequency is $\frac{1}{T} = 21.6Hz$ corresponding to gear 3's rotating frequency. Therefore, we can determine that gear 3 has a fault by time-frequency analysis. Compared the result of Figure 50, Figure 51 and Figure 52, the proposed method is more clear and intuitionistic than the other two methods.

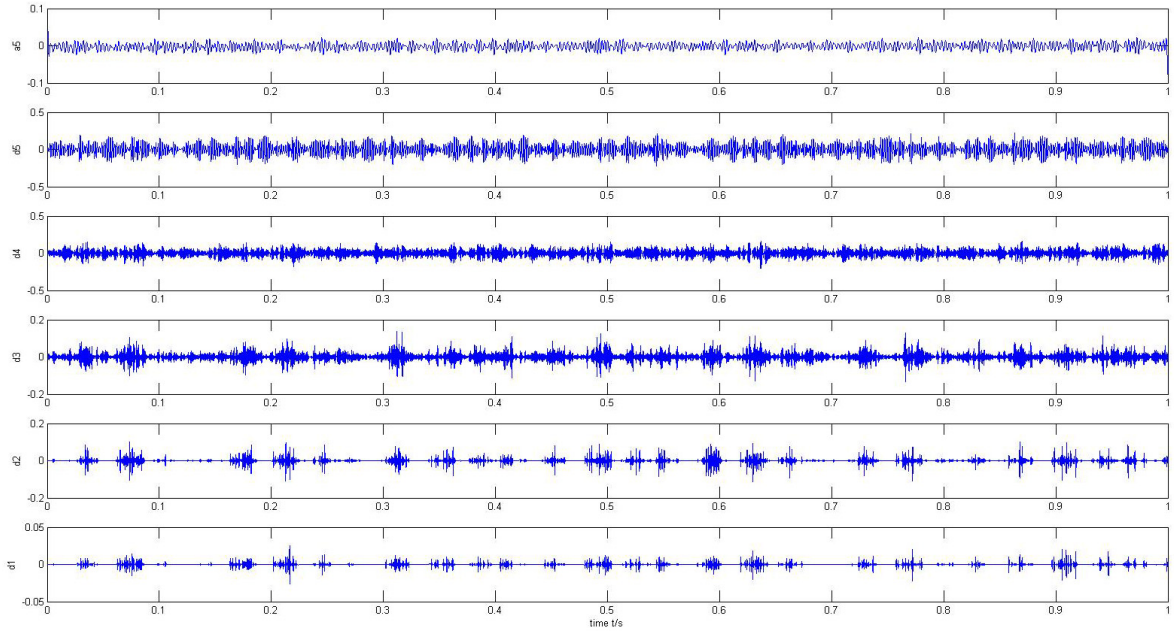

Figure 48 Approximation signal and detail signals for the gear with 80% crack

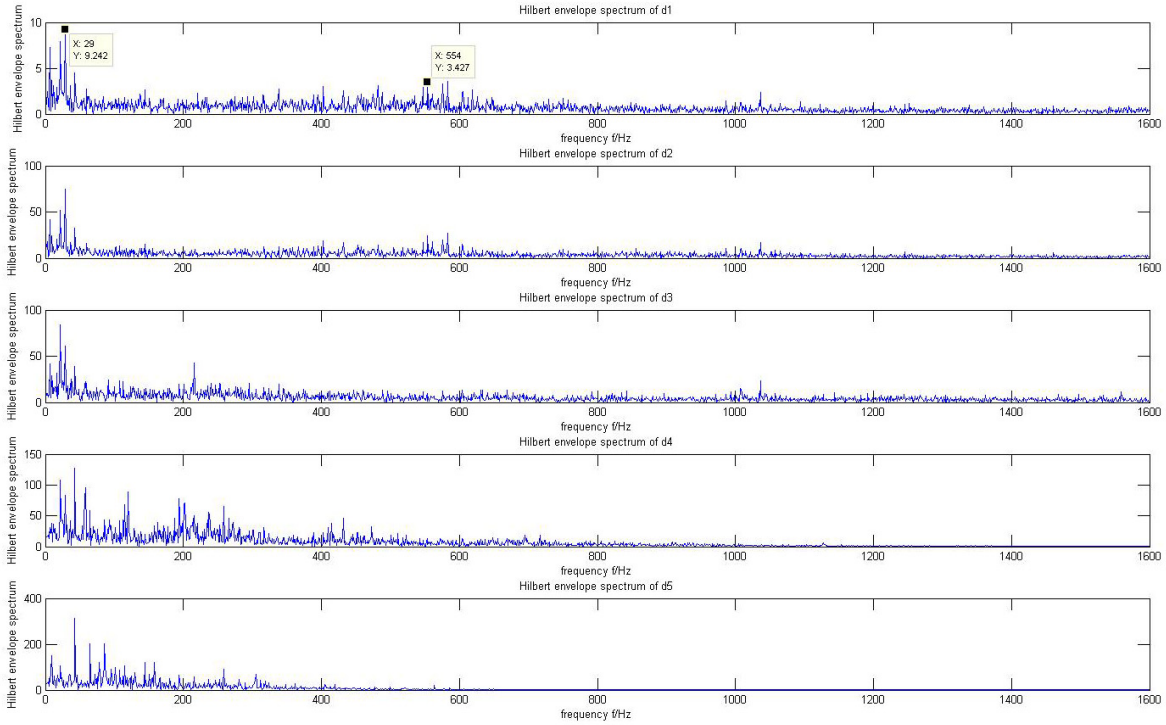

Figure 49 Hilbert envelope spectrum analysis for the gear with 80% crack

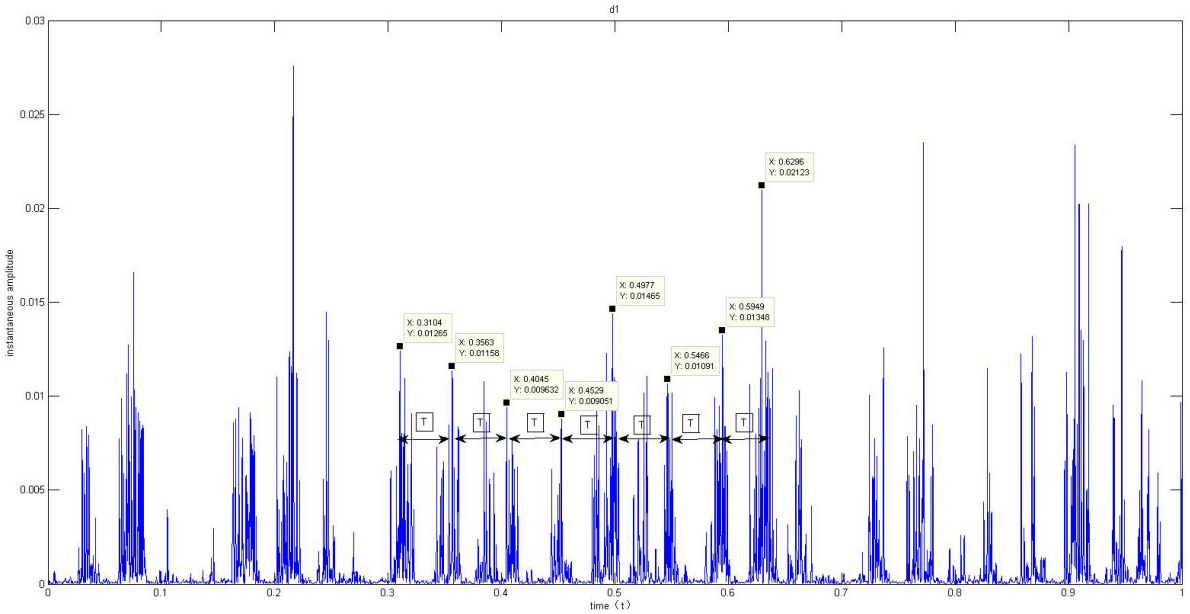

Figure 50 Instantaneous amplitude of d1 for the gear with 80% crack

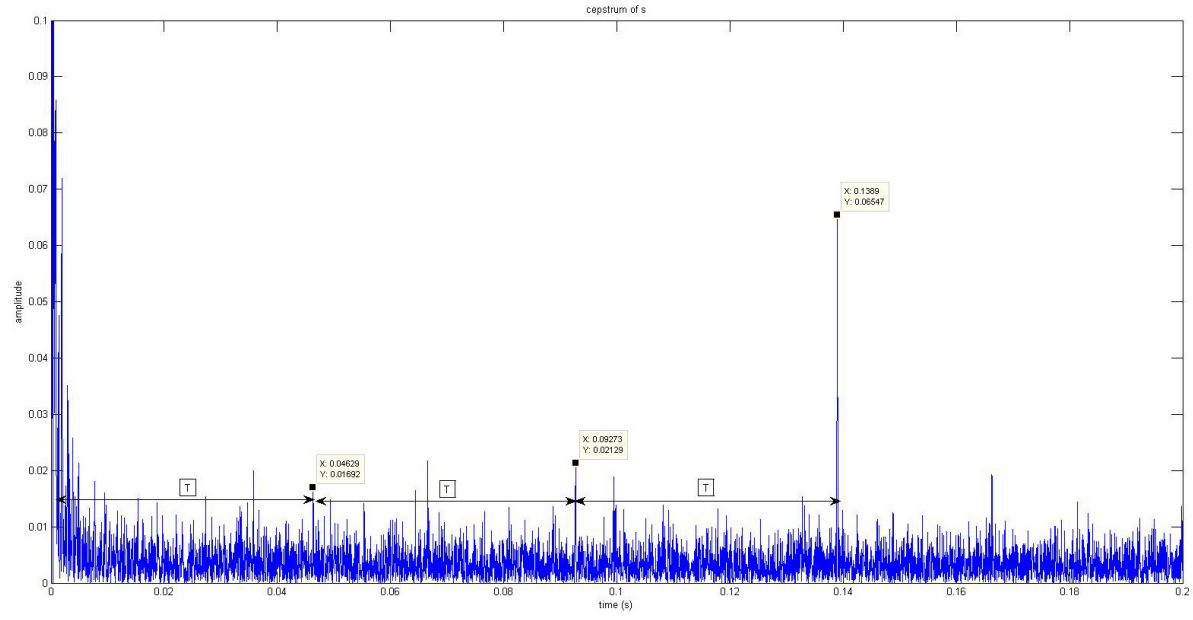

Figure 51 Cepstrum analysis of the entire original signal for the gear with 80% crack

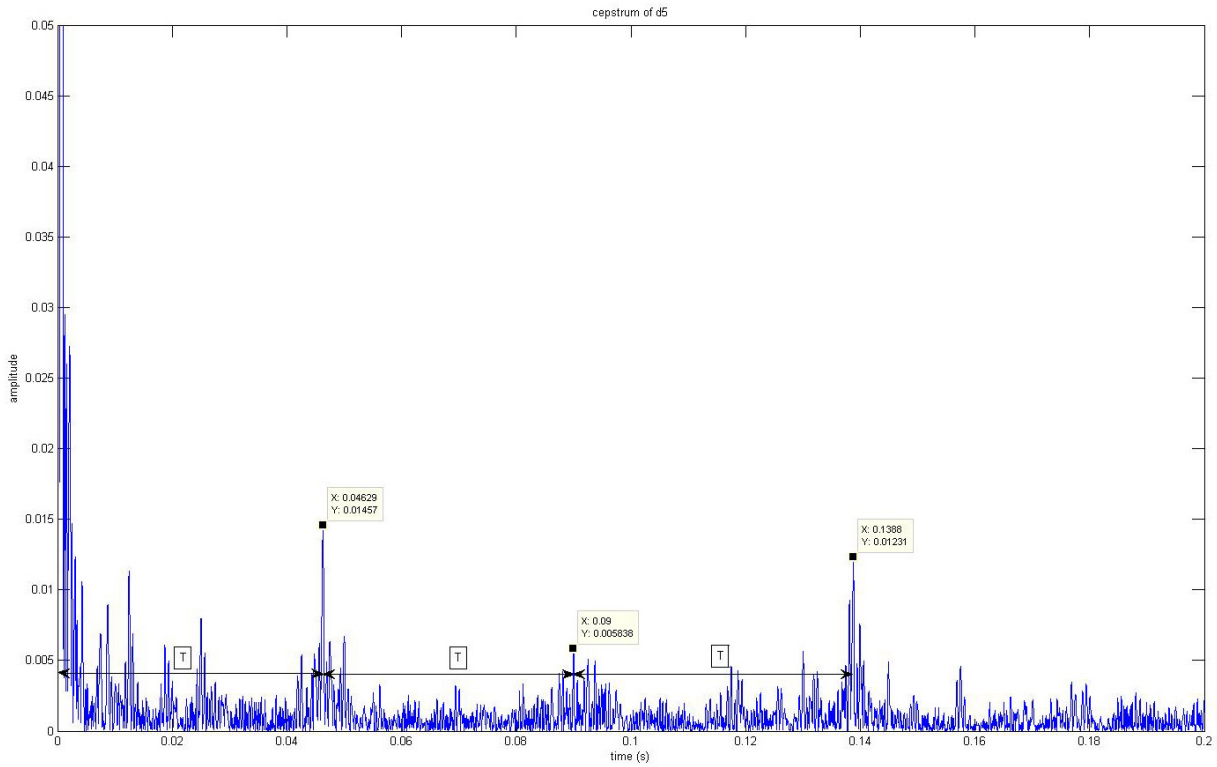

Figure 52 Cepstrum analysis of d5 for the gear with 80% crack

4.3.3 The HHT method

Due to HHT's particular noise immunity, we use the original raw signal directly. After decomposing the collected data into a series of IMFs through EMD, we apply Hilbert spectral analysis to extract the features from the IMFs for gear fault diagnosis.

4.3.3.1 Healthy gear

Figure 53 to Figure 56 show the total 11 IMFs and the residue of the signals that decomposed by EMD. Then we apply Hilbert spectral analysis to analyze IMF1, which contains the most information of the signal. Figure 57 shows the power spectrum of IMF1 that reflect the frequency distribution of the signal and there exists a peak value (28, 107.3) corresponding to gear 3's rotating frequency. Figure 58 shows IMF1's instantaneous envelope spectrum analysis

that present the instantaneous amplitude. The Hilbert marginal spectrum of the signal is shown in Figure 59.

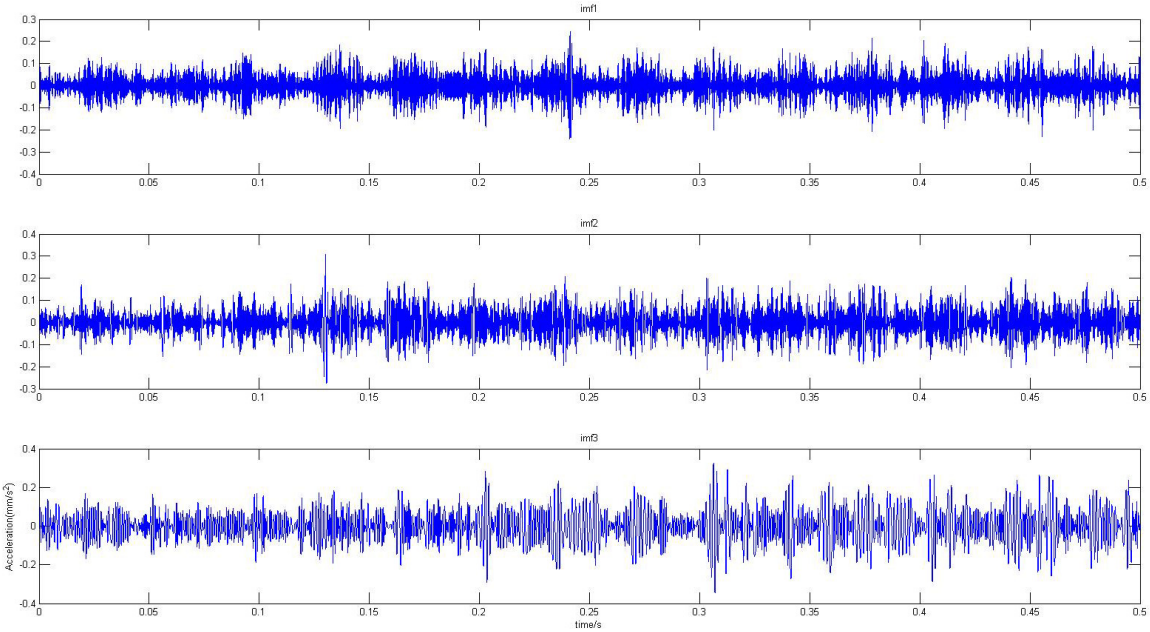

Figure 53 IMF1-IMF3 for the healthy gear

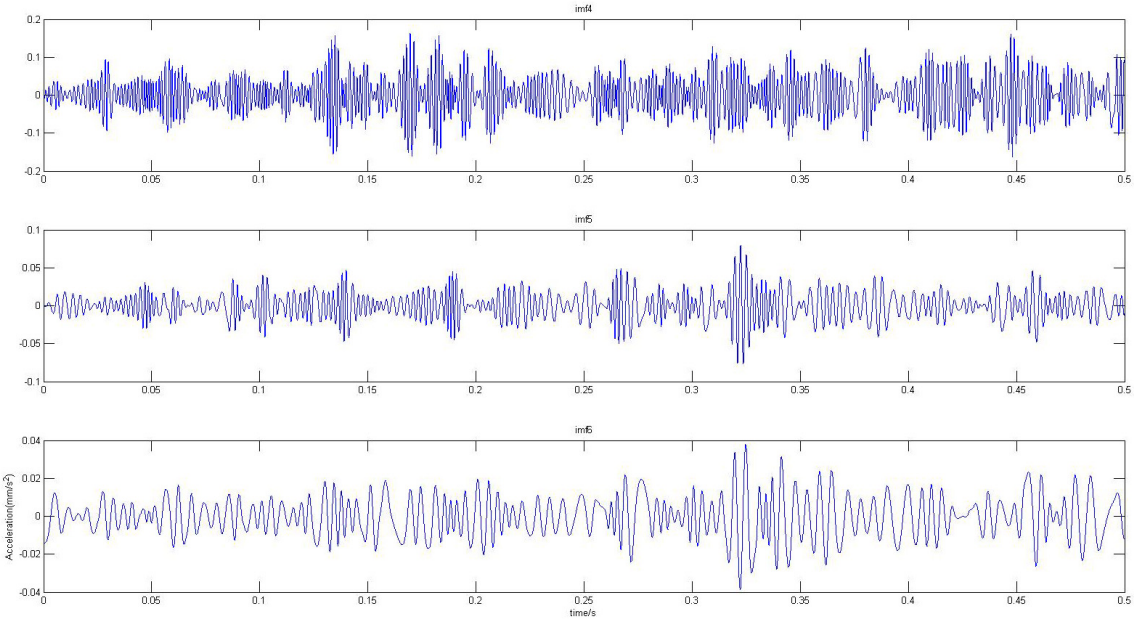

Figure 54 IMF4-IMF6 for the healthy gear

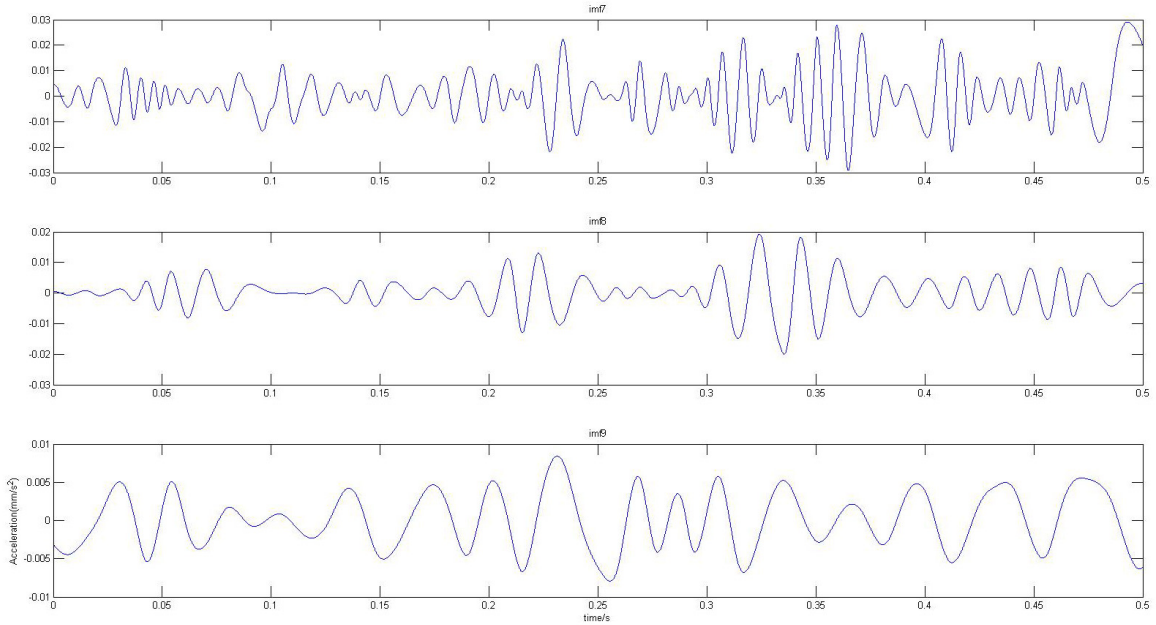

Figure 55 IMF7-IMF9 for the healthy gear

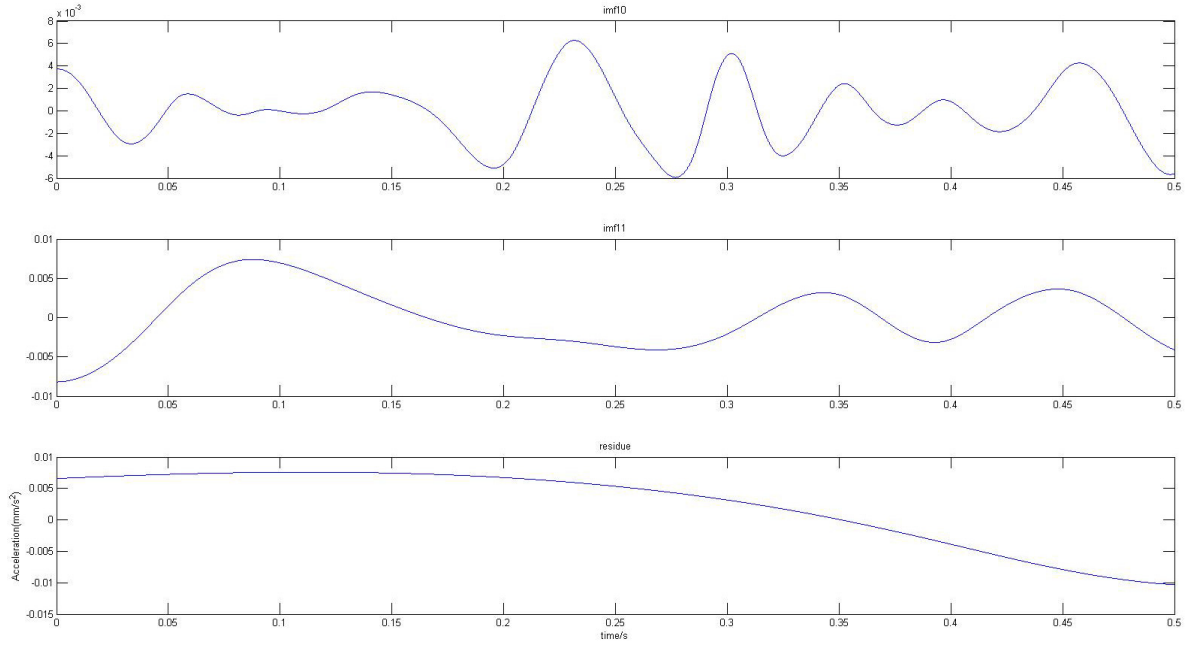

Figure 56 IMF9-IMF10 and residue for the healthy gear

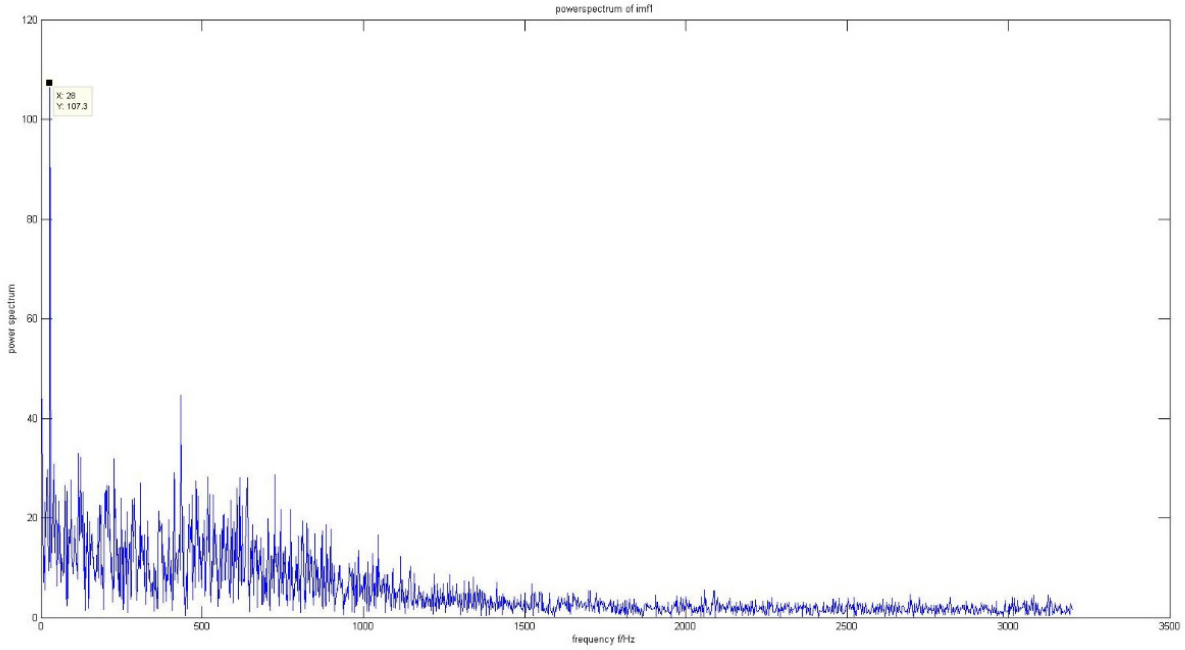

Figure 57 The power spectrum of IMF1 for the healthy gear

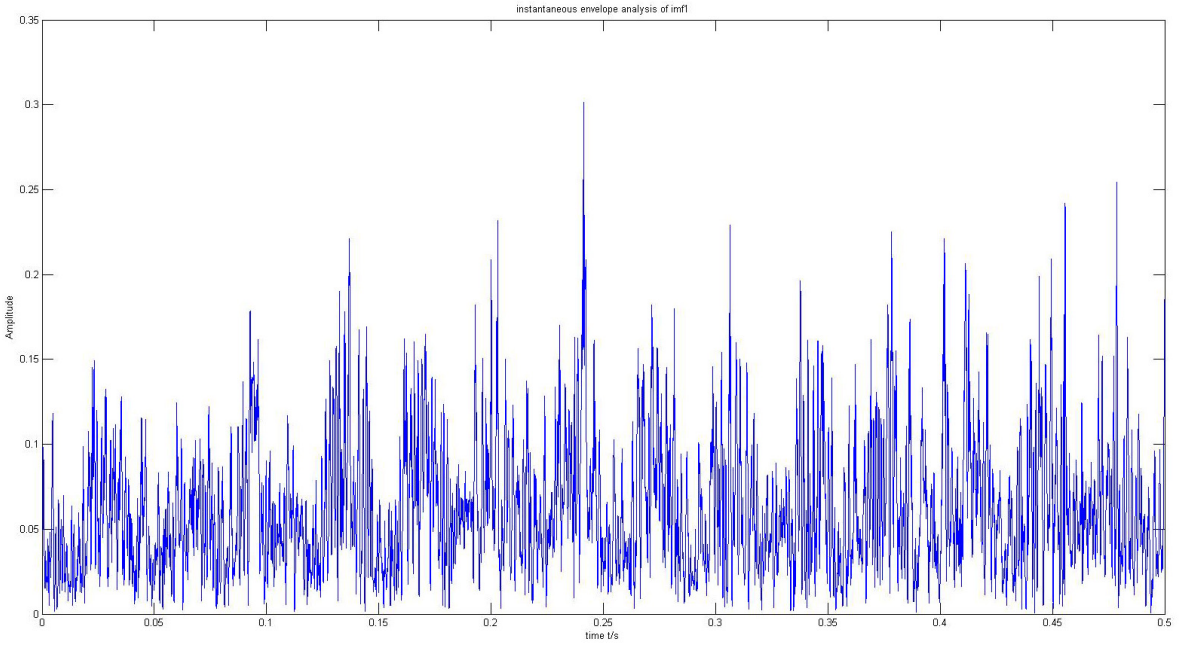

Figure 58 IMF1's instantaneous envelope spectrum analysis for the healthy gear

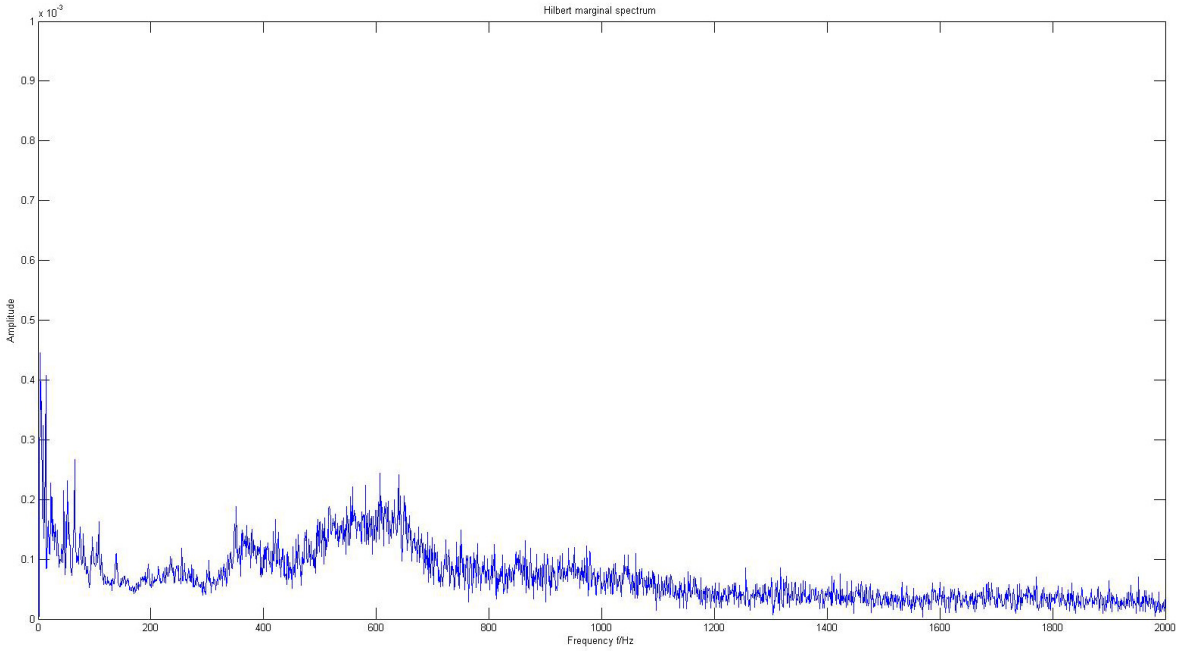

Figure 59 Hilbert marginal spectrum of the signal for the healthy gear

4.3.3.2 Gear with 25% crack

Since most information of the signal is contained in first several IMFs, we only show IMF1 - IMF3 in Figure 60. Figure 61 shows the power spectrum of IMF1 and there doesn't exist the frequency corresponding to the faulty gear. Figure 62 shows IMF1's instantaneous envelope spectrum analysis but there doesn't exist obvious period of the impact. The Hilbert marginal spectrum of the signal is shown in Figure 63, which also doesn't have the information of the faulty gear.

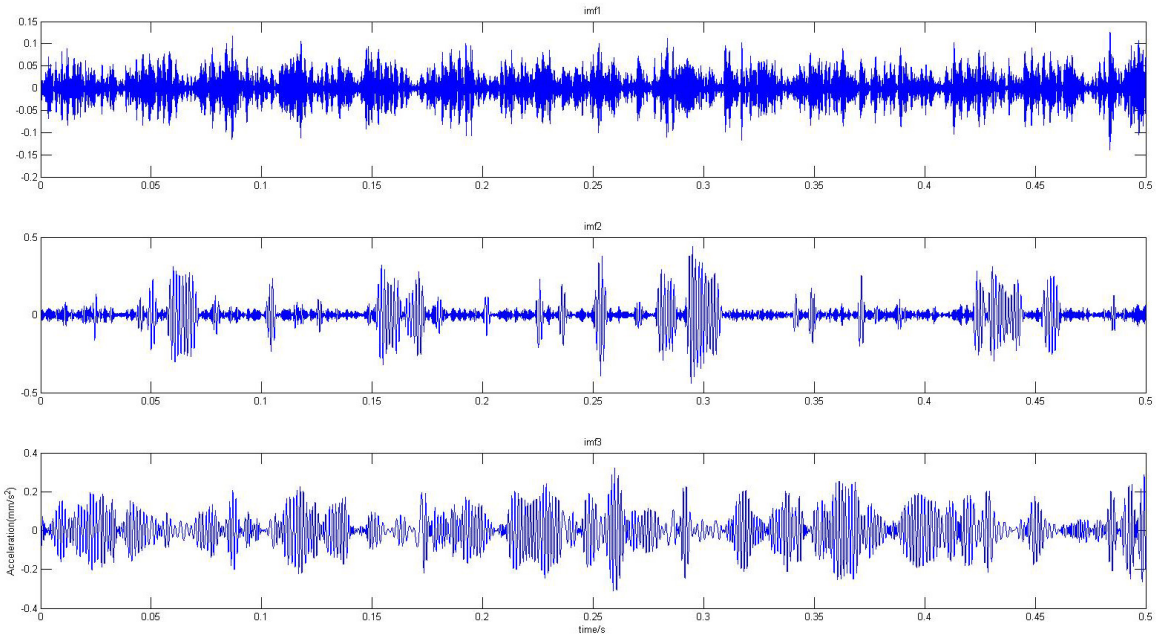

Figure 60 IMF1-IMF3 for the gear with 25% crack

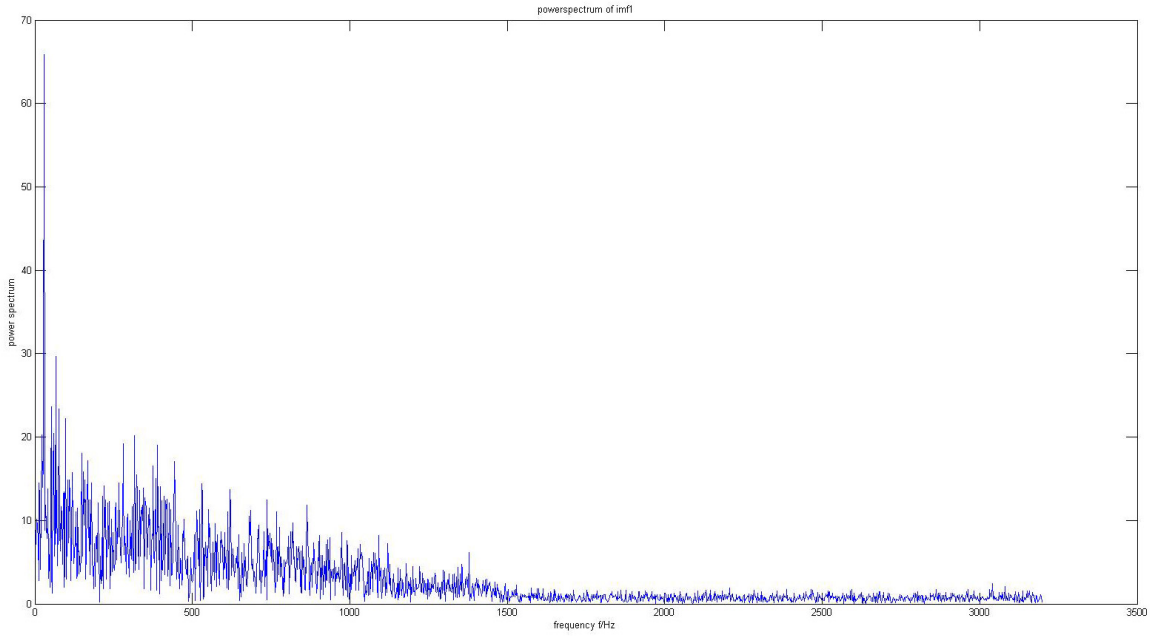

Figure 61 The power spectrum of IMF1 for the gear with 25% crack

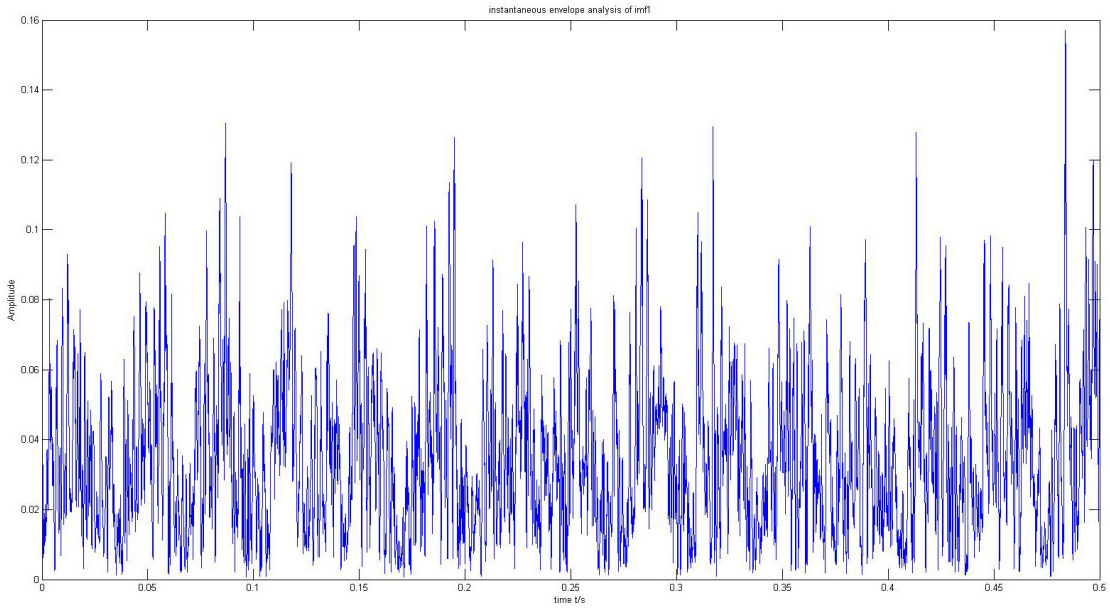

Figure 62 IMF1's instantaneous envelope spectrum analysis for the gear with 25% crack

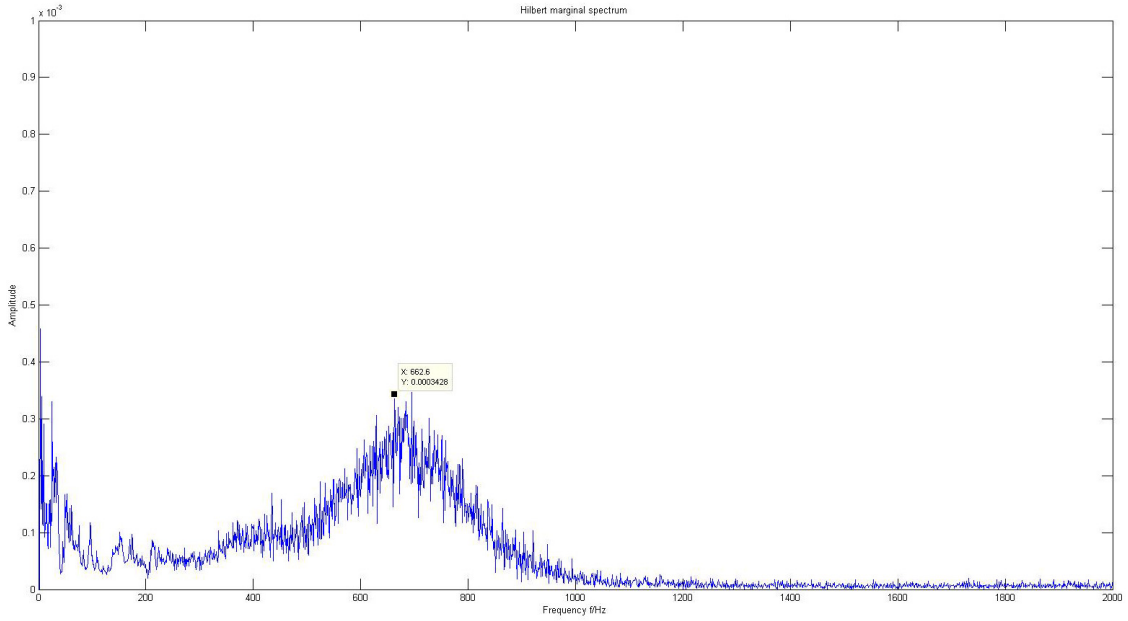

Figure 63 Hilbert marginal spectrum of the signal for the gear with 25% crack

4.3.3.3 Gear with 40% crack

Figure 64 shows the IMF1 - IMF3 of the gear's root cut in 40% degree. Figure 65 is the power spectrum of IMF1 where there are peak value (28, 136.9) corresponding to gear 3's rotating frequency, (518, 47.98) & (1034, 40.61) corresponding to gear 3's meshing frequency and its second harmonic frequency. Compared with the peak value (28, 107.3) of the healthy gear, it has highly increased. Figure 66 shows IMF1's instantaneous envelope spectrum analysis but the period of the impulses is not obvious enough. The Hilbert marginal spectrum of the signal is shown in Figure 67, and the frequency corresponding to the peak is 519.6Hz is corresponding to gear 3's meshing frequency. Even though the time domain analysis is not clear enough, we can still determine that there is a fault on gear 3 based on frequency domain analysis.

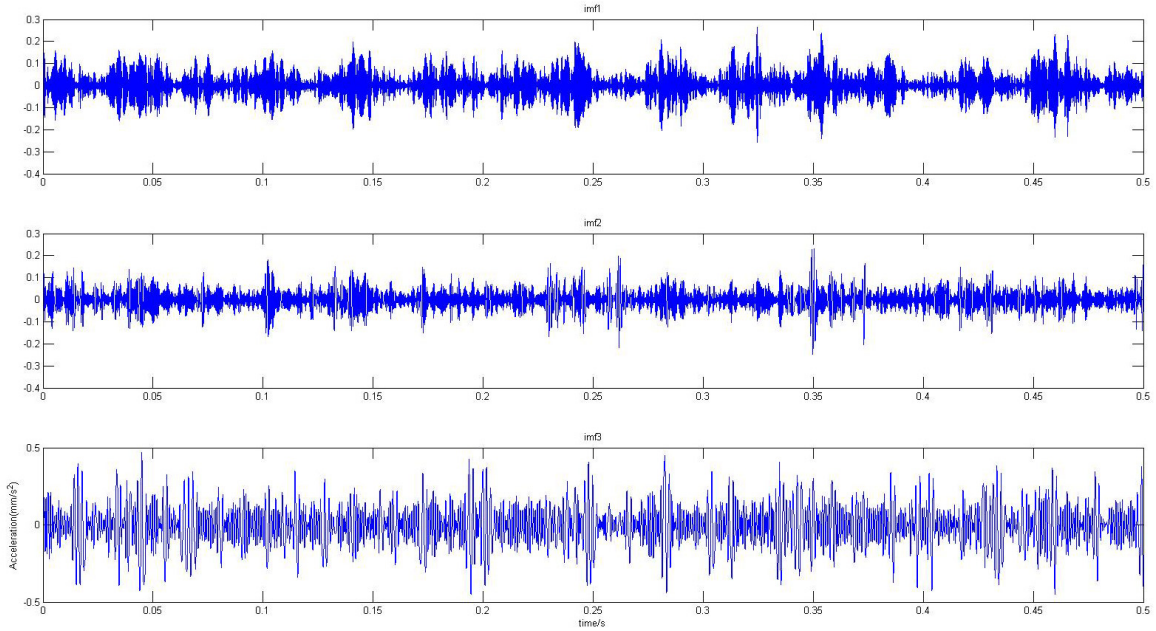

Figure 64 IMF1-IMF3 for the gear with 40% crack

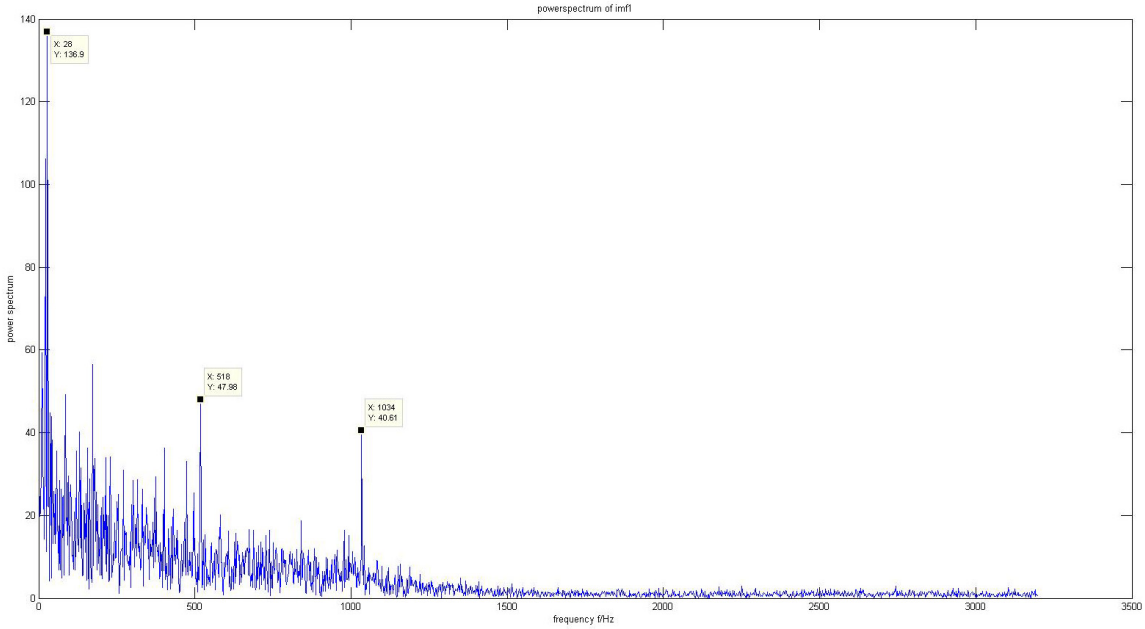

Figure 65 The power spectrum of IMF1 for the gear with 40% crack

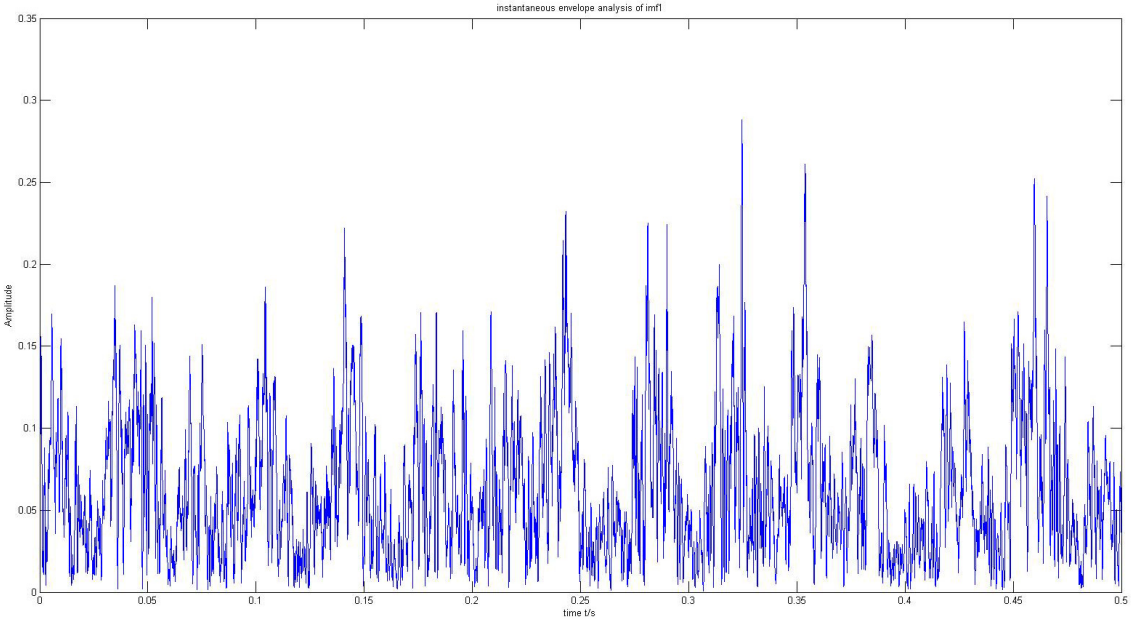

Figure 66 IMF1's instantaneous envelope spectrum analysis for the gear with 40% crack

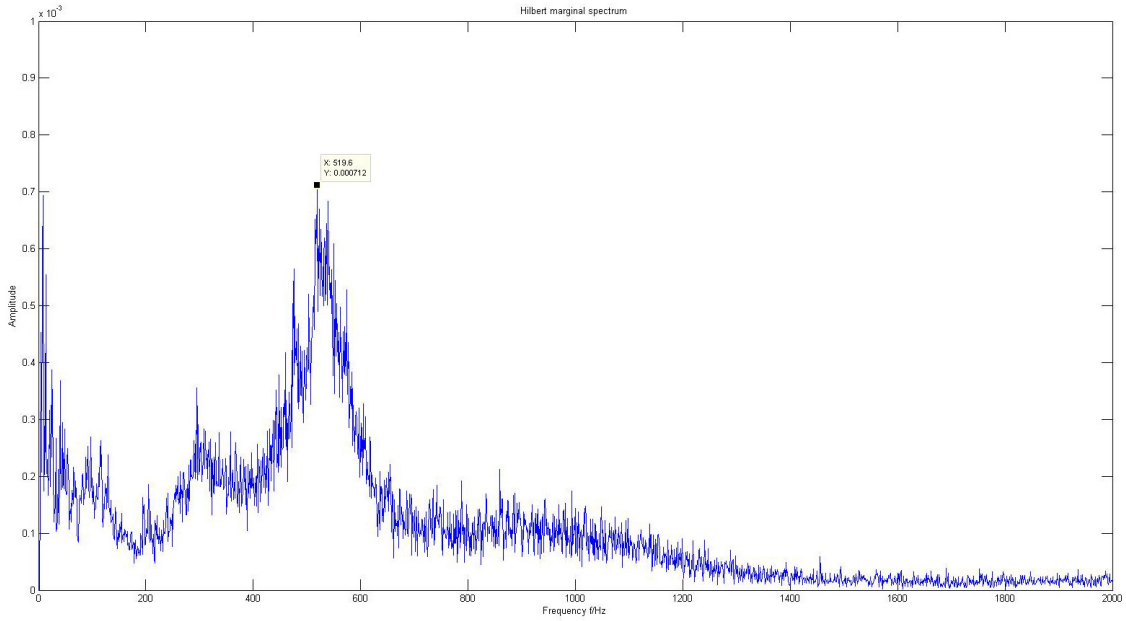

Figure 67 Hilbert marginal spectrum of the signal for the gear with 40% crack

4.3.3.4 Gear with 60% crack

Figure 68 presents the IMF1 - IMF3 of the gear's root cut in 60% degree. In the power spectrum of IMF1 (Figure 69), there are peak value (28, 120.2) corresponding to gear 3's rotating frequency, (518, 45.21) & (1036, 73.96) corresponding to gear 3's meshing frequency and its second harmonic frequency. Compared with peak value (28, 107.3) of the healthy gear, the value has increased. In Figure 70, there are the period of the impulses $T \approx 0.035s$ with the frequency $\frac{1}{T} = 28.5Hz$ which is close to gear 3's rotating frequency. In Figure 71, there are the corresponding frequencies 536.6Hz and 951.6Hz of the peaks, which are gear 3's meshing frequency and its harmonic frequency. Then the fault information of the gear 3 can be extracted by time-frequency domain analysis.

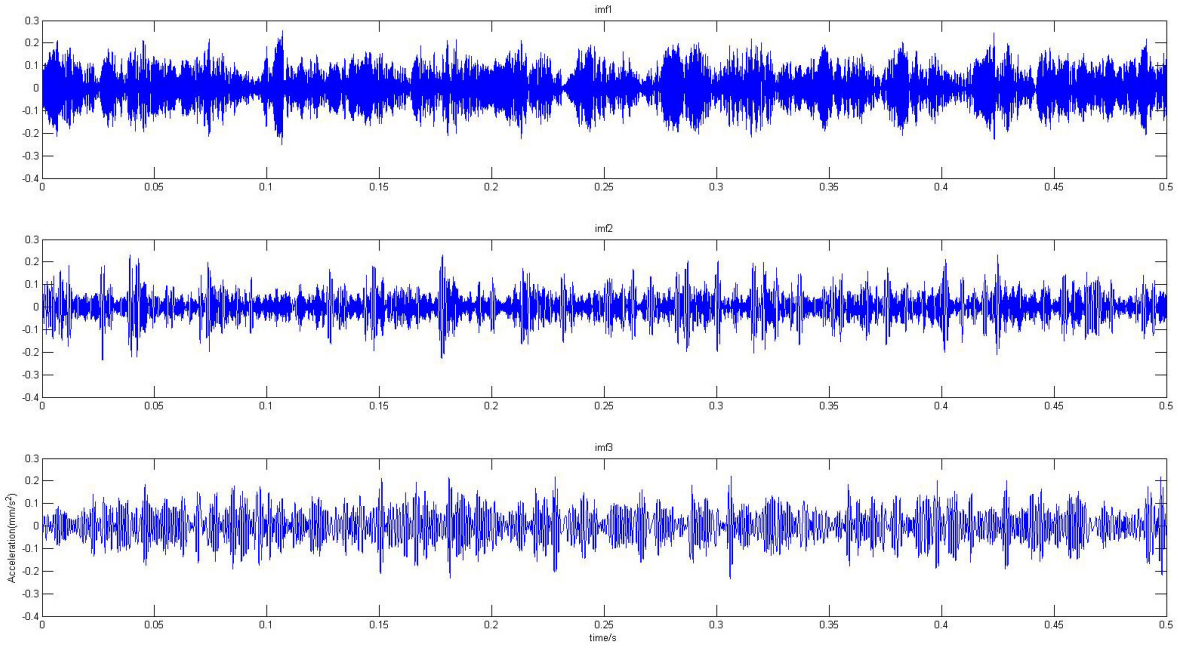

Figure 68 IMF1-IMF3 for the gear with 60% crack

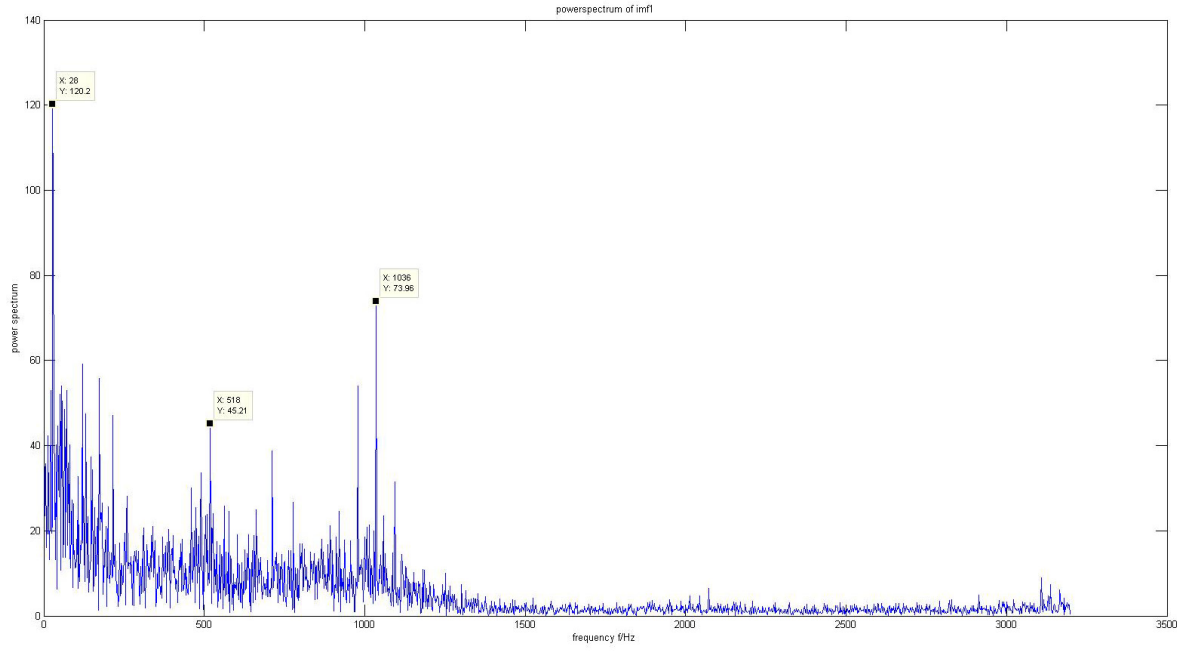

Figure 69 The power spectrum of IMF1 for the gear with 60% crack

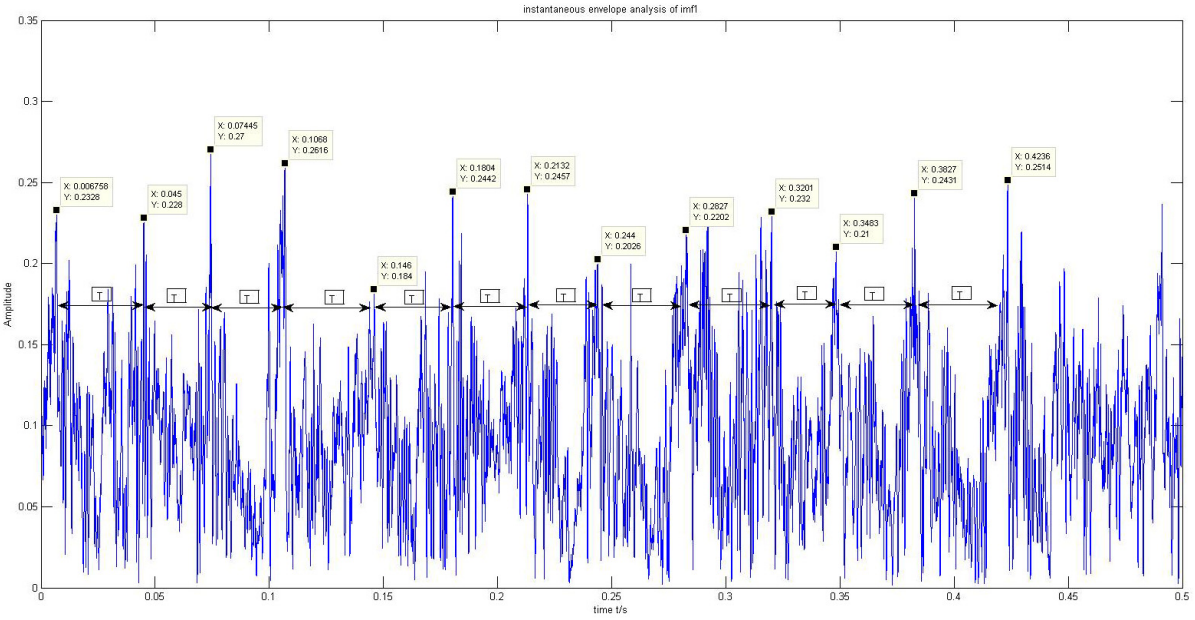

Figure 70 IMF1's instantaneous envelope analysis for the gear with 60% crack

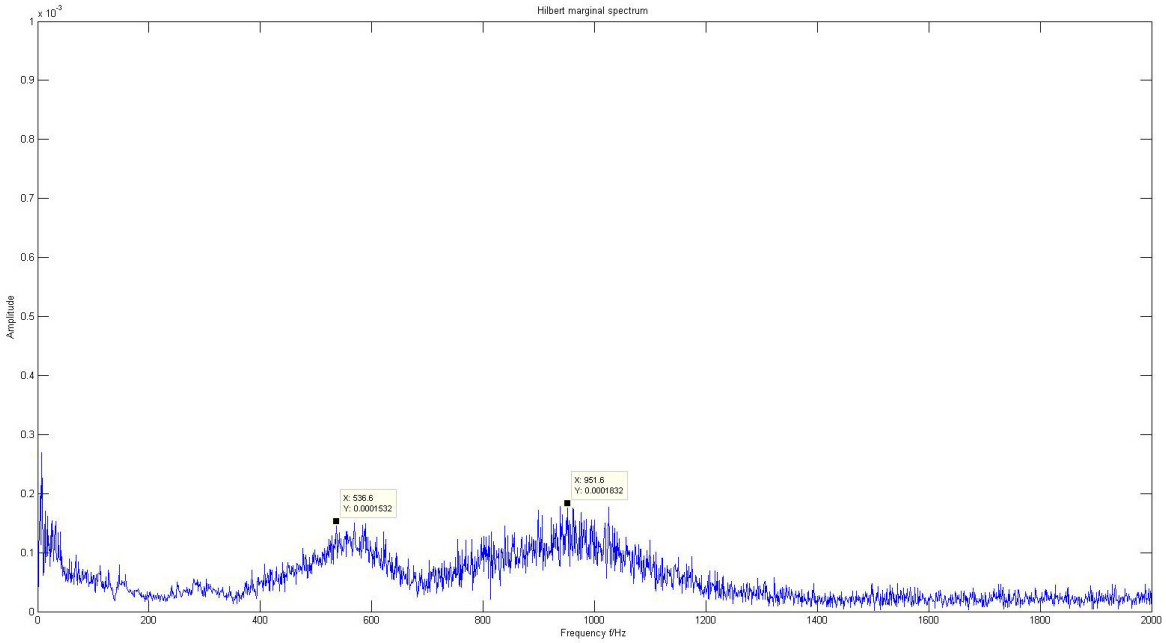

Figure 71 Hilbert marginal spectrum for the gear with 60% crack

4.3.3.5 Gear with 80% crack

Figure 72 shows that IMF1 has clear periodicity. In Figure 73, there are peak points (28, 136.4) corresponding to gear 3's rotating frequency, (576, 55.29) & (1036, 34.77) corresponding to gear 3's meshing frequency and its second harmonic frequency. Compared with peak value (28, 107.3) of the healthy gear, it has increased highly. There are the obvious period of the impulses with $T \approx 0.038s$ and its frequency is $\frac{1}{T} = 26.3Hz$, which is near gear 3's rotating frequency.

Figure 74 shows IMF1's instantaneous envelope analysis. Figure 75 shows the Hilbert marginal spectrum of the signal, where peak values' corresponding frequency is 543.6Hz, which is gear 3's meshing frequency. Therefore, HHT analysis works well on fault diagnosis of the gear with 80% crack.

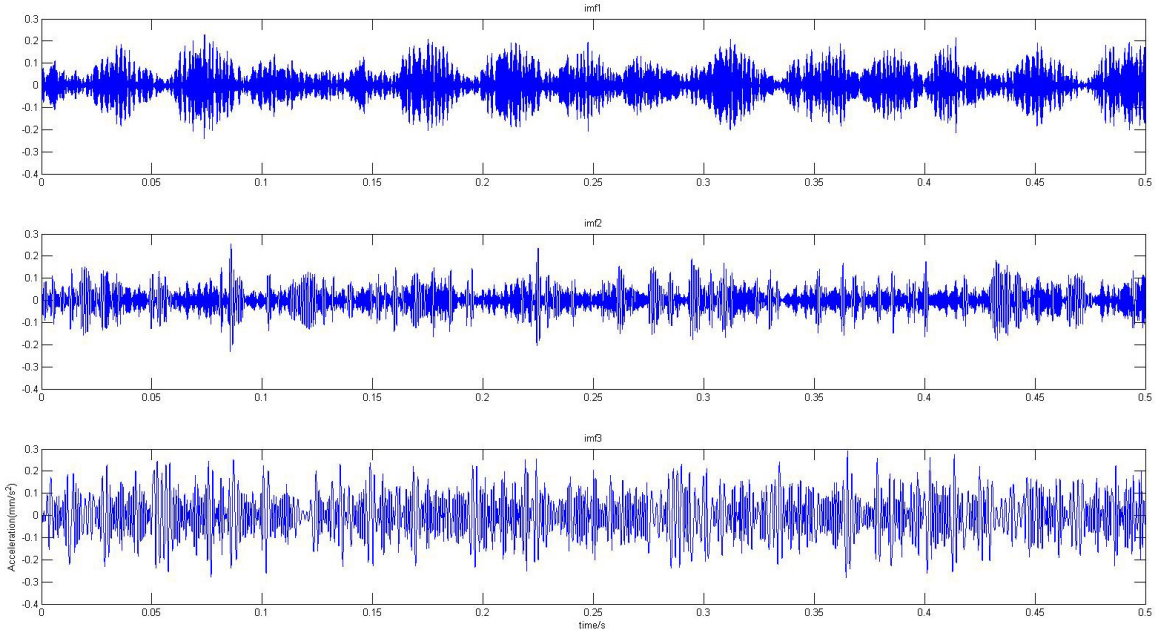

Figure 72 IMF1-IMF3 for the gear with 80% crack

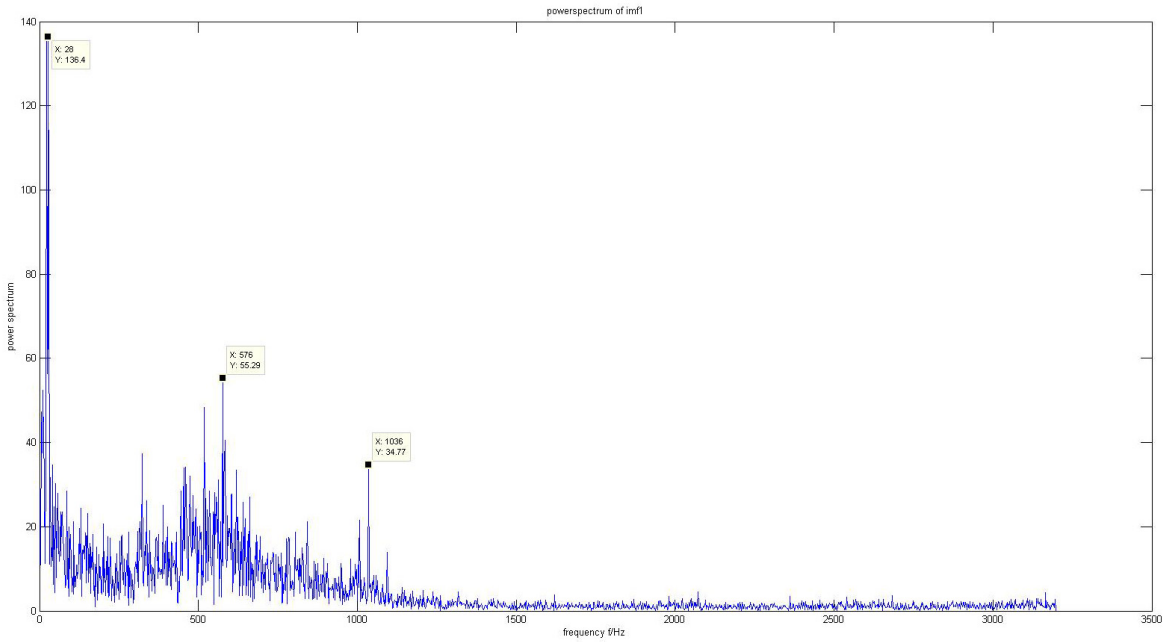

Figure 73 The power spectrum of IMF1 for the gear with 80% crack

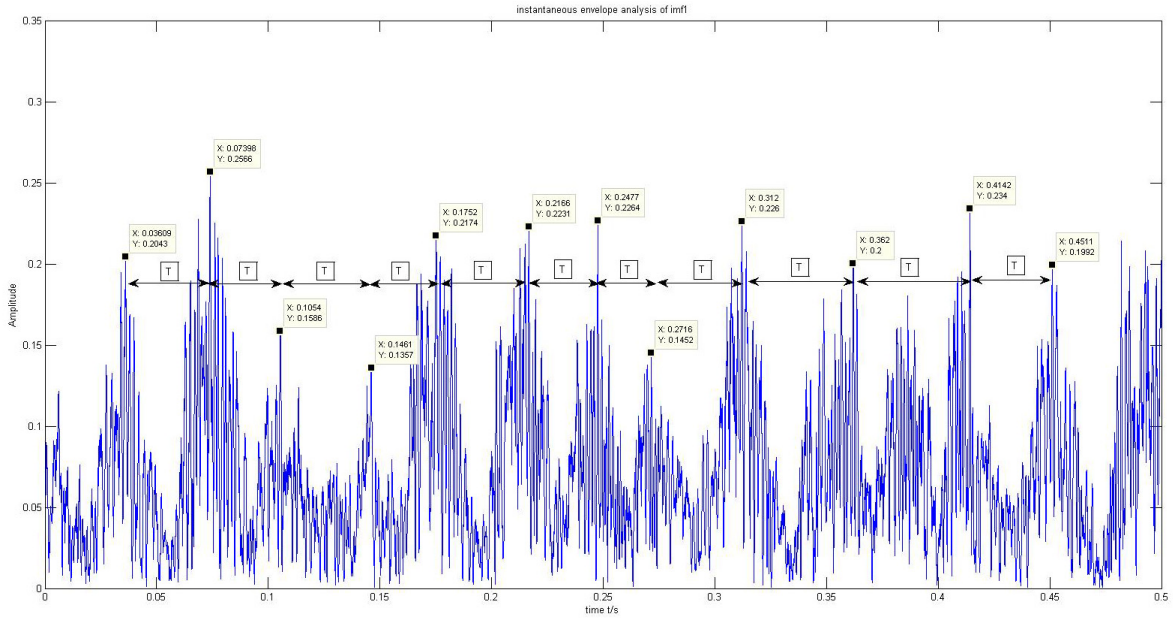

Figure 74 IMF1's instantaneous envelope analysis for the gear with 80% crack

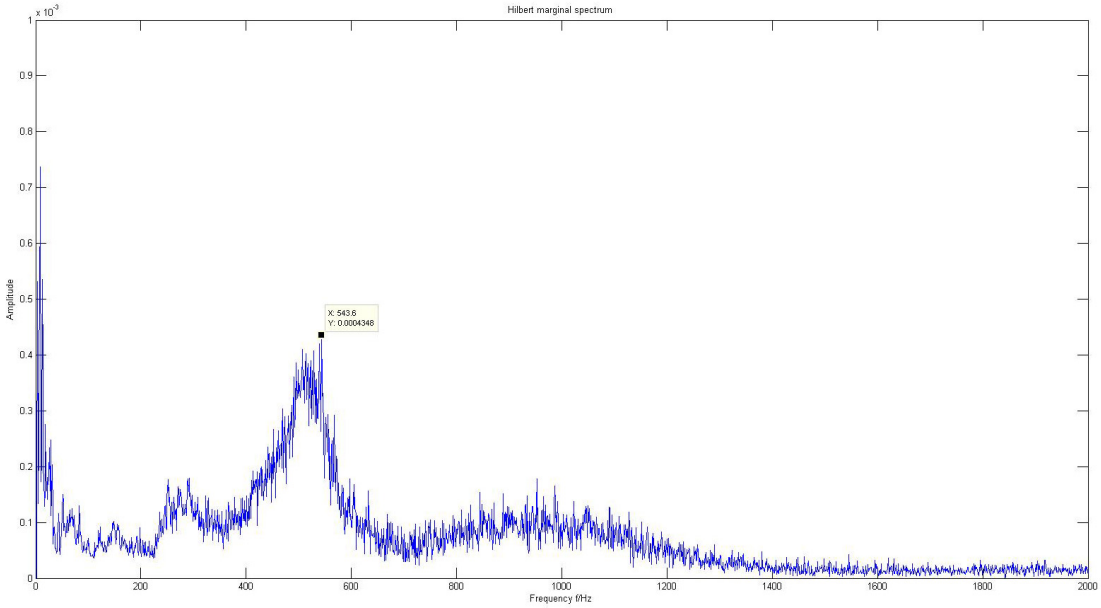

Figure 75 Hilbert marginal spectrum of the signal for the gear with 80% crack

According to the above results, we can find that all the methods cannot diagnose the fault of the damage in 25% degree. Perhaps it is because the energy of the damage is too weak to be collected by the accelerometer or it is 'masked' by the others frequency components such as noise and etc.

The HHT method performs more sensitive in frequency domain analysis than the other two methods. It can make fault diagnose of the gear after 40% crack while the other two methods can do it with the gear after 60% crack.

The proposed method shows its advantage in analyzing the periodic impulses in time domain than the other two methods. It also performs better than the existing methods of applying Cepstrum analysis directly. Its results are more intuitive and accurate.

Chapter 5

5. Case study on bearing fault diagnosis

5.1 Case introduction

The experimental data of the bearing is from our lab's collaborative partner: Green Power Monitoring Systems Company. The vibration signals were collected from the bearing with inner race fault (Figure 76) and outer race fault (Figure 77) respectively. The input shaft rate is 50Hz and the sampling frequency is 97656Hz. The bearing's parameters are shown in Table 2. Based on Eq. (34) and Eq. (35), we can calculate the faulty characteristic frequencies shown in Table 3.

Figure 76 Bearing with inner race fault

Figure 77 Bearing with outer race fault

Table 2 Bearing parameters

Parameter	No. of the rolling elements b	Ball bearing diameter d	Bearing pitch diameter e	Bearing contact angle β
Value	8	0.235	1.245	0

Table 3 Bearing faulty characteristic frequency

Name	Inner race fault	Outer race fault
Value(Hz)	237.75	162.25

5.2 Comparison of the methods

In this section, we compare the time-frequency methods mentioned above in fault diagnosis of the bearing with inner race fault and outer race fault respectively.

5.2.1 Time-wavelet energy spectrum

5.2.1.1 Healthy bearing

We first analyze the healthy bearing as a comparison. The time-domain waveform of the healthy gear collected from the gearbox is shown in Figure 78 and the Fast Fourier transform is shown in Figure 79. No periodic impulses can be found in the Frequency distribution of the time-wavelet spectrum shown in Figure 80. There is not obvious peak value that is corresponding to any faulty characteristic frequency in time-wavelet spectrum shown in Figure 81.

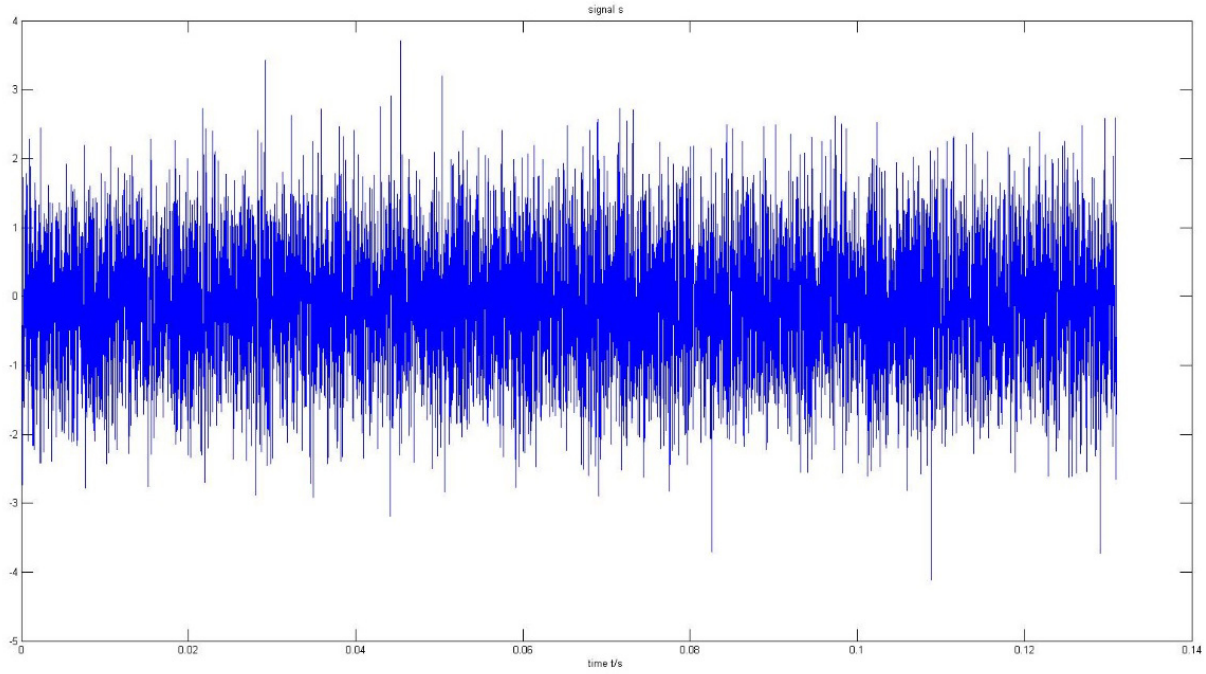

Figure 78 Time-domain waveform for the healthy bearing

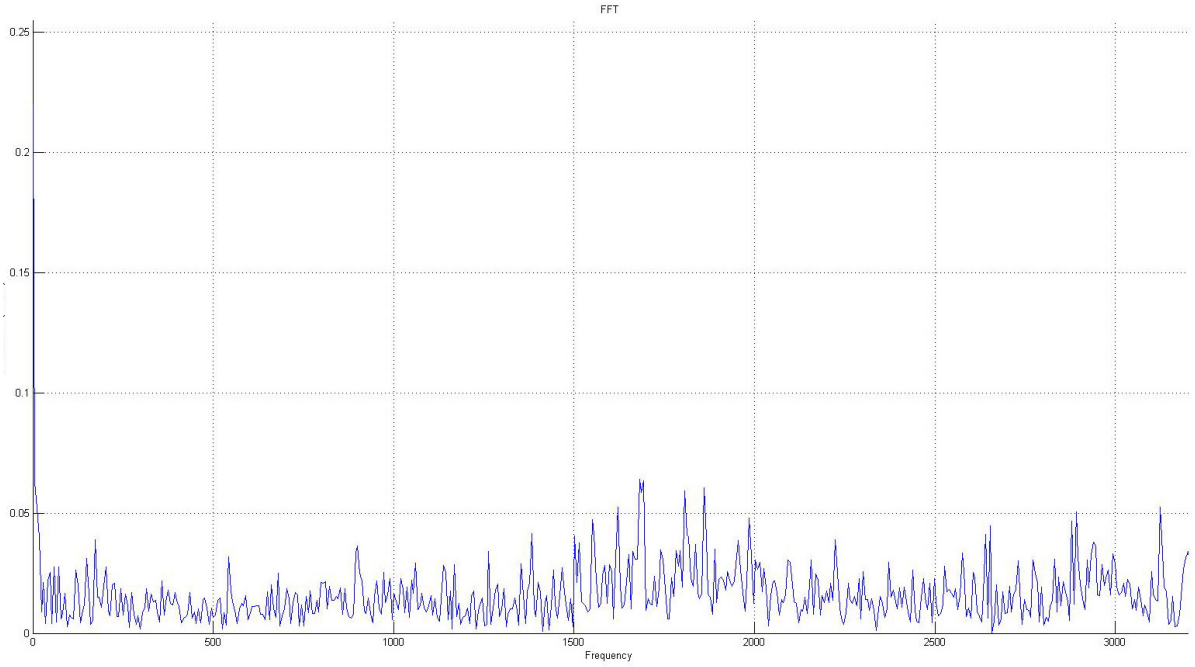

Figure 79 FFT for the healthy bearing

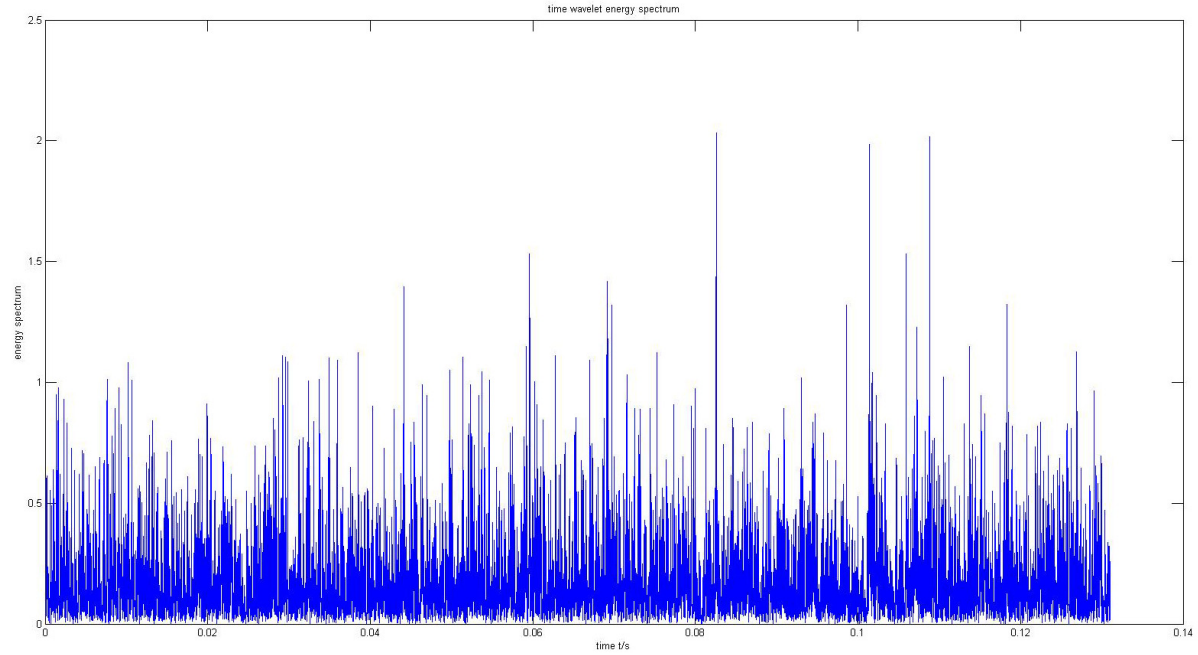

Figure 80 Time-wavelet spectrum for the healthy bearing

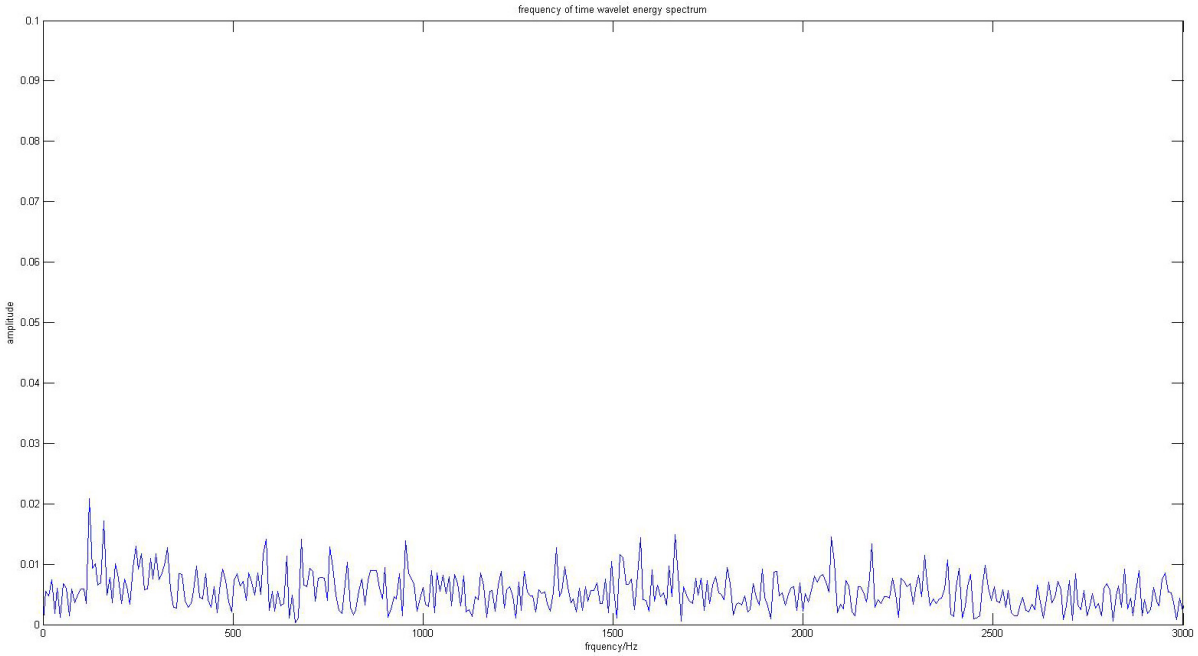

Figure 81 Frequency distribution of the time-wavelet spectrum for the healthy bearing

5.2.1.2 Bearing with inner race fault

We apply the method to analyze the signal collected from the bearing with inner race fault. Figure 82 is the time-domain waveform where we can find there are many obvious impulses. But there is no peak values that is corresponding to the characteristic frequency of the inner race fault in Figure 83 (the Fast Fourier transform). There are obvious vibration periods in Figure 84 with $T \approx 0.0042s$ and its frequency is $\frac{1}{T} = 238.09Hz$, which is correspond to the characteristic frequency of the inner race fault (237.75Hz). There are frequency values of the two highest peak 236.5Hzand 473Hz which is corresponding to the bearing's faulty characteristic frequency and its second harmonic in Figure 85. Hence, we can conclude that the bearing has an inner race fault.

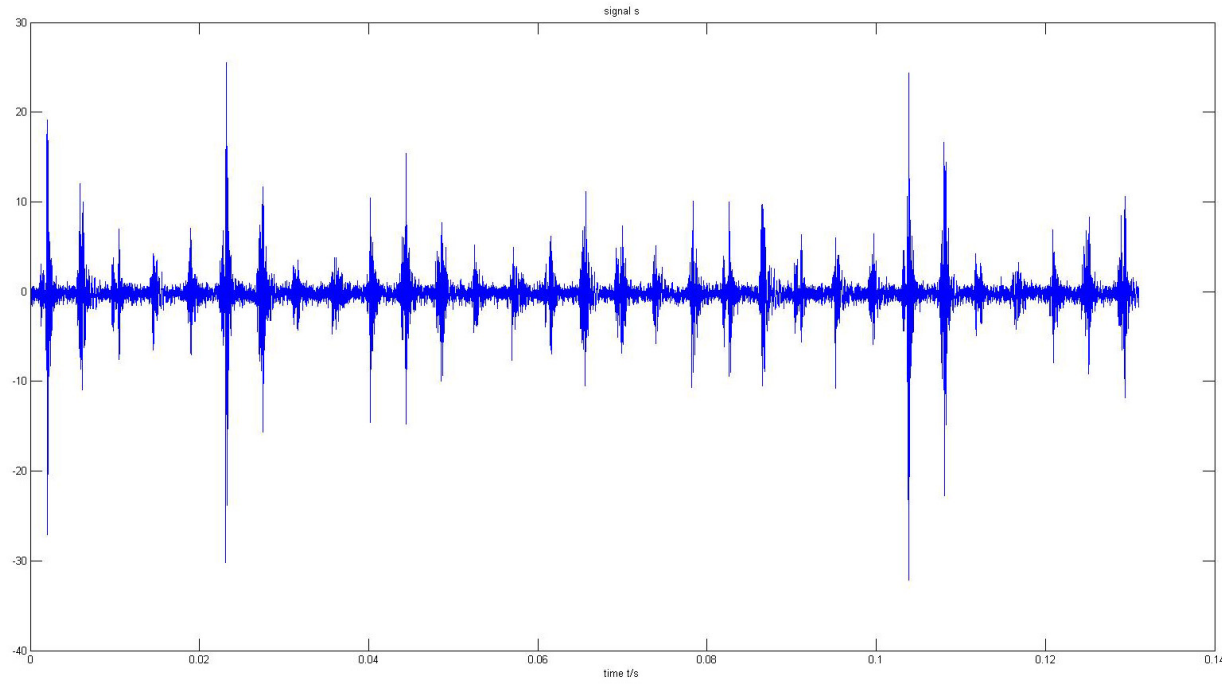

Figure 82 Time-domain waveform for the bearing with inner race fault

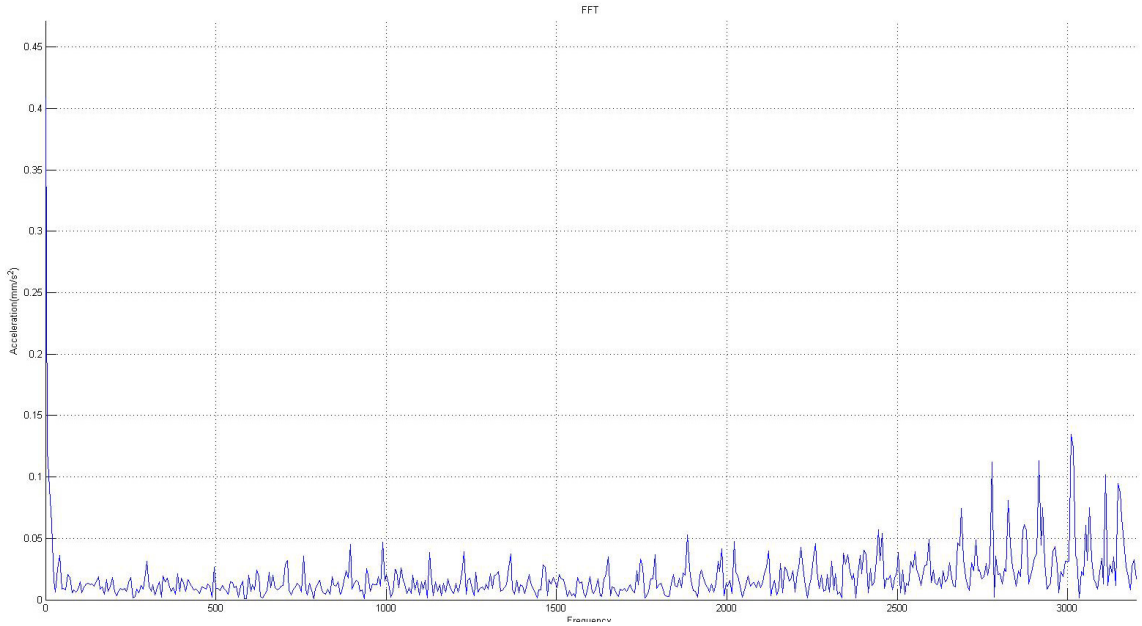

Figure 83 FFT for the bearing with inner race fault

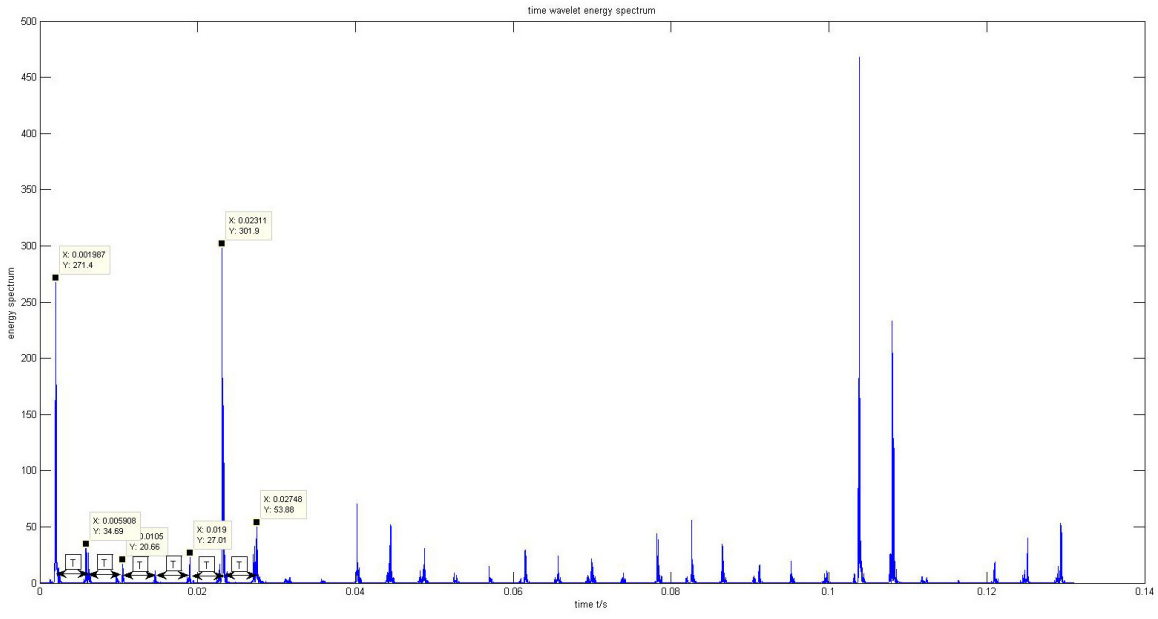

Figure 84 Time-wavelet spectrum for the bearing with inner race fault

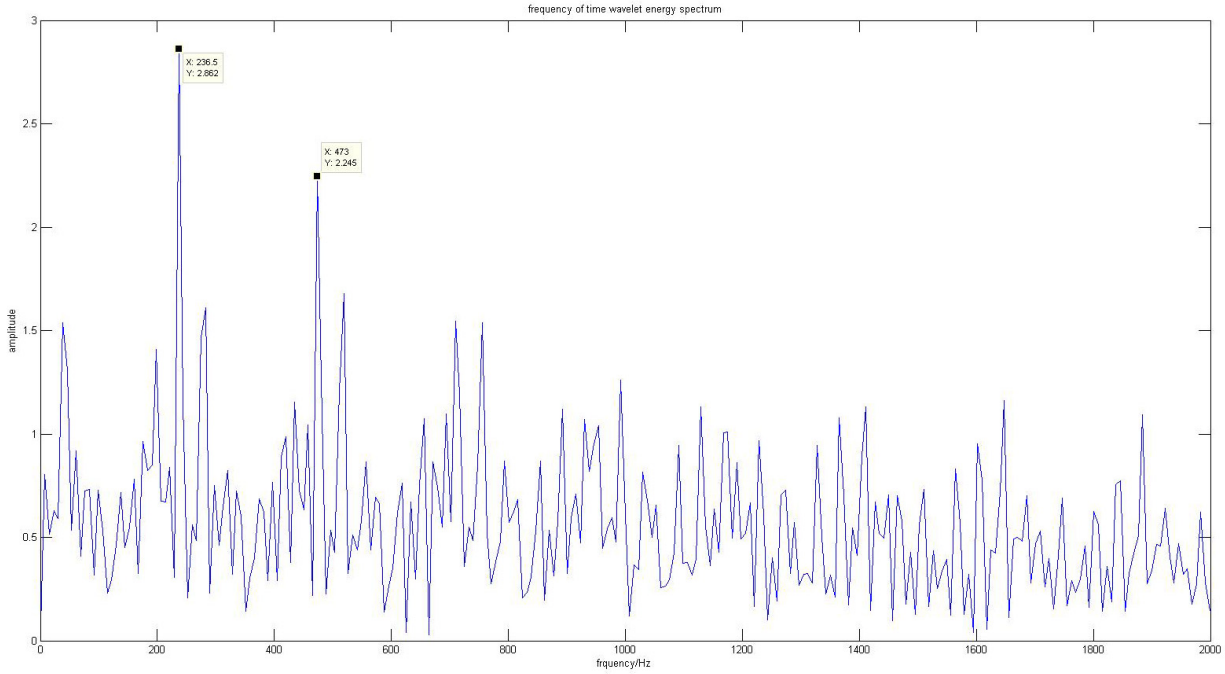

Figure 85 Frequency distribution for the bearing with inner race fault

5.2.1.3 Bearing with outer race fault

The time-domain waveform of the signal collected from the bearing with outer race fault is shown in Figure 86. We can find there are many obvious impulses in it. But there is no frequency values of the peak that is corresponding to the characteristic frequency of the outer race fault in Figure 87 (the Fast Fourier transform). There are obvious vibration period in Figure 88 with $T \approx 0.0062s$ and its frequency is $\frac{1}{T} = 161.29Hz$, which is corresponding to the characteristic frequency of the outer race fault (162.25Hz). There are obvious peak value points 160.2Hz and 320.2Hz, which are corresponding to the bearing's faulty characteristic frequency and its second harmonic in Figure 89. Hence, we can conclude that the bearing has an outer race fault.

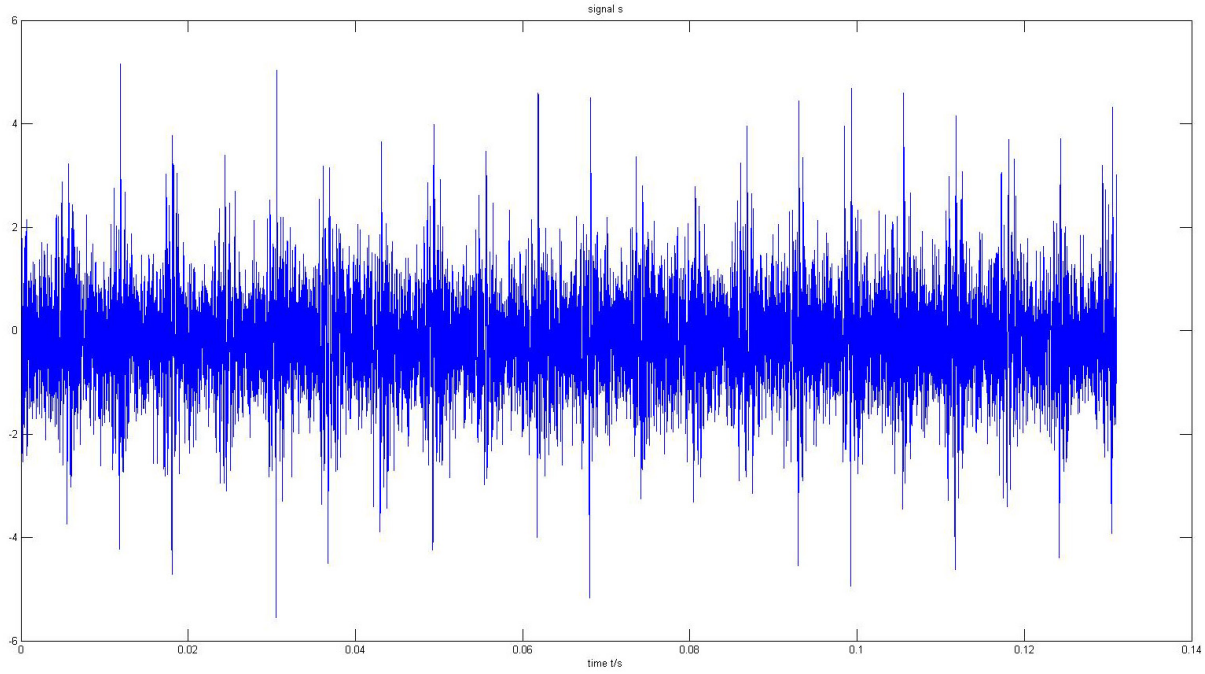

Figure 86 Time-domain waveform for the bearing with outer race fault

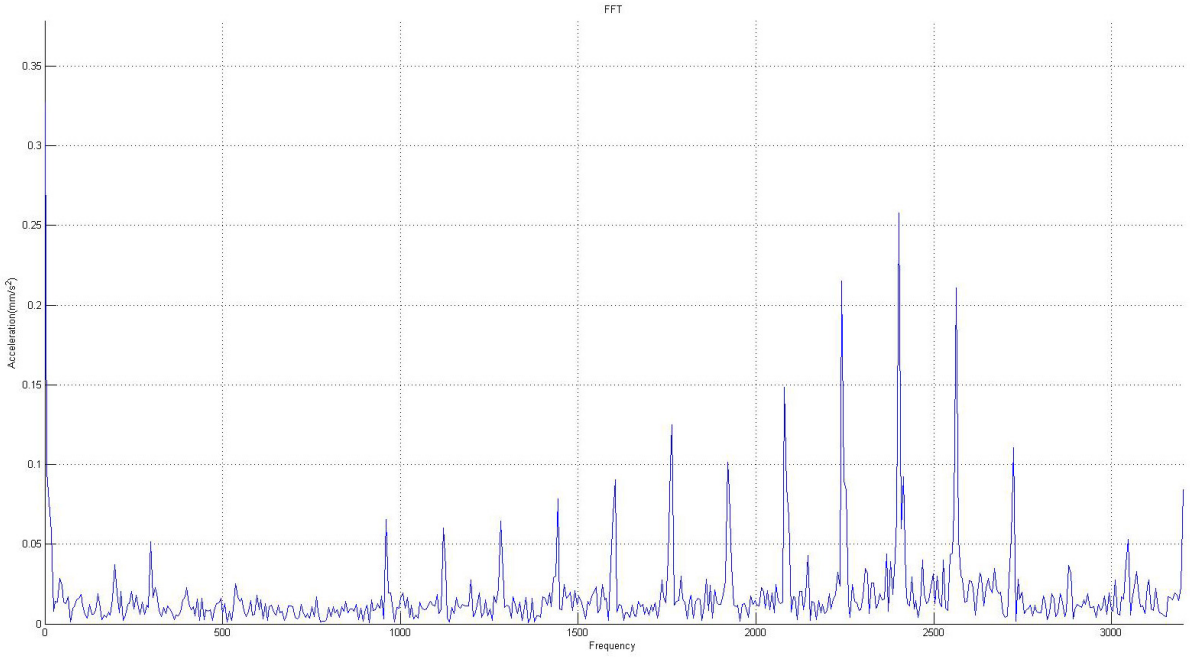

Figure 87 FFT for the bearing with outer race fault

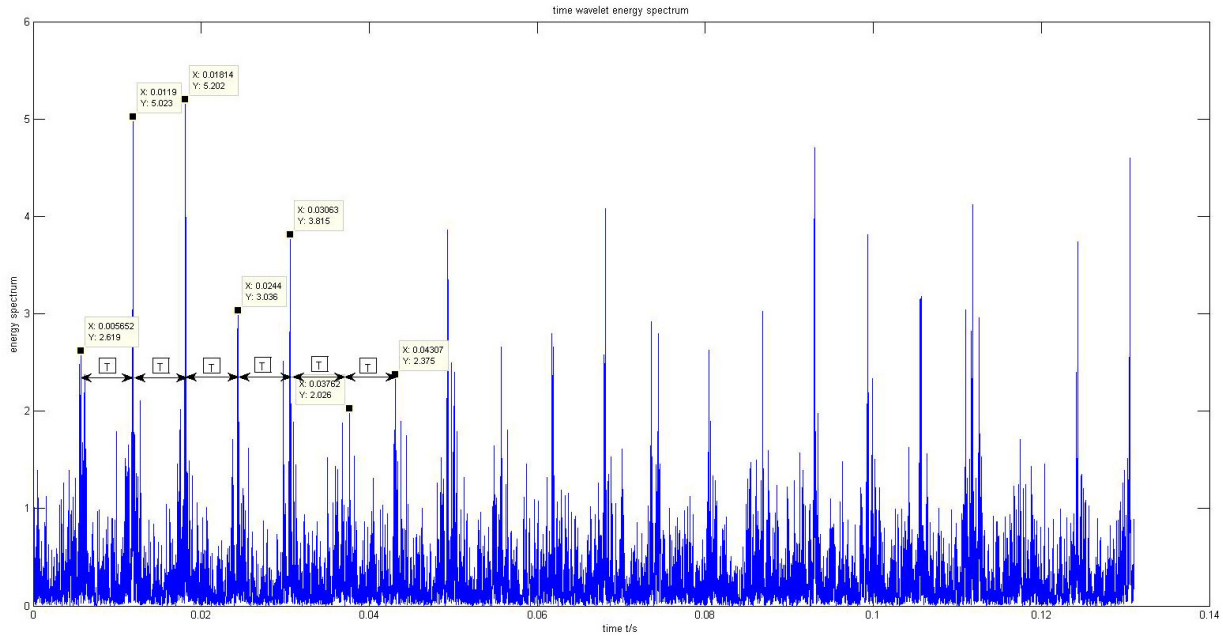

Figure 88 Time-wavelet spectrum for the bearing with outer race fault

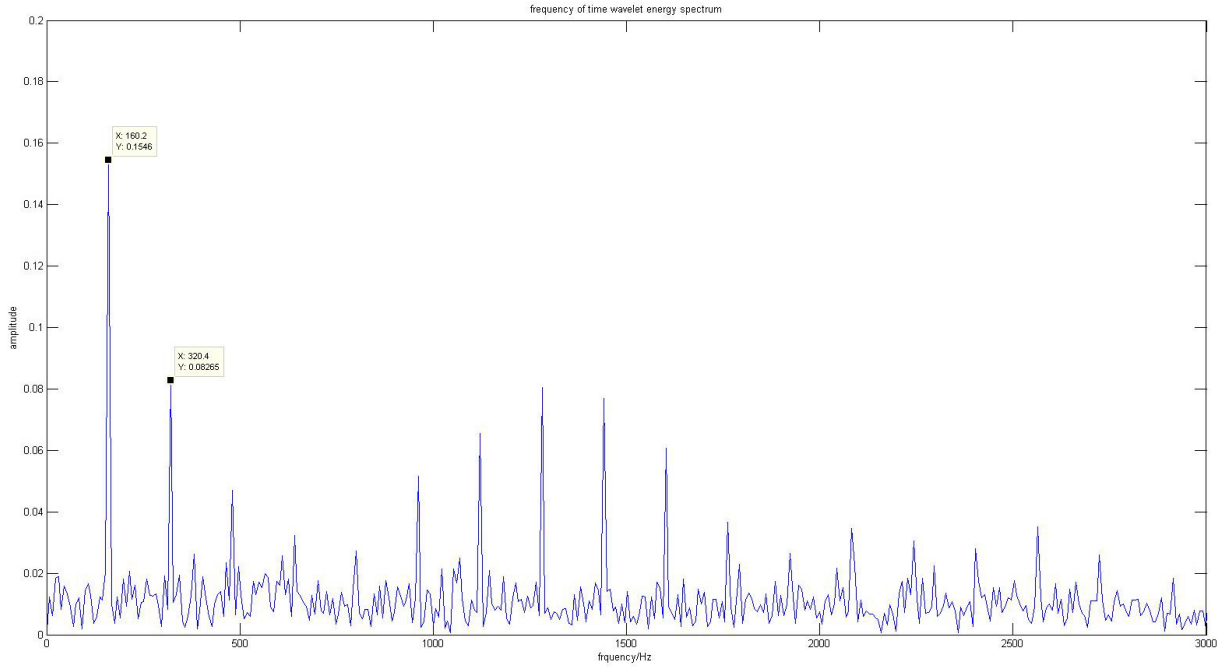

Figure 89 Frequency distribution for the bearing with outer race fault

5.2.2 The improved DWT method

In this section, we still use DB 20 (Daubechies 20) wavelet to obtain the approximation signal and the detail signals. We also apply the Cepstrum analysis to analyze the whole original signal as a comparison.

5.2.2.1 Healthy bearing

Figure 90 is the Hilbert envelope spectrum analysis from d1 to d5, where no peak values are found to be corresponding to the characteristic of the faulty bearing. No obvious impulse periods can be found in the Cepstrum of the whole signal (Figure 91), the instantaneous envelope analysis (Figure 92) of d1 and the Cepstrum analysis of d1 (Figure 93).

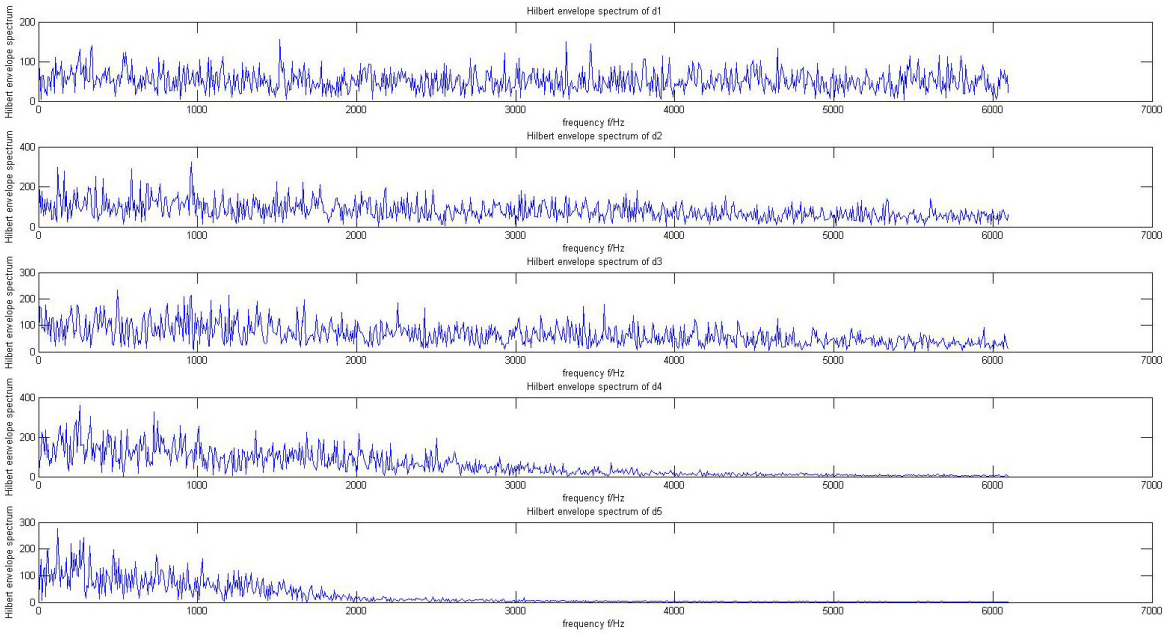

Figure 90 Envelope spectrum analysis for the healthy bearing

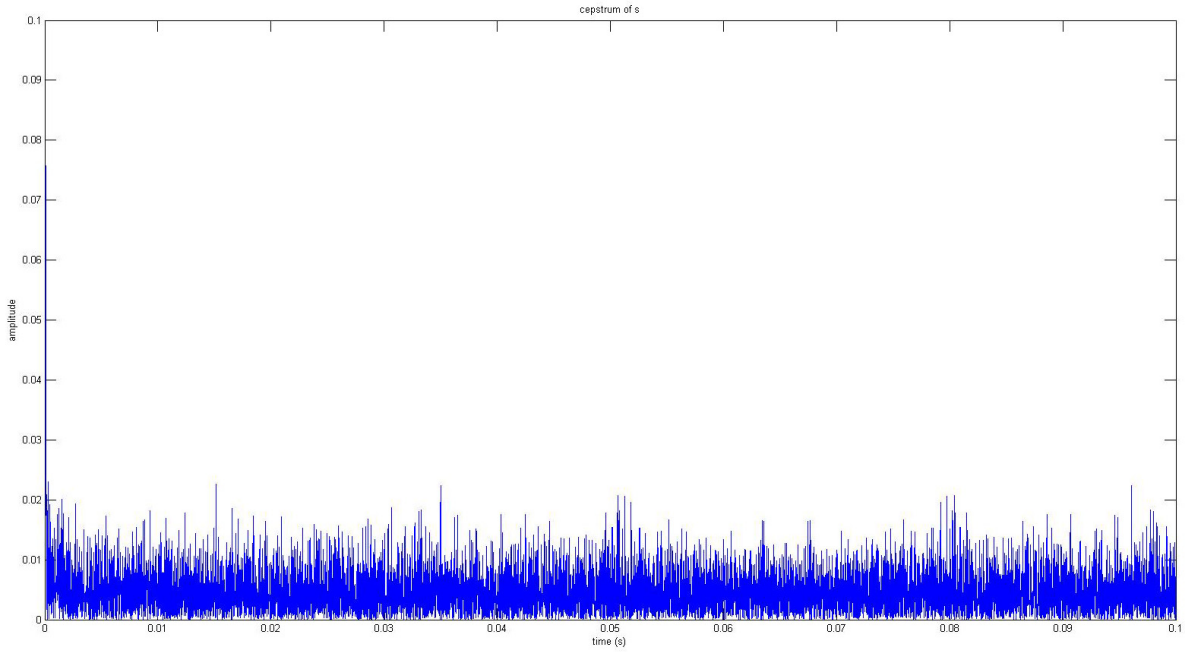

Figure 91 Cepstrum analysis for the original signal the healthy bearing

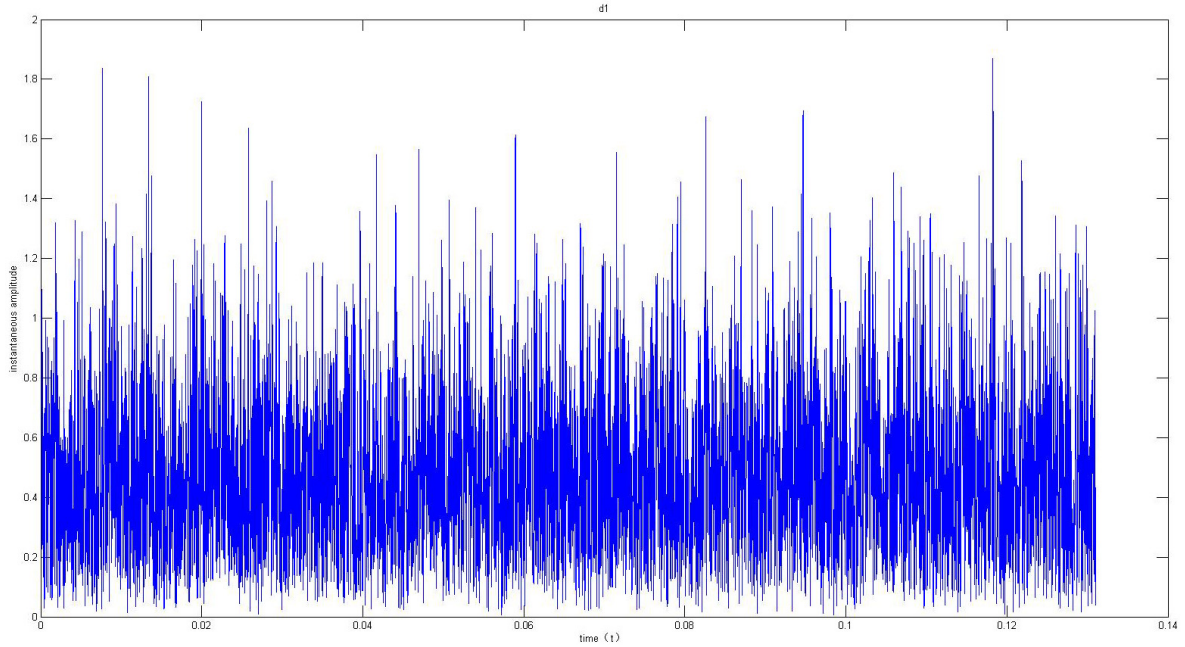

Figure 92 Instantaneous amplitude of d1 for the healthy bearing

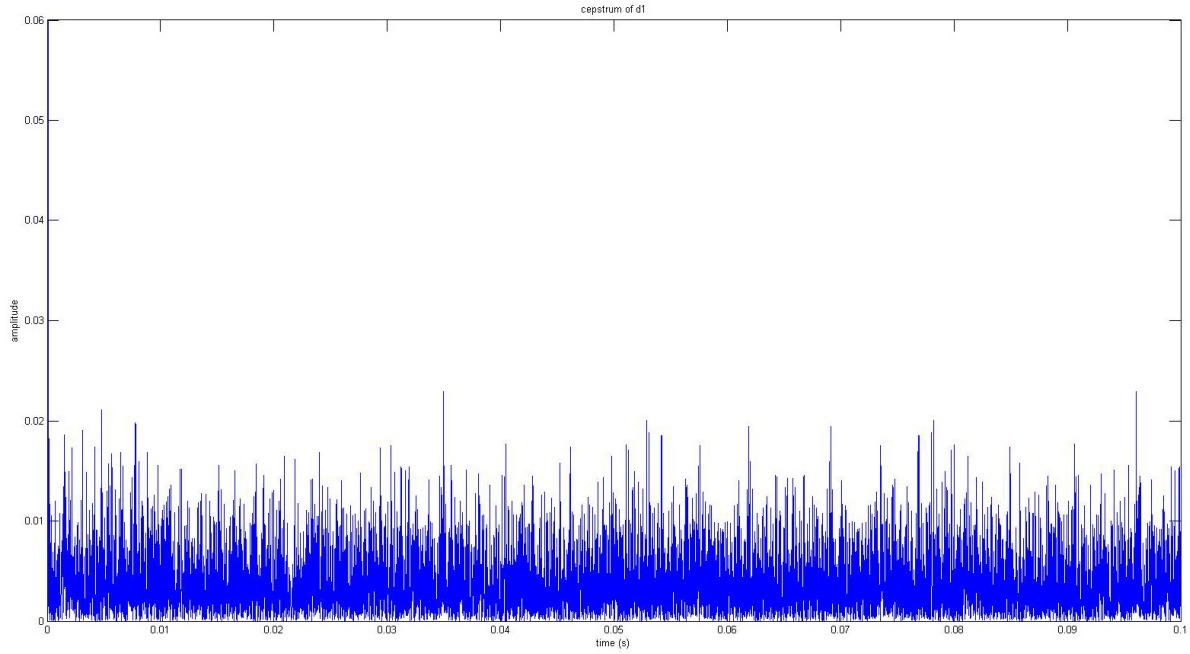

Figure 93 Cepstrum analysis of d1 for the healthy bearing

5.2.2.2 Bearing with inner race fault

Figure 94 is the Hilbert envelope spectrum analysis from d1 to d5, where the frequencies of two highest peaks are 236.5Hz and 473 Hz respectively. They are corresponding to the characteristic frequencies of the inner race fault (237.75Hz) and its second harmonic. The impulse's period T of the Cepstrum of the whole signal (Figure 95), instantaneous envelope analysis of d1 (Figure 96) and in Cepstrum analysis of d2 (Figure 97) are all the same with $T \approx 0.0042s$ and its frequency is $\frac{1}{T} = 238.1Hz$, which is close to the characteristic frequency of the inner race fault. Hence, we can conclude that there is an inner race fault of the bearing. Besides, compared Figure 95 with Figure 97, we can find that the result of the proposed method is more clear and has less noise than applied Cepstrum analysis directly.

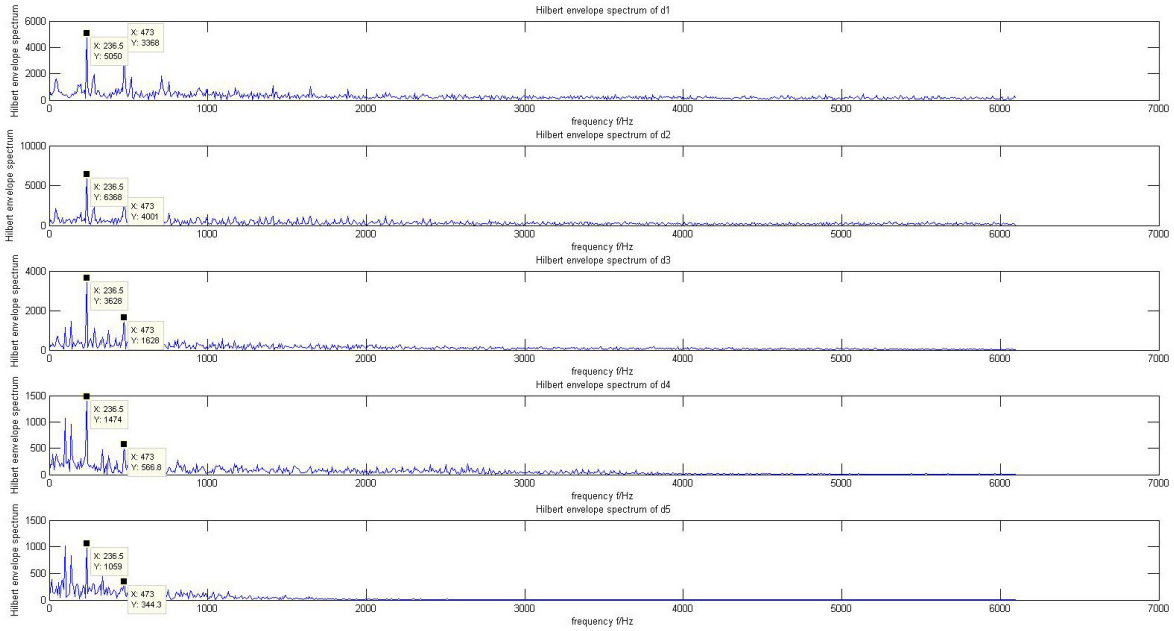

Figure 94 Envelope spectrum analysis for the bearing with inner race fault

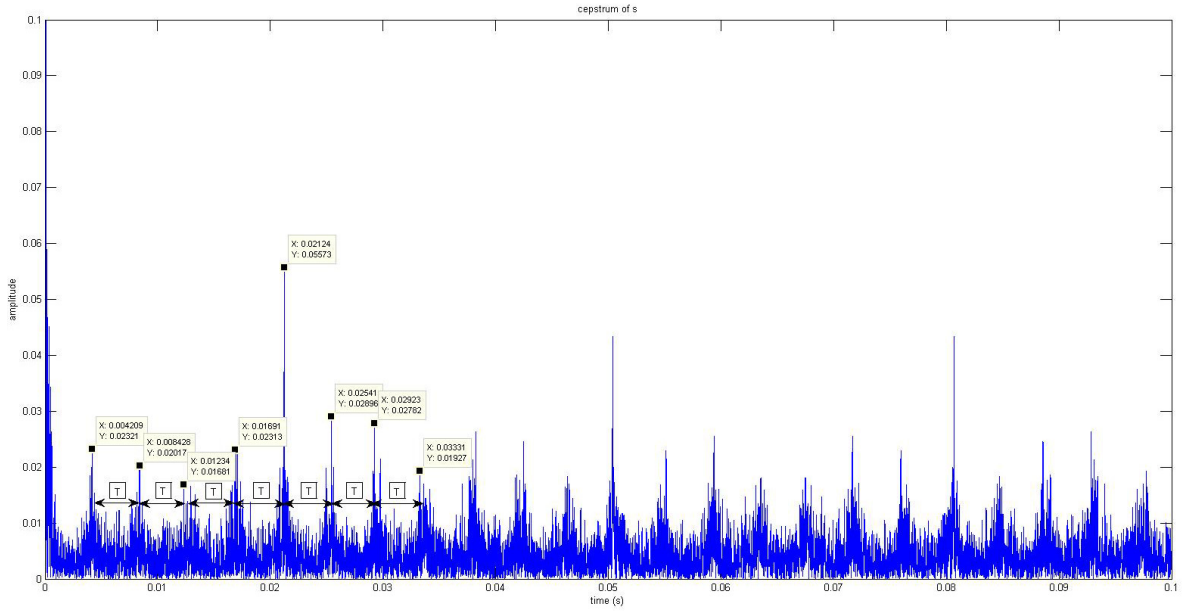

Figure 95 Cepstrum analysis of the original signal for the bearing with inner race fault

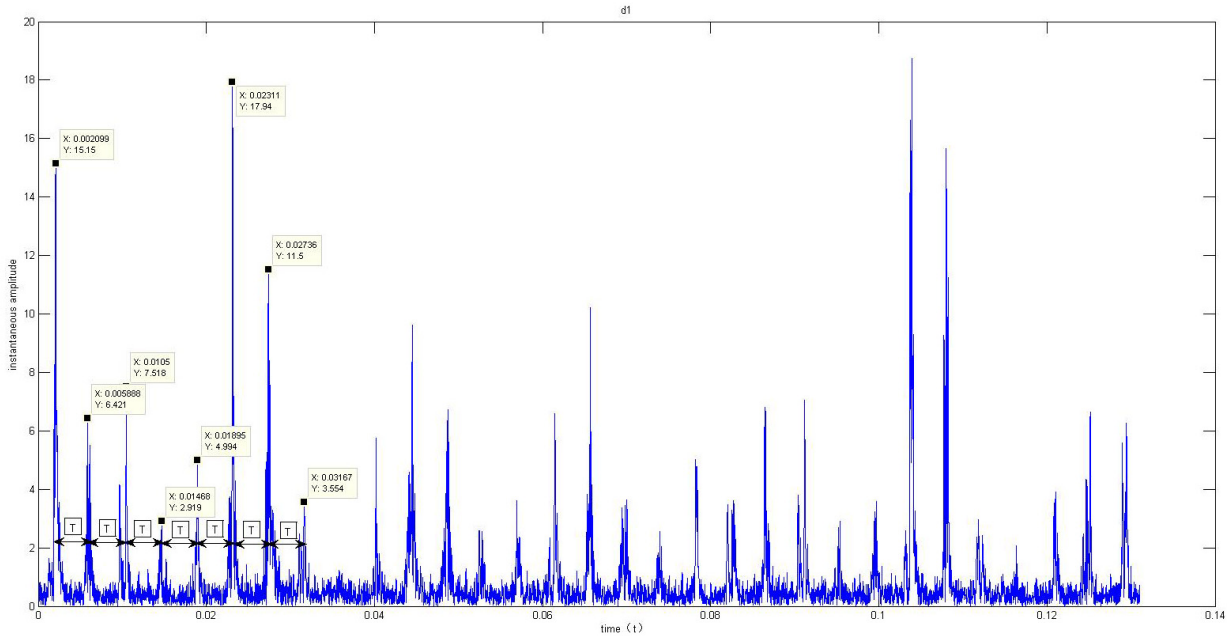

Figure 96 Instantaneous amplitude of d1 for the bearing with inner race fault

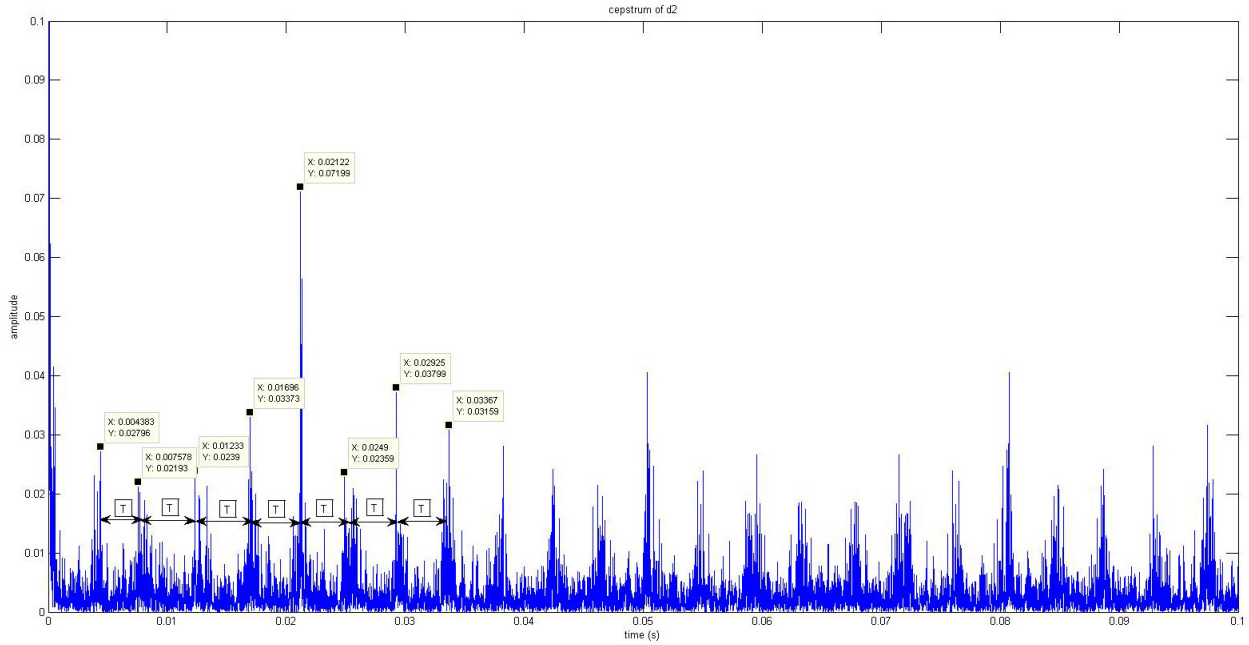

Figure 97 Cepstrum analysis of d2 for the bearing with inner race fault

5.2.2.3 Bearing with outer race fault

In the Hilbert envelope spectrum analysis from d1 to d5 shown in Figure 98, the frequencies of peaks values are 160.5Hz and 320.4 Hz, which are corresponding to the characteristic of the outer race fault (162.25Hz) and its second harmonic. The impulse's period T of the Cepstrum of the whole signal (Figure 99) is $T \approx 0.0062s$ with the frequency is 160.29Hz. The impulse's period in the instantaneous envelope analysis of d1 (Figure 100) is $T \approx 0.0061s$ and its frequency is 163.9Hz. The impulse's period of the Cepstrum analysis of d5 in Figure 101 is $T \approx 0.0063s$ and its frequency is 158.73Hz. All of them are close to the characteristic frequency of the outer race fault. Hence, we can conclude that there is an outer race fault of the bearing. Furthermore, we can find that the result obtained by the proposed method is clearer than the other two methods, and it also has less noise than applied Cepstrum analysis directly.

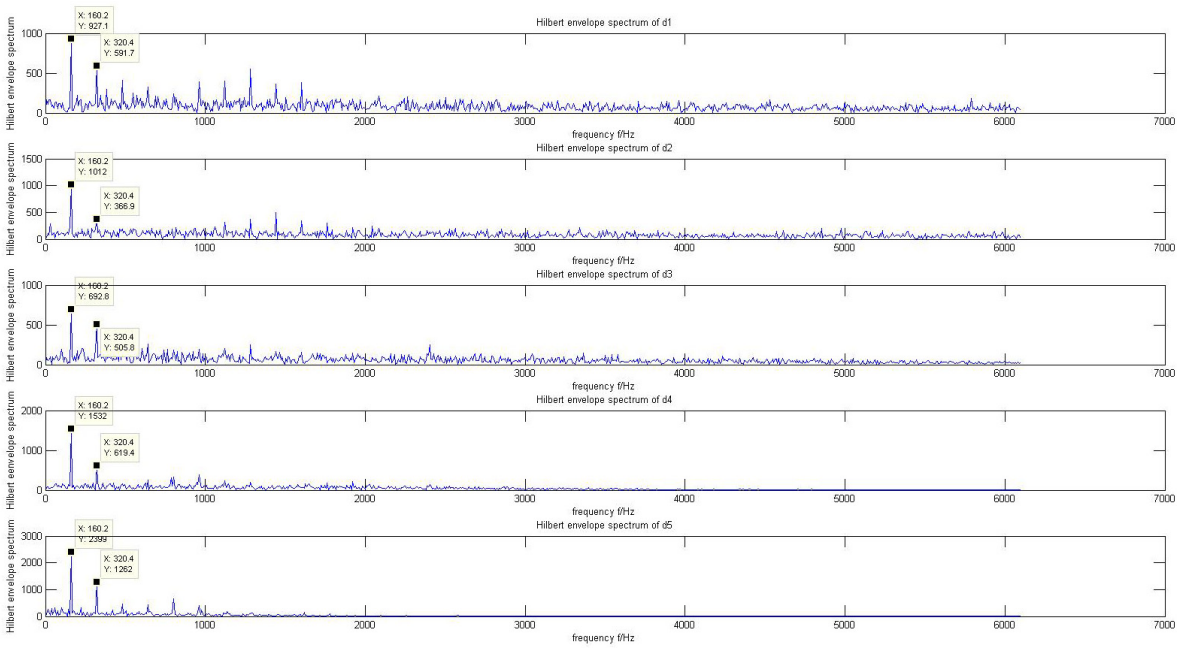

Figure 98 Envelope spectrum analysis for the bearing with outer race fault

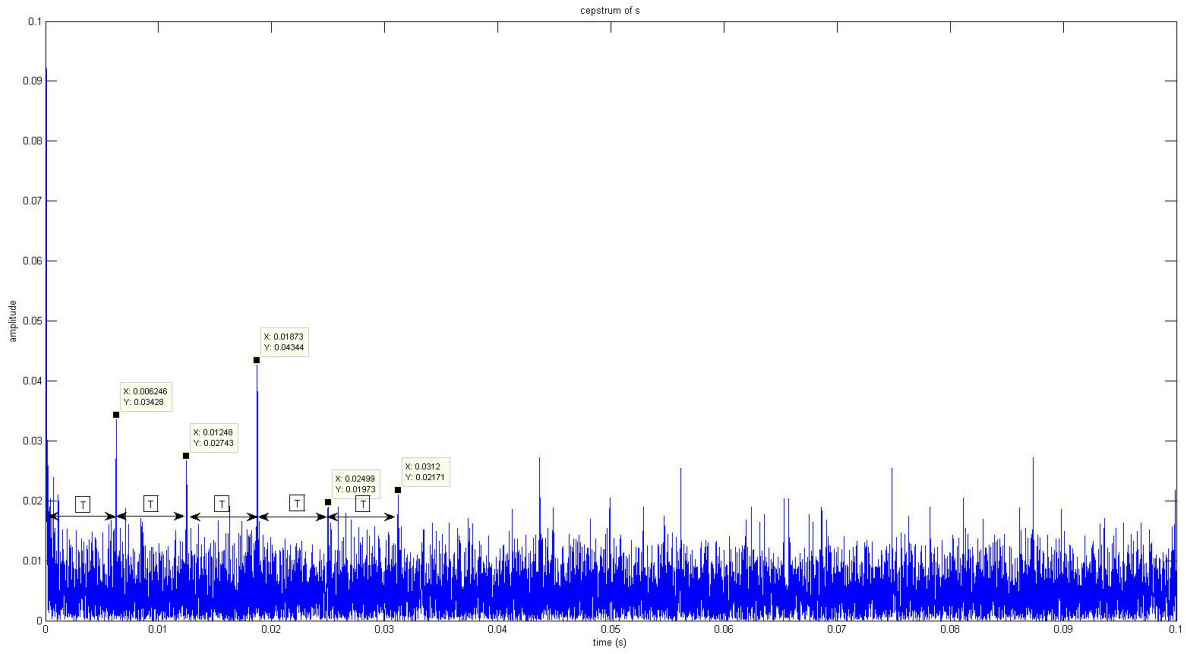

Figure 99 Cepstrum analysis of the original signal for the bearing with outer race fault

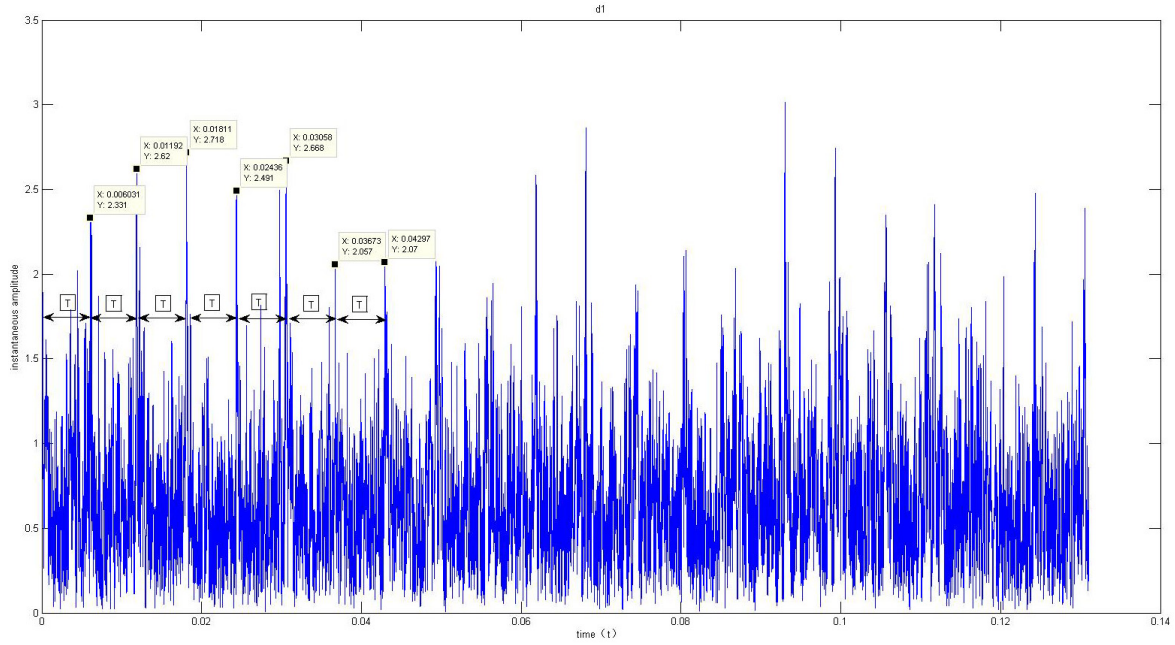

Figure 100 Instantaneous amplitude of d1 for the bearing with outer race fault

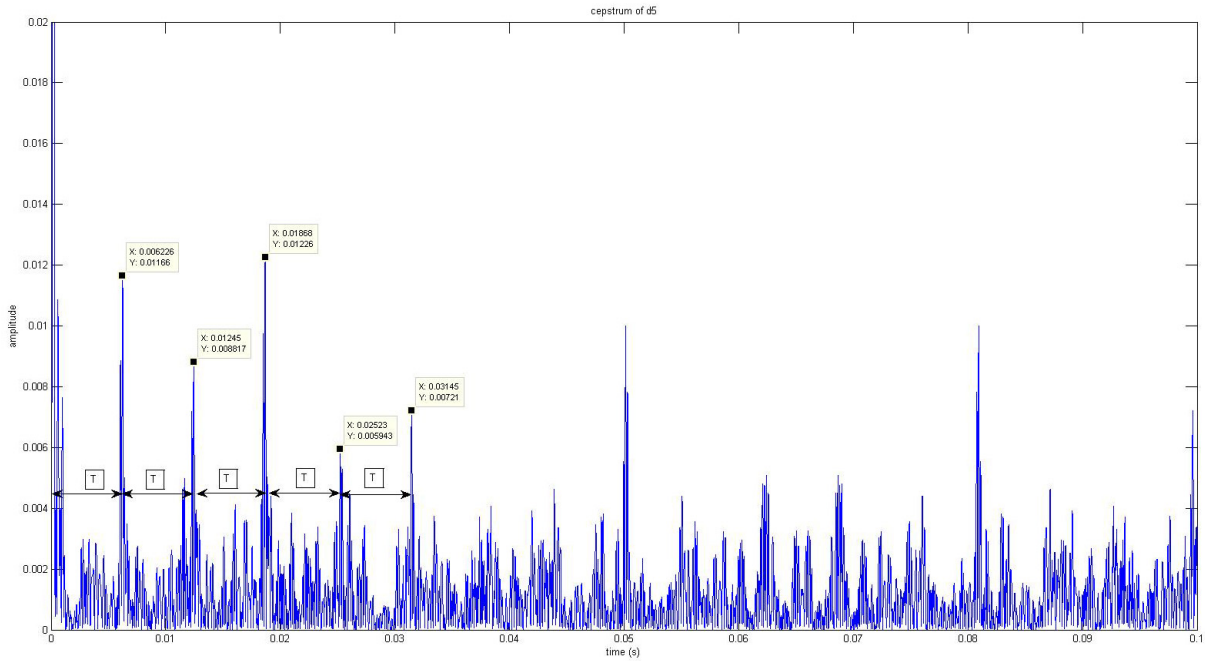

Figure 101 Cepstrum analysis of d5 for the bearing with outer race fault

5.2.3 HHT analysis

We apply EMD to decompose the collected data into a series of IMFs. Then we apply Hilbert spectral analysis to extract the features from the corresponding IMFs for Bearing fault diagnosis.

5.2.3.1 Healthy bearing

We apply Hilbert spectral analysis to analyze IMF1 and get its power spectrum shown in Figure 102, where there is no frequency of the peaks that is corresponding to the characteristics of the faulty bearing. There are no periodic impulses in Figure 103.

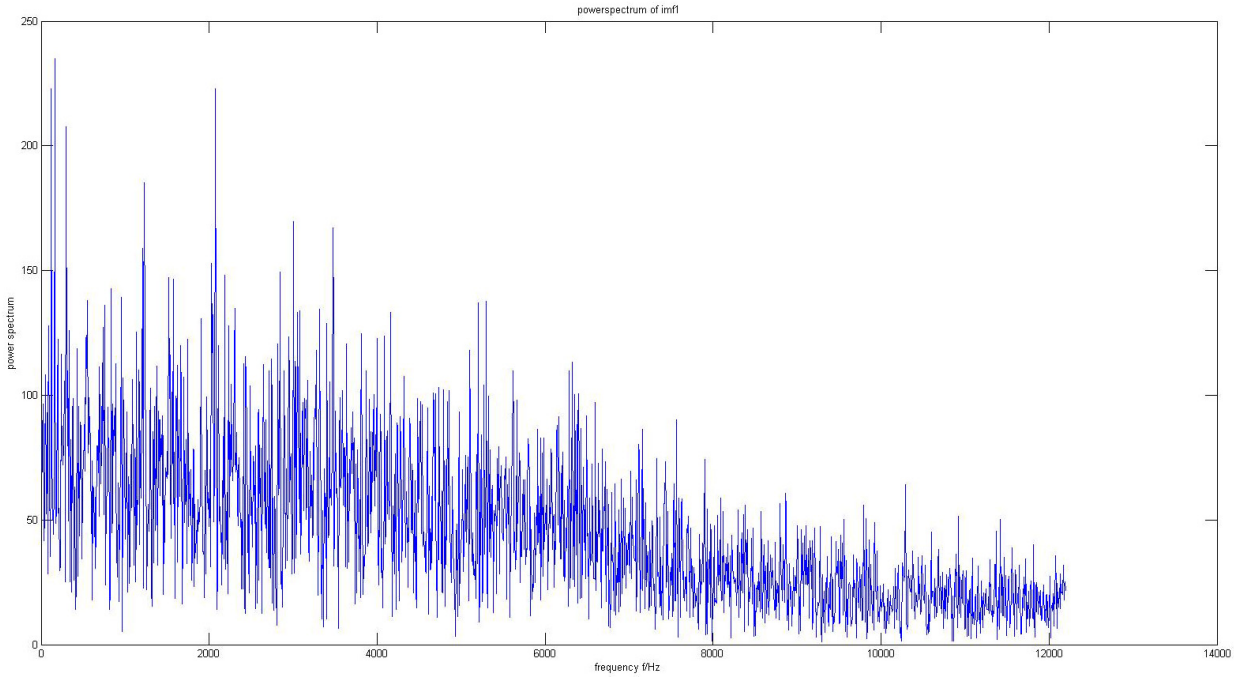

Figure 102 The power spectrum of IMF1 for the healthy bearing

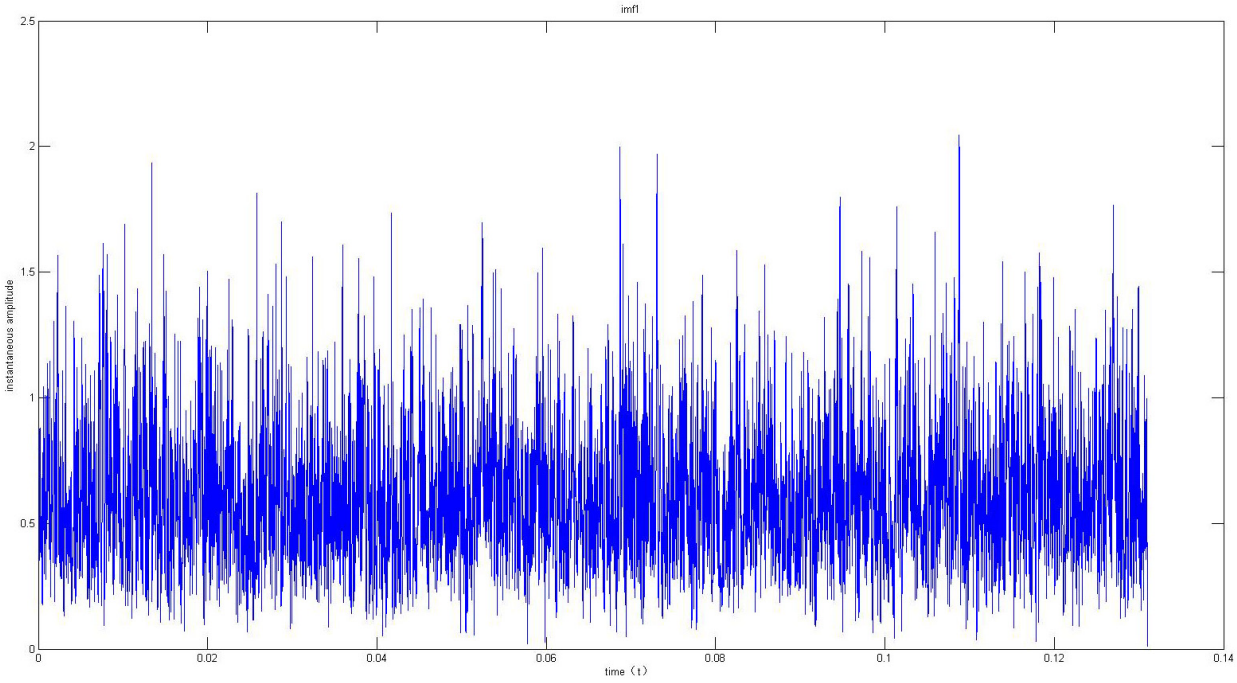

Figure 103 IMF1’s instantaneous envelope spectrum analysis for the healthy bearing

5.2.3.2 Bearing with inner race fault

Figure 104 is the power spectrum analysis of IMF1, where we can find that the frequencies of the two highest peaks values are 236.5Hz and 473 Hz respectively. They are corresponding to the characteristic frequency of the inner race fault (237.75Hz) and its second harmonic. The impulse's period T of the IMF1's instantaneous envelope analysis (Figure 105) is $T \approx 0.0042s$ and its frequency is $\frac{1}{T} = 238.1Hz$, which is corresponding to the characteristic frequency of the inner race fault. Hence, we can conclude that there is an inner race fault of the bearing.

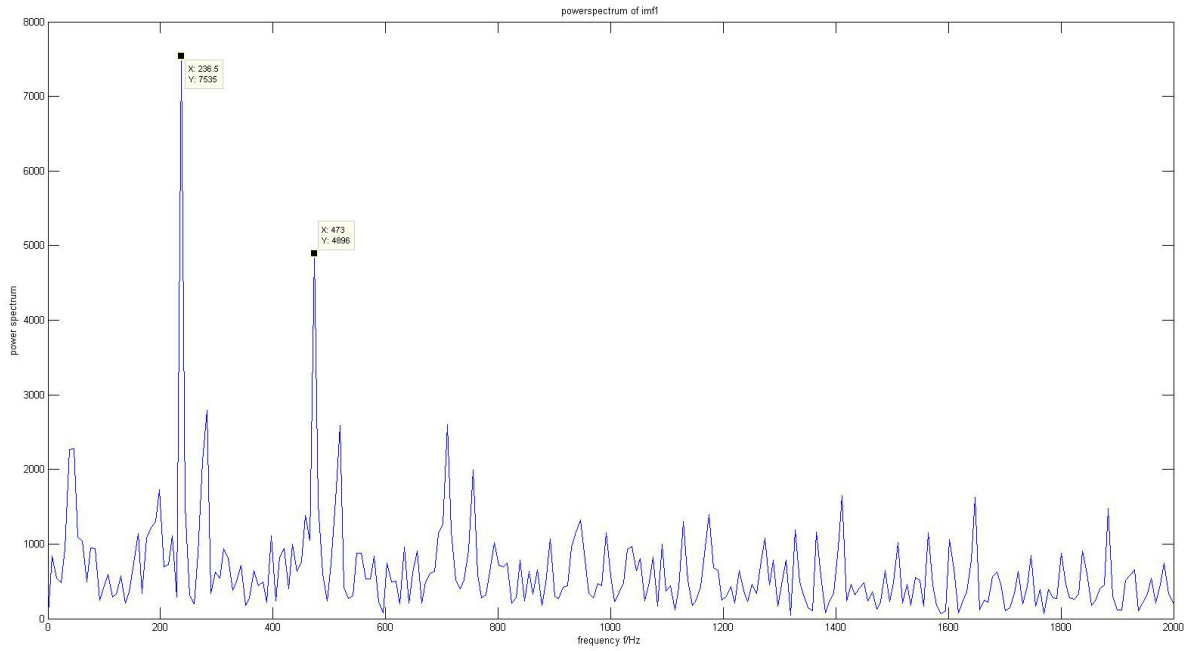

Figure 104 The power spectrum of IMF1 for the bearing with inner race fault

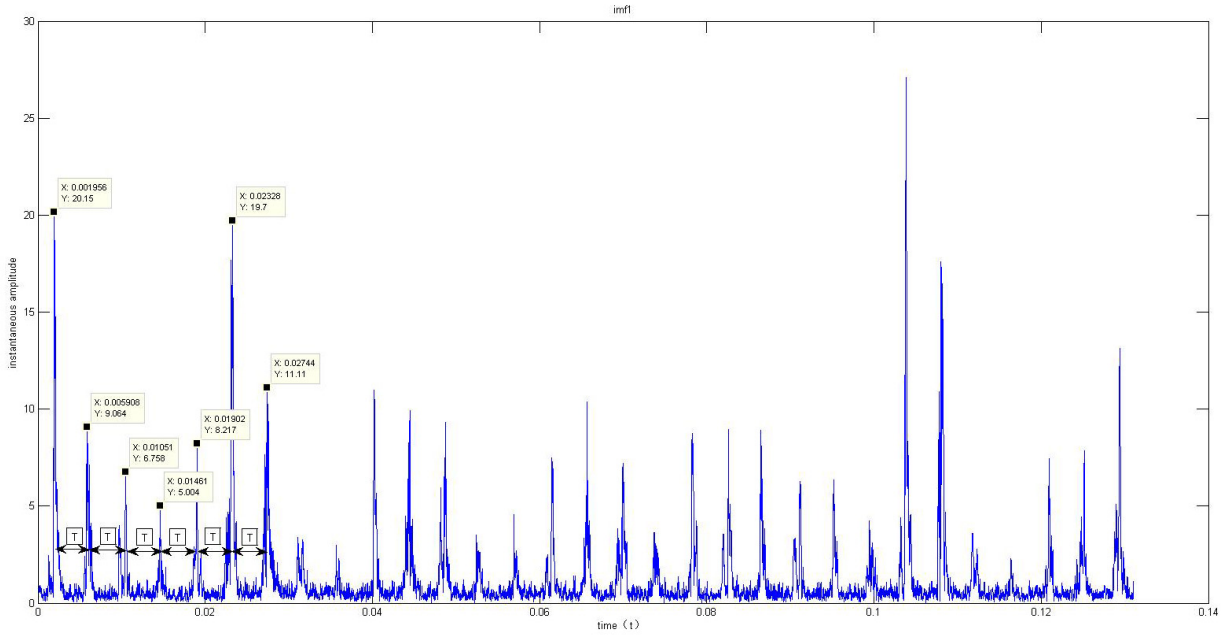

Figure 105 IMF1's instantaneous envelope analysis for the bearing with inner race fault

5.2.3.3 Bearing with outer race fault

The power spectrum analysis of IMF1 is shown in Figure 106. We can find the frequency of the two highest peaks are 160.2Hz and 320.4Hz, which are corresponding to the characteristic frequency of the inner race fault (162.25Hz) and its second harmonic respectively. The impulse's period T of the IMF1's instantaneous envelope analysis (Figure 107) is $T \approx 0.0062s$ and its frequency is $\frac{1}{T} = 161.29Hz$, which is corresponding to the characteristic frequency of the outer race fault. Hence, we can conclude that the bearing has an outer race fault. Moreover, the periodic impulses shown by the proposed method (Figure 101) is more intuitive than that of HHT.

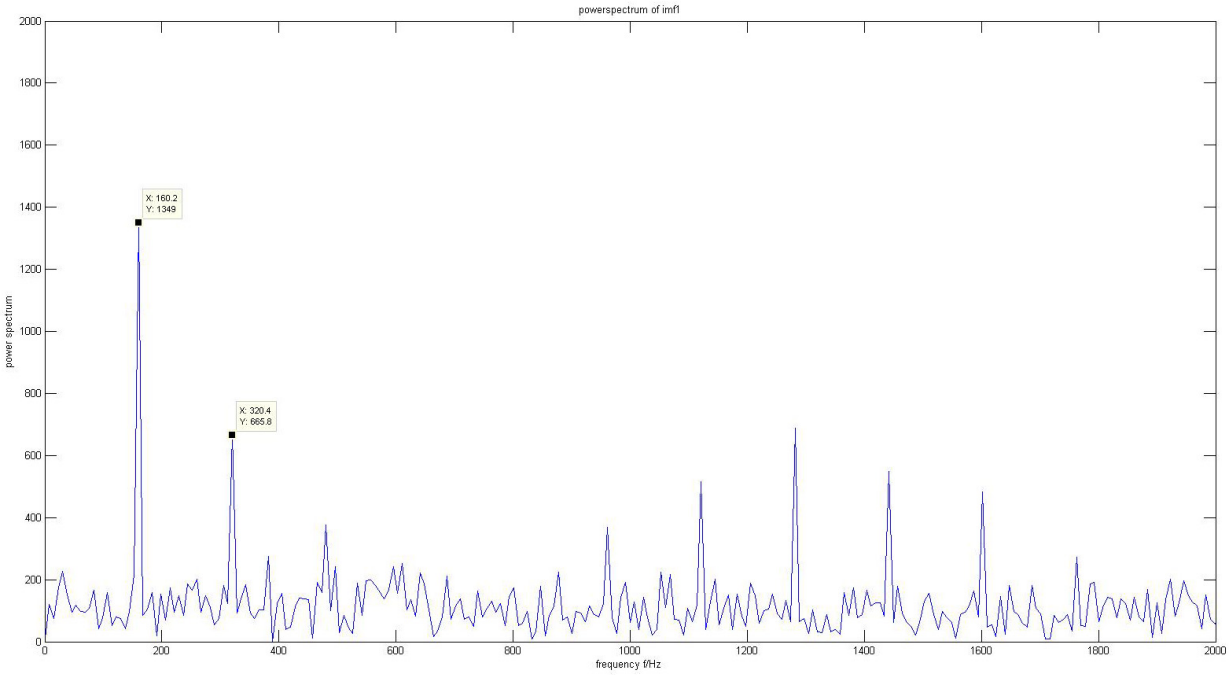

Figure 106 The power spectrum of IMF1 for the bearing with outer race fault

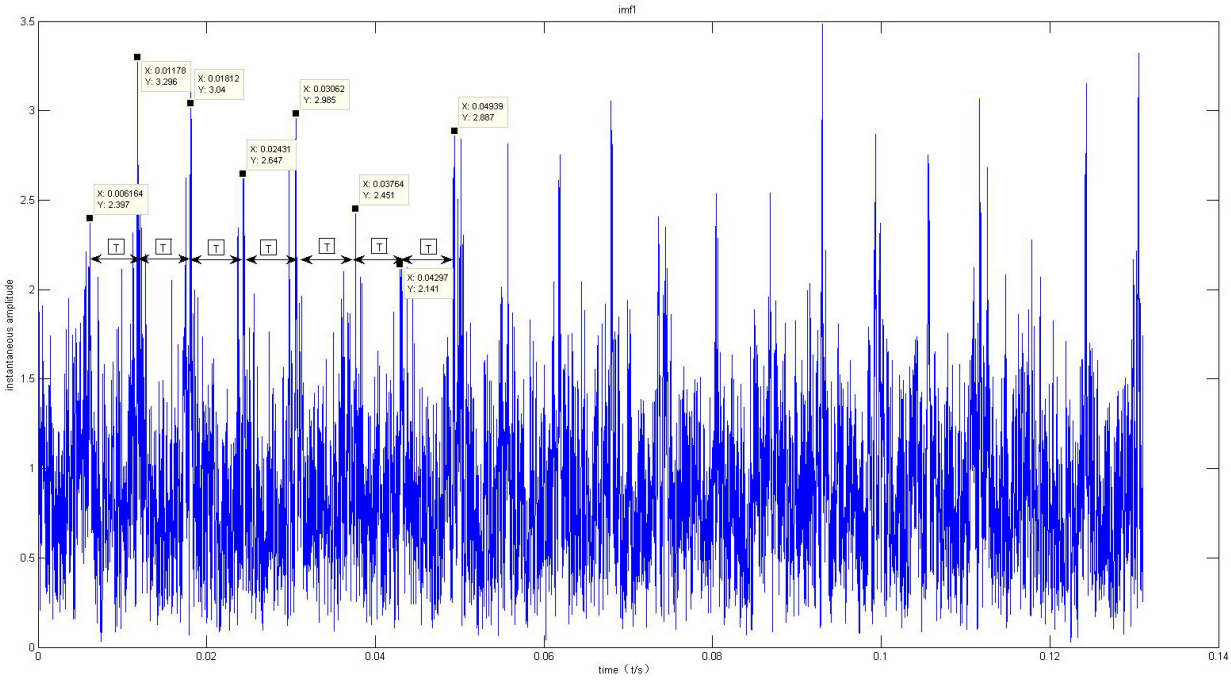

Figure 107 IMF1’s instantaneous envelope analysis for the bearing with outer race fault

Based on the results above, we can find that all the three methods can perform effective fault diagnosis of bearings. They can extract faulty characteristics and analyze them in frequency domain. Their performance are almost the same in analyzing the periodic impulses caused by the bearing's inner race fault in time domain. However, the CWT methods and the proposed methods can detect the fault more clearly than the HHT method in analyzing the periodic impulses caused by the bearing's outer race fault.

Chapter 6

6. Conclusion and future work

6.1 Conclusion

In this thesis, we investigate fault diagnosis of rotating machinery by using one set for gear condition monitoring data and one set for bearing condition monitoring data. We propose an improved DWT method integrating Cepstrum analysis which can improve the analytical capacity of the periodic impulses in time domain. The results show that it performs better than the existing methods of applying Cepstrum analysis directly. Furthermore, it has better performance in time domain analysis than Hilbert spectral analysis in analyzing the periodic impulses contained in the detail signals.

A comprehensive study is conducted to compare the following three methods in fault diagnosis of the gears and bearings: (1) The CWT method using time-wavelet energy spectrum, (2) the improved DWT method using Cepstrum analysis, and (3) the HHT method.

In fault diagnosis of the gearbox, we can conclude as follows:

- The HHT method performs more sensitive in frequency domain than the other two methods. It can extract the faulty characteristic frequency of the gear after 40% crack while the other two methods can diagnose the faulty characteristic frequency after 60% crack. Besides, the HHT method has better noise immunity.

- The improved DWT method is good at analyzing the periodic impulses caused by the fault in time domain. The results of the proposed methods are more intuitive and accurate than the other two methods.

In fault diagnosis of the bearing, all the methods can detect and identify the bearing's inner race fault and outer race fault. The fault can be more clearly detected using the CWT and improved DWT methods in analyzing the periodic impulses that caused by the outer race fault of the bearing. The results obtained in this thesis can assist researchers and practitioners to select suitable methods for fault diagnosis of gears and bearings.

6.2 Future work

As there are more and more complex rotating machinery being designed and manufactured, the requirement of fault diagnosis analysis will increase significantly. Hence, many research of fault diagnosis can be done in the future.

1. In the case study on gearbox fault diagnosis, we collect five sets of data with the sizes of the crack at the gear tooth root are: 0% (healthy gear), 25%, 40%, 60%, and 80%. In the future, we can collect more sets of data with the sizes of the crack changing little by little, for example, the size of the crack can be 0%, 10%, 20%… 80%, 90%. Thus the comprehensive study of the three methods above can be more detailed. We can also change the load and the motor speed in the experiment so that more sets of data can be collected to investigate fault diagnosis of gears and bearings.
2. In this thesis, we use data collected from the two-stage gearbox where there is a faulty gear. In the future, we can collect data from a gearbox where there are two or more

faulty gears. Moreover, we can also collect data from some more complex gearboxes, such as planetary gearboxes. Then the three methods above can be applied to investigate the capacity of fault diagnosis.

3. As there are also many effective methods have been presented in fault diagnosis of rotating machinery, we can apply these methods in our experimental data to compare their capacity in fault diagnosis of the gears and bearings. For example, the methods based on the wavelet package transform, which can offer better time-frequency localization of signals, has been widely used in fault diagnosis. An improved EMD method called as B-Spline based EMD that can overcome the disadvantage of EMD also has been proposed in fault diagnosis. These methods can be applied in our data and compared the results with the three methods above.

Bibliography

[1] X.F. Fan, M.J. Zuo, Gearbox fault detection using Hilbert and wavelet packet transform, Mechanical Systems and Signal Processing. 20 (2006) 966-982.

[2] A.K.S. Jardine, D.M. Lin, D. Banjevic, A review on machinery diagnostics and prognostics implementing condition-based maintenance, Mechanical Systems and Signal Processing 20 (2006) 1483-1510.

[3] I. Yesilyurt, Fault detection and location in gears by the smoothed instantaneous power spectrum distribution, NDT & E International 36 (2003) 535-542.

[4] B. Boashash, Time–Frequency Signal Analysis and Processing: A comprehensive Reference, Elsevier Science, Oxford, (2003) ISBN 0080443354.

[5] P. Bonato, R. Ceravolo et al, Bilinear time–frequency transformations in the analysis of damaged structures, Mechanical Systems and Signal Processing 11 (1997) 509-527.

[6] D.L. Jones, T.W. Parks, A resolution comparison of several time-frequency representations, IEEE Transactions on Signal Processing 40 (2) (1992) 413-420.

[7] N.E. Huang, Z. Shen et al, The empirical mode decomposition and the Hilbert Spectrum for nonlinear and non-stationary time series analysis, Processing of the Royal Society Series A 454 (1998) 903-995.

[8] Z.K. Peng, P.W. Tsea, F.L. Chu, A comparison study of improved Hilbert–Huang transform and wavelet transform: Application to fault diagnosis for rolling bearing, Mechanical Systems and Signal Processing 19 (2005) 974-988.

[9] J.A. Antonino-Daviu, M. Riera-Guasp et al, A critical comparison between DWT and Hilbert–Huang-based methods for the diagnosis of rotor bar failures in induction machines, IEEE Transactions on Industry Applications 45 (5) (2009) 1794-1803.

[10] S.X. Yang, J.S. Hu et al, The comparison of vibration signals' time frequency analysis between EMD-based HT and WT method in rotating machinery, Proceeding of the CSEE, 23 (6) (2003) 102-107.

[11] B.F. Yan, A. Miyamoto, A comparative study of modal parameter identification based on wavelet and Hilbert–Huang Transforms, Computer-Aided Civil and Infrastructure Engineering 21 (2006) 9-23.

[12] S.T. Quek, P.S. Tua et al, Comparison of Hilbert-Huang, Wavelet and Fourier Transforms for selected applications, The Hilbert-Huang transform in engineering, CRC Press, (2005) ISBN 0849334225.

[13] N.Tandon, A comparison of some vibration parameters for the condition monitoring of rolling element bearings, Measuremnt 12 (1994) 285-289.

[14] P. Vecer, M.kreidl et al, Condition indicators for gearbox condition monitoring systems, Acta Polytechnica 45 (6) (2005) 35-43.

[15] E. Bechhoefer, M. Kingsley, A review of time synchronous average algorithms, Annual Conference of the Prognostics and Health Management Society, (2009).

[16] G. Dalpiaz, A. Rivola et al, Effectiveness and sensitivity of vibration processing techniques for local fault detection in gears, Mechanical Systems and Signal Processing 14 (2000) 387-412.

[17] G. Kaiser, A friendly guide to wavelets, Birkhauser, (1994) ISBN 0817637117.

[18] J.O. Smith III, Mathematics of the Discrete Fourier Transform (DFT): with Audio Applications, W3K Publishing, (2007) ISBN 097456074X.

[19] A. Aherwar, Md. Khalid, Vibration analysis techniques for gearbox diagnostic: a review, International Journal of Advanced Engineering Technology Vol.III Issue III (2012).

[20] G. Betta, C. Liguori et al, A DSP-based FFT-analyzer for the fault diagnosis of rotating machine based on vibration analysis, IEEE Intrumentation and Measurement Technology Conference, Vol.1 (2001) 572-577.

[21] V.K. Rai, A.R. Mohanty, Bearing fault diagnosis using FFT of intrinsic mode functions in Hilbert-Huang transform, Mechanical Systems and Signal Processing 21 (2007) 2607-2615.

[22] H. Ahmadi, Z. Khaksar, Power spectral density technique for fault diagnosis of an electromotor, Communications in Computer and Information Science Vol.165 (2011) 105-112.

[23] W. Zhang, Q.X. Bi, Power chart analysis method applied to bearing breakdown monitoring and measurement of pump, China Mining Magazine 16 (6) (2007) 56-59.

[24] K.Heidarbeigi, H. Ahmadi et al, Fault diagnosis of Massey Ferguson gearbox using power spectral density, Proceedings of the 2008 International Conference on Electrical Machines, Paper ID 1397 (2008) 1-4.

[25] J. Cusidó, L. Romeral et al, Fault detection in induction machines using power spectral density in wavelet decomposition, IEEE Transactions on Industrial Electronics 55 (2) (2008) 633-643.

[26] X.F. Zhang, J.S. Ye et al, The roller bearing fault diagnosis based on EMD method and power spectrum, Mechanical Engineer Vol.12 (2012) 24-26.

[27] C.M. Harris, A.G. Piersol, Harris' Shock and Vibration Handbook, McGraw-Hill, (2002) ISBN 0071370811.

[28] M.P.Norton, D.G.Karczub, Fundamentals of Noise and Vibration Analysis for Engineering, Cambridge University Press, (2003) ISBN 0521499135.

[29] N.T. Van der Merwe, A.J. Hoffman, A modified cepstrum analysis applied to vibrational signals, Digital Signal Processing of 14th International Conference, Vol.2 (2002) 873–876.

[30] R. Bajric, D. Sprecic et al, Review of vibration signal processing techniques towards gear pairs damage identification, International Journal of Advances in Engineering &Technology 11 (04) (2011) 124-128.

[31] L. Nacib, K.M. Pekpe et al, Detecting gear tooth cracks using cepstral analysis in gearbox of helicopters, International Journal of Advances in Engineering & Technology 5 (2) (2013) 139-145.

[32] C.B. Fan, L.B. Zhang et al, Using inverse spectrum analysis method to diagnose complex fault of wind power dynamotor gearbox, Science Technology and Engineering 6 (2) (2006) 187-189.

[33] W. Teng, X. Wu et al, Cepstrum analysis of vibration signals of wind turbine gear box, Proceedings of the 30th Chinese Control Conference, (2011) 4237-4240.

[34] H.B. Zhao, L. Wang, Tooth fracture diagnosis in gearbox based on Hilbert envelopment and cepstrum, Coal Mine Machinery 32 (05) (2011) 232-234.

[35] T. Yi, C.H. Liang et al, Fault diagnosis detection of roller bearing based on cepstrum technology, Machine Tool & Hydraulics 37 (09) (2009) 272-274.

[36] J. Ma, C.J. Li, Gear effect detection through model-based wideband demodulation of vibrations, Mechanical Systems and Signal Processing 10 (5) (1996) 653-665.

[37] F.X. Zhou, G.G. Cheng et al, Fault diagnosis technology based on wavelet analysis and resonance demodulation, Proceedings of the 5th World Congress on Intelligent Control and Automation, Vol.2 (2004) 1746-1750.

[38] R.N. Bracewell, The Fourier Transform and its applications, McGraw, (1999) ISBN 0071160434.

[39] J.F. Wang, F.C. Li, Signal processing methods in fault diagnosis of machinery-analyses in frequency domain, Noise and Vibration Control 33 (1) (2012) 173-180.

[40] A. Medoued, A. Lebaroud et al, Application of Hilbert transform to fault detection in electric machines, Advances in Difference Equations 2013 (2) (2013).

[41] S.K. Ahamed, S. Karmakar et al, Diagnosis of broken rotor bar fault of induction motor through envelope analysis of motor startup current using Hilbert and Wavelet transform, Innovative Systems Design and Engineering 2 (4) (2011) 163-176.

[42] H.L. Wang, H.X. Pan, Gearbox fault detection research using Hilbert and Wavelet Packet node energy method, Coal Mine Machinery 31 (5) (2010) 251-254.

[43] I. Moumene, N. Ouelaa, Gears and bearings combined faults detection using Hilbert transform and Wavelet multiresolution analysis, Condition Monitoring of Machinery in Non-stationary Operations, Springer Berlin Heidelberg, ISBN 9783642287671 (2012) 319-328.

[44] D. Wang, Q. Miao et al, Rolling element bearing fault detection using an improved combination of Hilbert and Wavelet transforms, Journal of Mechanical Science and Technology 23 (2009) 3292-3301.

[45] A.V. Oppenheim, R.W. Schafer et al, Discrete-Time Signal Processing, Prentice-Hall, (1999) ISBN 0137549202.

[46] O. Rioul, M. Vetterli, Wavelets and signal processing, IEEE Signal Processing Magazine 8 (4) (1991) 14-38.

[47] S.V. Nese, O. Kilic et al, Analysis of wind turbine blade deformation with STFT method, Energy Education Science and Technology Part A: Energy Science and Research, 29 (1) (2012) 679-686.

[48] M. Cocconcelli, R. Zimroz et al, STFT based approach for ball bearing fault detection in a varying speed motor, Condition Monitoring of Machinery in Non-Stationary Operations, Springer Berlin Heidelberg, (2012) 41-50 ISBN 9783642287671.

[49] M.K. Kiymik, I. Guler et al, Comparison of STFT and wavelet transform methods in determining epileptic seizure activity in EGG signals for real-time application, Computers in Biology and Medicine 35 (2005) 603-616.

[50] J. Long, J. Wu, Application of short time Fourier transform and Hilbert-Huang transform in fault diagnosis of rolling bearing of windmill, Noise and Vibration Control 33 (4) (2013) 219-222.

[51] L. Debnath, Wavelet transforms and their applications, Birkhauser, (2002) ISBN 0817642048.

[52] F.K.Choy, D.H.Mugler et al, Damage identification of a gear transmission using vibration signatures, Journal of Mechanical Design 125 (2) (2003) 394-403.

[53] Q.M. Meng, L.S. Qu, Rotating machinery fault diagnosis using Wigner distribution, Mechanical Systems and Signal Processing 5 (3) (1991) 155-166.

[54] N. Baydar, A. Ball, A comparative study of acoustic and vibration signals in detection of gear failures using Wigner-Ville distribution, Mechanical Systems and Signal Processing 15 (6) (2001) 1091-1107.

[55] R.B. Pachori, P. Sircar, A new technique to reduce cross terms in the Wigner distribution, Digital Signal Processing 17 (2) (2007) 466-474.

[56] W.J. Wang and P.D. McFadden, early detection of gear failure by vibration analysis-I. Calculation of the time-frequency distribution, Mechanical Systems and Signal Processing 7 (3) (1993) 193-203.

[57] B.P. Tang, W. Liu et al, Wind turbine fault diagnosis based on Morlet wavelet transform and Wigner-Ville distribution, Renewable Energy 35 (12) (2010) 2862-2866.

[58] H. Li, H.Q. Zheng et al, Wigner-Ville distribution based on EMD for faults diagnosis of bearing, Fuzzy Systems and Knowledge Discovery, Springer Berlin Heidelberg, (2006) ISBN 9783540459163.

[59] F.X. Qiao, Introduction to Wavelet-A Tutorial, workshop 118 on Wavelet Application in Transportation Engineering, (2005).

[60] P.S. Vikhe, N.S. Nehe et al, Heartsound abnormality detection using short time Fourier transform and continuous wavelet transform, Second International Conference on Emerging Trends in Engineering and Technology, (2009) 50-54.

[61] J. Lin, Feature extraction of machine sound using wavelet and its application in fault diagnosis, NDT & E International 34 (2001) 25-30.

[62] N. Baydar, A. Ball, Detection of gear failures via vibration and acoustic signals using wavelet transform, Mechanical Systems and Signal Processing 17 (2003) 787-804.

[63] H. Zheng, Z. li et al, Gear fault diagnosis based on continuous wavelet transform, Mechanical Systems and Signal Processing 16 (2–3) (2002) 447-457.

[64] R. Rubini, U. Meneghetti, Application of the envelope and wavelet transform analysis for the diagnosis of incipient faults in ball bearings, Mechanical Systems and Signal Processing 15 (2) (2001) 287-302.

[65] F. Elbarghathi, T. Wang et al, Two stage helical gearbox fault detection and diagnosis based on continuous wavelet transformation of time synchronous averaged vibration signals, 25th International Congress on Condition Monitoring and Diagnosis Engineering, (2012).

[66] I. Daubechies, Ten lectures on wavelets, SIAM, (1992) ISBN 0898712742.

[67] B. Lu, M. Paghda, Induction motor rotor fault diagnosis using wavelet analysis of one-cycle average power, Applied Power Electronics Conference and Exposition of 23th Annual IEEE, (2008) 1113-1118.

[68] S. Prabhakar, A.R. Mohanty et al, Application of discrete wavelet transform for detection of ball bearing race faults, Tribology International 35 (2002) 793-800.

[69] R.H. Su, F. Qi, Wavelets applied to early fault analysis of hoist gearbox, Journal of Coal Science & Engineering 18 (2) (2012) 201-206.

[70] Z.Y. Liu, K.X. Fang et al, Application study of wavelet analysis in the fault diagnosis of gears, Noise and Vibration Control 4 (2009) 58-60.

[71] S.K. Ahamed, Diagnosis of broken rotor bar fault of induction motor through envelope analysis of motor startup current using Hilbert and Wavelet Transform, Innovative Systems Design and Engineering 2(4) (2011) 163-176.

[72] N. Saravanan, K.I. Ramachandran, Incipient gearbox fault diagnosis using discrete wavelet transform for feature extraction and classification using artificial neural network, Expert Systems with Applications 37 (6) (2010) 4168-4181.

[73] X.S. Lou, K.A. Loparo, Bearing Fault diagnosis based on wavelet transform and fuzzy inference, Mechanical Systems and Signal Processing 18 (5) (2004) 1077-1095.

[74] S. Ergin, S. Tezel et al, DWT-based fault diagnosis in induction motors by using CVA, Innovations in Intelligent Systems and Applications (2011) 129-132.

[75] N.E. Huang, S.P. Shen, Hilbert-Huang Transform and its applications, World Scientific, (2005) ISBN 9812569768.

[76] M. Datig, T. Schlurman, Performance and limitations of the Hilbert-Huang Transformation (HHT) with an application to irregular water waves, Ocean Engineering 31 (14-15) 1783-1834.

[77] M.E. Montesinos, J.L. Munoz-Cobo et al, Hilbert-Huang analysis of BWR detector signals: application to DR calculation and to corrupted signalanalysis, Annals of Nuclear Energy, 30 (2003) 715-727.

[78] D.J. Yu, J.S. Cheng, Application of EMD method and Hilbert Spectrum to the fault diagnosis of roller bearings, Mechanical Systems and Signal Processing 19 (2005) 259-270.

[79] R.Q. Yan, R.X. Gao, Hilbert-Huang transform-based vibration signal analysis for machine health monitoring, IEEE Transactions on instrumentation and measurement 55 (6) (2006) 2320-2329.

[80] H. Li, Hilbert-Huang transform and marginal spectrum for detection and diagnosis of localized defects in roller bearings, Journal of Mechanical Science and Technology 23 (2009) 291-301.

[81] D.J. Yu, Y. Yang, Application of time-frequency entropy method based on Hilbert-Huang transform to gear fault diagnosis, Measure 40 (2007) 823-830.

[82] L.R. Han, Gear fault detection and diagnosis based on Hilbert-Huang transform, Third International Congress on Image and Signal Processing, Vol.7 (2010) 3323-3326

[83] F.C. Cao, H.X. Pan, The fault diagnosis research of gearbox based on Hilbert-Huang Transform, International Journal of Education and Management Engineering Vol.2 (2012) 71-77.

[84] J.S. Cheng, D.J. Yu et al, Application of frequency family separation method based upon EMD and local Hilbert energy spectrum method to gear fault diagnosis, Mechanism and Machine Theory 43 (2008) 712-723.

[85] Z.Y. Su, Y.M. Zhang et al, Gear fault identification and classification of singular value decomposition based on Hilbert Huang transform, Journal of Mechanical Science and Technology 25 (2) (2011) 267-272.

[86] X.M. Wang, Z. Ren, A sensor fault diagnosis method research based on wavelet transform and Hilbert-Huang Transform, Fifth conference on Measuring Technology and Mechatronics Automation, (2013) 81-84.

[87] Z.K. Peng, F.L. Chu, Application of the wavelet transform in machine condition monitoring and fault diagnostics: a review with bibliography, Mechanical Systems and Signal Processing 18 (2004) 199-221.

[88] J. Lin, M.J. Zuo, Gearbox fault diagnosis using adaptive wavelet filter, Mechanical Systems and Signal Processing 17 (6) (2003) 1259-1269.

[89] Z.K. Peng, P.W.Tsea et al, An improved Hilbert-Huang transform and its application in vibration signal analysis, Journal of Sound and Vibration 286 (2005) 187-205.

[90] L. Xiang, A.J. Hu, Comparison of methods for different time-frequency analysis of vibration signal, Journal of Software 7 (1) (2012) 68-74.

[91] T.R. Babu, S. Srikanth et al, Hilbert-Huang transform for detection and monitoring of crack in a transient rotor, Mechanical Systems and Signal Processing 22 (2008) 905-914.

[92] B. Liu, S. Riemenschneider et al, Gearbox fault diagnosis using empirical mode decomposition and Hilbert spectrum, Mechanical Systems and Signal Processing 20 (2006) 718-734.

[93] J. Zhang, Z.P. Feng et al, Extraction of rolling bearing fault feature based on time-wavelet energy spectrum, Journal of Mechanical Engineering 9 (2001) 44-49.

[94] J.S. Cheng, D.J. Yu Dejie et al, Time-energy density analysis based on wavelet transform, NDT&E International 38 (2005) 569-572.

[95] J. Zhang, Z.P. Feng et al, Gearbox fault diagnosis using time-wavelet energy spectral analysis, Condition Monitoring of Machinery in Non-Stationary Operations, Springer, (2012) 223-230.

[96] S. Mallat, A wavelet tour of signal processing, Academic Press, (1998) ISBN 0124666051.

[97] R. Polikar, S.S. Udpa, Frequency Invariant classification of ultrasonic weld inspection signals, IEEE Transactions on Ultrasonics, Ferroelectrics and Frequency Control, 45 (3) (1998) 614-625.

[98] R. Polikar, The wavelet tutorial, 1996.

[99] X.F. Fan, M. Liang et al, A joint wavelet lifting and independent component analysis approach to fault detection of rolling element bearings, Smart Materials and Structures 16 (2007) 1973-1987.